DESIGN OF A
HIGH RELIABILITY TRANSPORT MECHANISM

by

FRANK JOSEPH PENNISI, JR.

B.S., Mechanical Engineering and Materials Engineering
University of California, Berkeley (1992)

Submitted to the Department of
Mechanical Engineering
in partial fulfillment of the requirements
for the Degree of

MASTER OF SCIENCE IN MECHANICAL ENGINEERING

at the

MASSACHUSETTS INSTITUTE OF TECHNOLOGY
May, 1994

Signature of Author _____
Department of Mechanical Engineering
May, 1994

Certified by _____
Dr. Andre Sharon
Thesis Supervisor

Accepted by _____
Prof. Ain A. Sonin
Departmental Committee on Graduate Studies
Department of Mechanical Engineering

DESIGN OF A
HIGH RELIABILITY TRANSPORT MECHANISM

by

FRANK JOSEPH PENNISI, JR.

Submitted to the Department of Mechanical Engineering
on May 6, 1994 in partial fulfillment of the requirements for
the Degree of Master of Science in Mechanical Engineering

ABSTRACT

High volume automated manufacturing lines often run at efficiencies as low as seventy percent--even for well-understood, mature products. Despite continuous improvement efforts over the last two decades that resulted in increased line speed, overall line efficiency (the actual number of parts produced divided by the maximum number of parts the line is capable of producing) has typically remained below eighty percent. It is argued in this thesis that increasing efficiency provides a greater financial return on investment than increasing line speed, yield, or flexibility, and should be the focus of future improvement efforts.

Further studies of efficiency within disposable consumer goods manufacturing reveal that the key cause of downtime is not machine reliability, but transfer/transition point jams. Numerous transfer points between machines, feeders, and tracks can force efficiencies below sixty percent, even with reliabilities as high as 1 jam per 50,000 parts. Clearly, the most effective means of reducing transfer/transition points is to grab positively each part once and not let it go until it completes its route through the entire manufacturing process.

This thesis describes the development, design and construction of a prototype transfer line in which parts are positively held and oriented as they are carried from one manufacturing operation to the next, greatly reducing the number of transfer/transition points and potentially raising efficiency dramatically. The prototype can operate at a rate of 840 parts per minute, and can be easily upgraded to 2500 parts per minute. This transfer line concept can theoretically operate efficiently at rates as high as several thousand parts per minute, but is in fact limited by current part feeding technologies.

Thesis Advisor: Dr. Andre Sharon
Title: Executive Officer, The Manufacturing Institute

ACKNOWLEDGMENTS

I'd first like to extend my deepest gratitude to Dr. Andre Sharon, my thesis advisor. He has provided me with more resources and experience than I feel I have deserved. Thanks for all the advice and encouragement, academic and personal, Andre. I consider you to be both an influential contact and a valuable friend.

If Fred Coté had paid for my thesis in addition to sharing with me some of his unending wisdom and patience, he'd have given Andre a quite a contest for that renowned first paragraph. If he wasn't around, my design wouldn't be half as practical as it is now. I'll never forget the design advice and machining tricks you've taught me, Fred. I hope someday there's a way I can repay you. Thanks also to Gerry Wentworth and Norm Berube, who helped out with my other machining needs--if it wasn't for Gerry, I'd still be machining parts.

Then there's my longtime (about sixty-seven years, I think) lab companions, Eric Ask, Dave Phillips, and Susie Ward. Eric, you hung around and reassured me during some of my hardest times here. I hope your (our) time at General Electric is great--just don't start competing directly against me. Thanks to Dave for always being willing to scratch his head for any kind of problem I had. No matter what the question was, you always gave the right answer, if you know what I mean; I've matured quite a bit because of you. And you, Sus, congratulations to you and your main squeeze, and thanks for helping with that frustrating cap analysis thing.

Next comes Miguel, Wayne, Tiina, and Andrés, my short-term (supposedly) lab companions. Thanks to all you guys for your criticism, suggestions, and willingness to move heavy things with me. W, special thanks for garaging my truck!

Just to show everyone that the order shouldn't matter too much, I want to thank Dan Alvarado and Leslie Regan in the middle, though they both deserve alot more credit. Without them, I'd have no parts, no good Mexican food, and no money. They've both carried me through the necessary administrative garbage with exemplary performances. Good luck at Stanfurd, Dan! Visit me when you get there, and hire me when you graduate!

When I was up you-know-what creek, Hal, Bill, and Wes were here to throw me a paddle. Harold Ackler, my messy Australian drinking buddy and roommate, helped me out with the insight of a grumpy Ph.D. student. Bill Davis, long-time friend from California (sigh), also provided that extra encouragement and help when the rewriting came. Thanks dude, we'll have to rage when I'm back

home. What should I say about Wes Williams? This guy comes out of nowhere and starts buying me dinner when I'm stuck at a machine all night, and offering beer and help whenever I needed it. I hope there's more guys like you around in this world, Wes. You can count on me to hire you if it ever comes to that--your outlook and your knowledge as an undergrad have really impressed me. (But don't get yourself killed.)

Carolyn Davis, my sweetie, my Luun, my elf, my frolicking wood nymph, deserves more than just a paragraph. Honey, I look forward to thanking you with more than just a few words on a page. I love you, and think you look really cute standing on a tensioning platform.

And last, but not least, I want to thank my family--Dad, Mom, Sam, Mary, and Grandpa Frank--they made me who I am and never stopped encouraging me through anything I chose to do. I think you guys have done a pretty good job. Keep up the good work. I'll try if you do.

CONTENTS

LIST OF FIGURES

LIST OF TABLES

CHAPTER 1: INTRODUCTION

From 1948 to 1989, the United States gross national product nearly quadrupled from 1.1 to 4.1 trillion dollars (adjusted to the 1982 dollar). During this same period, United States manufacturing closely followed, increasing from 239 to 929 billion dollars. In 1992, according to the United States Bureau of Labor [1], the manufacturing industry employed 18.2 million people, and several other types of jobs within the raw materials and service sectors depend on manufacturing. The International Productivity Journal [2] estimated the number of these manufacturing-related employees in the 1980s to be between 40 and 50 million. Thus manufacturing remains the key to economic growth and employment within the United States.

Two separate commissions on competitiveness [3, 4] however, rated the United States only third among the Group of Seven (G-7) nations, behind Japan and Germany. Many people believe erroneously that the high cost of United States labor contributes most significantly to this lack of competitiveness. In 1992, the average hourly manufacturing wage in the United States equaled that of Japan, and in Germany was actually sixty percent higher [5]. Despite this, a 1990 study conducted by Andersen Consulting [6] showed that even though labor costs averaged only ten to fifteen percent of total direct manufacturing costs, a typical United States manufacturer spent over seventy-five percent of its time trying to reduce them. Because of these misdirected efforts, low-cost labor nations have been used to assemble American products. These nations then build their own bases of skilled workers, making the United States even less competitive in the long run.

America clearly needs to take a different approach to increasing its manufacturing competitiveness. The Congressional Joint Committee on Taxation [2] reports that the United States' investment in capital (as a fraction of the gross national product) actually decreased in the 1980s from the 1970s. In contrast, the Manufacturers' Alliance for Productivity and Innovation (MAPI) [2] found that in the 1980s, Japan and Germany increased capital spending. These nations invested 15.8 and 8.3 percent of output; the United States invested only 5.2 percent. From this and other data, many have concluded that America's competitive stance would be improved most successfully by well-planned investments in capital. It was this approach that was taken and applied within this thesis.

To maximize a capital investment's potential, a product class whose manufacture is capital intensive was chosen. Many capital intensive products are small and produced in high volume on some sort of line requiring minimal human involvement. One class of parts fitting this description is disposable consumer goods, a category that includes pens and pencils, toothbrushes, flashlights, bottled and canned goods, razors, and measuring sticks.

Manufacture of these products usually involves a line that begins with a raw materials forming machine such as an injection molder or stamping press. Some products may require finishing or deburing by means of a numerically controlled machining tool or vibratory deburing machine. Typically, the part would then be labeled, painted, etc. Since an offset printer is most commonly used to accomplish this, the part would continue through an oven or dryer. After this, the part might be cleaned and/or prepared, joined to

other manufactured or purchased parts at assembly stations, then inspected. Testing of the product might also occur. From there, the finished product is taken to packaging.

This general plant layout can be applied to most disposable consumer goods. The cost analysis that follows in Chapter 2 assumes a layout similar to the one above, yet remains general. The chapter describes and compares the four most commonly employed methods of increasing productivity when investing in capital: raising yield, bettering efficiency, boosting line speed, and increasing flexibility. Chapter 2 establishes (qualitatively) that line efficiency provides the highest return on investment; in turn, Chapter 3 will break down inefficiency into its root causes and determine the best way to reduce it. The result is a machine whose design is described in Chapter 4. Chapter 5 presents briefly the results of the design, and Chapter 6 outlines conclusions and recommendations for further work. It should be noted, however, that as the thesis progresses, design restrictions will begin to require dimensions and characteristics for a specific product; therefore to prevent future complications, the product of choice will be a ball point pen, illustrated in Figure 1.

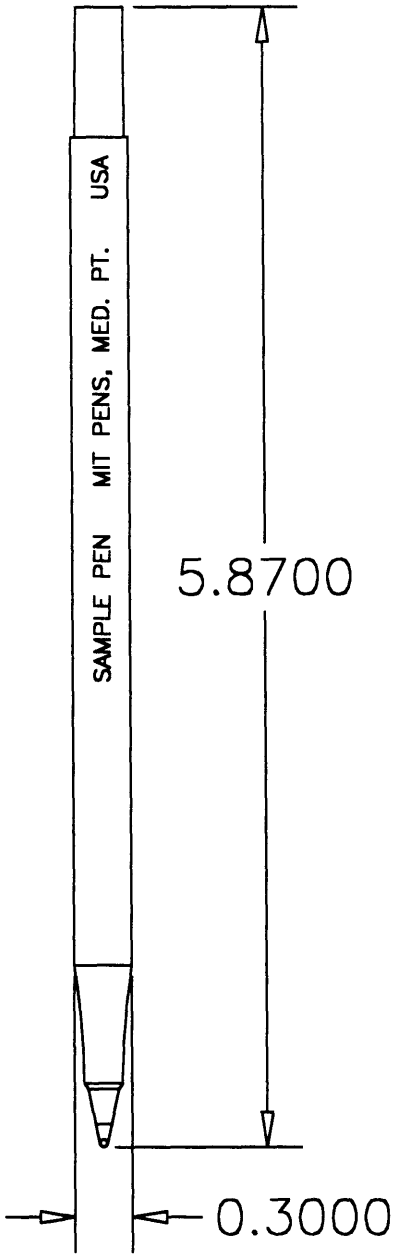

Figure 1: Typical disposable consumer good: a ball point pen.

CHAPTER 2: IMPROVEMENT ALTERNATIVES

The purpose of this chapter is to describe and evaluate the methods of improvement listed in Chapter 1, and to arrive at the method that is the most cost effective to implement. From here, a company can invest its funds in capital that best increases its productivity. For this analysis, assume that a ball point pen manufacturing facility wishes to improve its productivity through some capital investment. Four possible means of improvement to an existing (or new) manufacturing line deserve consideration: improving yield, efficiency, speed, and flexibility.

The first of the four means would improve the process's yield--the percentage of parts that emerge from the manufacturing line without defects. Typical yield values exceed ninety percent. Yield is often confused with the second means of improving a manufacturing process, improving line efficiency, which, in contrast to yield, is the ratio of the number of parts created within a given time to the maximum number of parts the line could produce within that time. An important aspect of line efficiency is the reliability of the machines and their ability to operate consistently at full capacity. A manufacturing line's efficiency can range from very low to as high as ninety-eight or ninety-nine percent. Increasing efficiency can typically increase line capacity more cost effectively than the third method: increasing the manufacturing line's speed, which is frequently the easiest to implement to a mild degree (it may involve simply turning a knob). However, harmful dynamic effects that may result from increased line speed decrease reliability, causing equipment damage that can prove costly and can actually reduce

throughput. The fourth and final improvement discussed within this thesis involves increasing overall line flexibility to accommodate several types of parts, or to accommodate a frequently changing product.

These suggestions for improvement translate into a working set of assumptions for building a cost analysis. Assume the ball point pen manufacturing line has a yield of 95 percent, an efficiency of 80 percent, produces 250 working parts per minute, and costs roughly five million dollars. The following plant layout will be used for this analysis: injection molders form three major components of the ball point pen, specifically, the body, the cartridge, and the lid. The parts are collected in bulk from the injection molding machines and are fed into the line via bowl feeders and feed tracks. The body moves to an offset printer where the brand name, make, and size are printed along its side. The printed ink dries onto the body as it travels through an oven; the pen is blown clean and transferred to an assembly station, after which the assembly station inserts the cartridge into a prefabricated tip, then fills it with ink. This assembly is placed into the body, sealed shut, and tested for proper ink flow. The station places a lid on the now-assembled pen, where it is inspected by a vision system and transferred to a packaging machine.

For both the layout described above and most manufacturing lines, the production and operating costs could be separated into five major categories: materials, labor, factory supplies, depreciation, and other costs. Materials include the costs of all raw materials, packaging materials, and contracted prefabricated parts. For a high-

volume manufacturing operation such as the one given here, materials often constitute the largest portion of total direct cost, ranging from roughly seventy to ninety percent. Labor costs, the second category, make up a significantly smaller portion of direct costs, ranging from ten to fifteen percent. These include not only the cumulative hourly wages of all line employees, supervisors, and engineers, but also overhead expenses and employee benefits. In a highly automated manufacturing line, the line employees' principal responsibilities are to keep the line running smoothly and to maintain and repair the equipment. The cost of spare parts and other equipment used to maintain these machines--such as replacement ink cartridges, grease, and bearings--falls under the third category, factory supplies costs, which typically embody the smallest portion of direct costs.

Indirect costs accumulate primarily through depreciation, the fourth category. As machines within the line age, their resale values drop; each value falls by a percentage defined by federal tax codes. The resulting depreciation cost is the amount lost after a hypothetical sale of the equipment. The remaining costs are also primarily indirect and more difficult to account for, and are therefore lumped into the fifth and final category, other costs.

To minimize the necessary financial resources, the costs described above will be loosely compared with one another for four hypothetical improvements:

(a) Yield has been increased from 95% to 99%.

(b) Efficiency has been increased from 80% to 96%.

(c) Line speed has been doubled to 500 parts per minute.

(d) Line is flexible enough to accommodate all products.

The demand for the pen (i.e., the annual production rate) is assumed not to change. In each case, only one means of improvement has been implemented, while all the other parameters remain constant. For example, in case (a), although the yield increases from 95 percent to 99 percent, the line still produces 250 parts per minute at 80 percent efficiency, and remains incapable of accommodating other products.

Upon implementing improvement (a), the results can be determined easily. First, it is assumed that all raw materials go toward creating the product, i.e., scrap, flash, and/or purging material is negligible. By assuming this, the percentage of material cost savings due to yield becomes the difference between the new yield and the old yield, or four percent. The change takes place within the machinery; additional labor and supplies are not necessary. It is also assumed that the cost to achieve this improvement in yield is negligible.

By improving efficiency, option (b), it is assumed the line operates with fewer periods of downtime due to jams. Savings in material costs are near zero; downtime rarely damages or sacrifices significant numbers of parts. Downtime, maintenance, and startups, however, are the leading reasons (if not the only reasons) for needing line employees. Past evidence has shown that in many high-volume plants, over half of the employees' complete job descriptions involve clearing part jams. Over fifty percent of the employees would become obsolete if these jams were reduced drastically or eliminated. This cuts labor costs roughly in half. Unfortunately, high

efficiency cannot be implemented as cost effectively as high yield. Startup and maintenance times cannot be reduced without more robust equipment and/or procedures, and jams cannot be reduced without implementing new technology. The cost of such replacements increases depreciation costs slightly. Factory supplies costs do not change. Although various parts may wear at slower rates, they will probably still be replaced at regular predetermined intervals, therefore not affecting costs.

Improvement option (c), which doubles the line speed, is the most frequently used option. Its ease of implementation--to a mild degree (such as a ten percent increase)--and apparent benefits seem to make this option the most attractive, but line speed ends up costing the most overall. As with efficiency, material costs remain unchanged--most parts will not be damaged or sacrificed if the appropriate safeguards and equipment are installed. Since only half the time is required to produce the line's annual capacity, labor costs are cut in half. However, since machinery is moving twice as quickly, the bearings and other parts of the line see higher forces, temperature increases, and wear rates, all of which increase factory supplies costs. Such an improvement also requires a complete redesign of most of the line, since faster speeds usually make necessary stronger and more dynamically resistant parts. Such a redesign is estimated to cost four to five times more than the cost of implementing higher efficiency, significantly increasing depreciation costs.

It would be unfair to claim that adding flexibility to a line is not beneficial; adapting a line to accommodate several products has

advantages that current manufacturing standards have only begun to measure. However, its high cost to implement and current level of development make it impractical to introduce into a high-volume manufacturing facility. Information theory has begun to place quantitative values on flexibility, but until the field is further developed, it will continue to appear to be an unwise investment to those looking solely at the bottom line.

In high volume manufacturing operations, greater flexibility and higher line speed are mistakenly the most sought after improvements because of the belief that these alternatives contribute most significantly to the bottom line. This is untrue. Flexibility has been shown to decrease the bottom line. Also, it is assumed that line speed can be doubled while maintaining the current efficiency, yet with current technology, this is not achievable. Comparing the alternatives above shows that efficiency provides the highest return on investment since increased efficiency cuts labor by roughly the same amount as high line speed without incurring large capital expenses and factory supplies costs. Cutting larger fractions of total cost--such as materials--produces savings only from higher yield. High efficiency surpasses high yield because yield is already so high in mature high-volume operations that it cannot be increased enough to render significant savings.

Along with producing the greatest savings, efficiency also increases the line's capacity. In moving from 80 to 96 percent efficiency, the line produces 297 parts per minute without increased line speed or additional costs. This impressive nineteen percent capacity increase is above and beyond the cost savings described.

With efficiency established as the best means for increasing manufacturing productivity, further decisions can be fine tuned.

CHAPTER 3: INCREASING EFFICIENCY

A manufacturing line that operates at one hundred percent efficiency would: 1) not require time to start up or stop, 2) be maintained as it operated without slowing its capacity, and 3) never stop due to jams or full buffers. In reality, designing a machine that eliminates each of these problems would be difficult, if not impossible. Instead, the approach was taken to break down efficiency into the components above via line observation, and determine the leading cause of inefficiency.

Close observations of a high-volume, eighty-percent efficiency manufacturing line over thirty hours revealed some significant findings. The machines that performed the manufacturing operations themselves, such as the printers and assemblers, ran quite reliably when the part was delivered to the machine at the proper intervals and in the right orientation. When this was not the case, however, the machine stopped because of a buffer or jamming problem, which occurred frequently. Line maintenance required only a small fraction of total downtime; startup and shutdown times were even smaller.

It was clear that the transfer mechanisms and buffers were the most significant contributors to the line's total downtime. Individually, these mechanisms may be inherently reliable; however, there are so many points of transfer between buffers, feed tracks, feeders, orienters, and machines that a probabilistic combination of these reliabilities would result in a significant amount of downtime. In the fictitious pen plant, for example, the following transfer points could occur:

Body

- Injection molder to conveyor
- Conveyor to printer buffer
- Printer buffer to printer's bowl feeder
- Bowl feeder to feed track
- Feed track to orienter
- Orienter to printer track (then through the printer)
- Printer track to assembly buffer
- Assembly buffer to assembly's bowl feeder #1
- Bowl feeder #1 to feed track
- Feed track to blower
- Blower to assembly station
- Assembly station to feed track
- Feed track to packaging buffer
- Packaging buffer to packaging's bowl feeder
- Bowl feeder to feed track
- Feed track to packaging

Cartridge

- Injection molder to conveyor
- Conveyor to assembly buffer
- Assembly buffer to assembly's bowl feeder #2
- Bowl feeder #2 to feed track
- Feed track to assembly station (where it joins the body)

Lid

- Injection molder to conveyor
- Conveyor to assembly buffer
- Assembly buffer to assembly's bowl feeder #3
- Bowl feeder #3 to feed track
- Feed track to assembly station (where it joins the body)

Pre-fabricated Tip

- Buffer to assembly's bowl feeder #4
- Bowl feeder #4 to feed track
- Feed track to assembly station (where it joins the body)

It is assumed that the assembly station fills the cartridge with ink, assembles all the parts, tests the pen, inserts the lid, and inspects the completed pen, all without transferring it. If the pens are to be packaged, an additional seven to fifteen transfer points should be added, depending on the packaging quantities and inter-part stacking complexities. The twenty-nine transfer points listed above represent a conservative estimate; realistically, one can expect a typical high-volume consumer product manufacturing line to have between thirty and fifty transfer points.

Even if each line shutdown takes only 90 seconds to correct, the decrease in efficiency from increased transfer points is staggering. In a line that produces 250 parts per minute, assume that a probability p exists that any transfer point on the line will jam. If there are no jams or machine failures, parts are produced at a rate of 250/e per minute, where e is the line's efficiency. This rate corresponds to 0.24e seconds between parts. If a jam does occur, 90 seconds pass before the next part is made. Including these breakdowns, parts are produced every 0.24 seconds. These facts can be placed into an expected time equation of the form

$$90(p) + 0.24e(1 - p) = 0.24. \qquad (1)$$

This equation states the expected time per part when taking the probability of breakdowns into account. Below is a table stating the resulting efficiencies, excluding startup times and maintenance, for various numbers of transfer points, assuming that each transfer point has a probability of failure of 0.00002 (1 jam per 50,000 parts):

Table I: Estimates of Line Efficiency vs. # of Transfer Points

# Transfers	Jamming Prob. p	Efficiency e
5	0.0001	0.963
10	0.0002	0.925
20	0.0004	0.850
30	0.0006	0.775
40	0.0008	0.701
50	0.0010	0.626

The calculations above assume that the machines operate at one hundred percent efficiency. Thus, any effort to improve machine reliability would still not raise efficiency above these values. Factoring in machine inefficiencies would decrease the resulting efficiencies even further. As can be seen, any line that must deal with several pieces, and therefore several transfer points, suffers a severe drop in efficiency.

Obviously, the number of transfer points must be decreased to increase line efficiency. The best (and perhaps the only) way to reduce the number of transfer points is to maintain positive control of all parts throughout the line; in other words, grab on to the part directly after it is formed, and do not let it go until it is placed into the packaging materials. All manufacturing operations should be performed on the part while it is held. Not only will this greatly increase efficiency, but it will also reduce both contamination and wear by preventing parts from continuously rubbing against feed tracks, feeders, and other parts. Once a part has been grabbed, the machines will always know the part's position with respect to the grips; accurate grip positioning will lead to accurate part positioning.

A mechanism that maintained positive control of the part throughout the entire line would virtually eliminate transfer points, dramatically increasing efficiency. This principle evolved into the concept described in this thesis, in which an individual part is placed into a carrier and held throughout the manufacturing process (Figures 2-4). Each carrier is transported, manipulated, and oriented in a positive, yet simple fashion, and every manufacturing operation is performed on the part as the carrier grips it.

Since parts are operated on in various orientations (horizontal during printing, vertical during assembly, etc.), the transport system had to be able to orient the carriers, and hence the parts, about their directions of travel without introducing additional transfer points, which would merely shift the problem from the parts to the carriers.

The cable/carrier system of Figures 2 through 4 provides all the benefits and features described above. It employs a series of carriers attached to one another by way of two cables (Figure 3). The carriers and cables resemble a rope ladder joined at its ends, with each "rung" of the ladder, or carrier on the chain, engaging between the teeth of a pair of modified roller chain sprockets (Figure 2). The sprockets are oriented with their axes of rotation parallel to the desired part orientation and drive the system similarly to a roller chain drive. In contrast to roller chain drives, however, this system can twist and orient the chain, and therefore the part, about its direction of travel by merely changing the sprocket axes (Figure 4). The parts are initially fed into the carriers by current means known to the art, such as the one depicted in Figure 5.

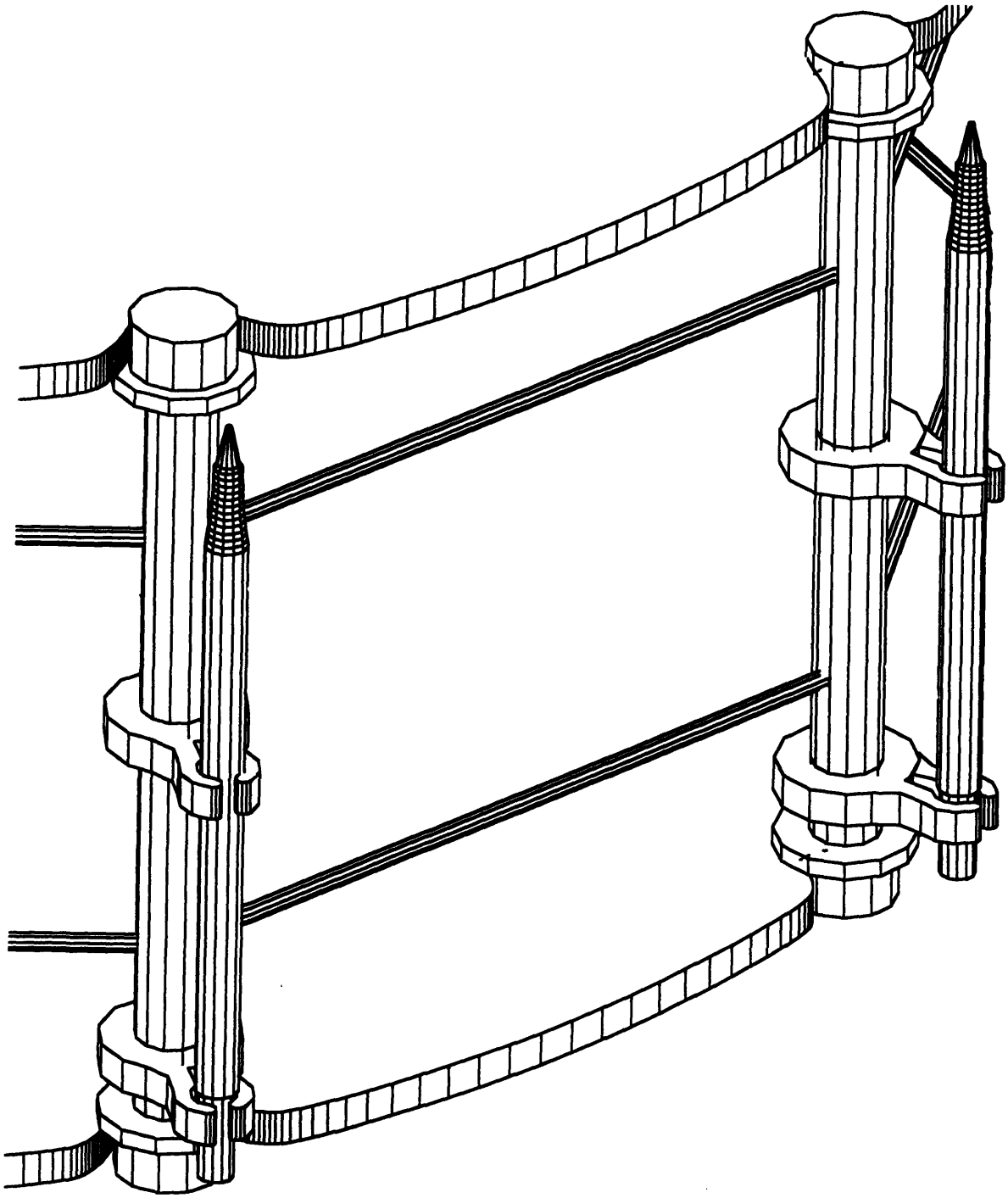

Figure 2: Closeup view of the cable/carrier mechanism's grips for a hypothetical axially symmetric part

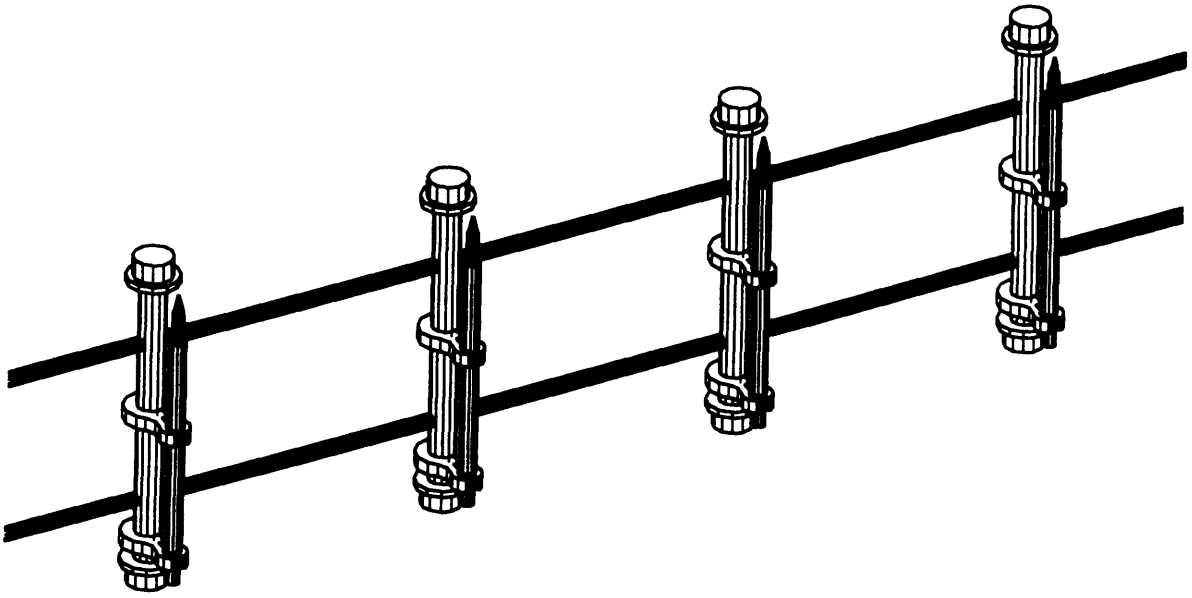

Figure 3: View of the cable/carrier mechanism between sprockets.

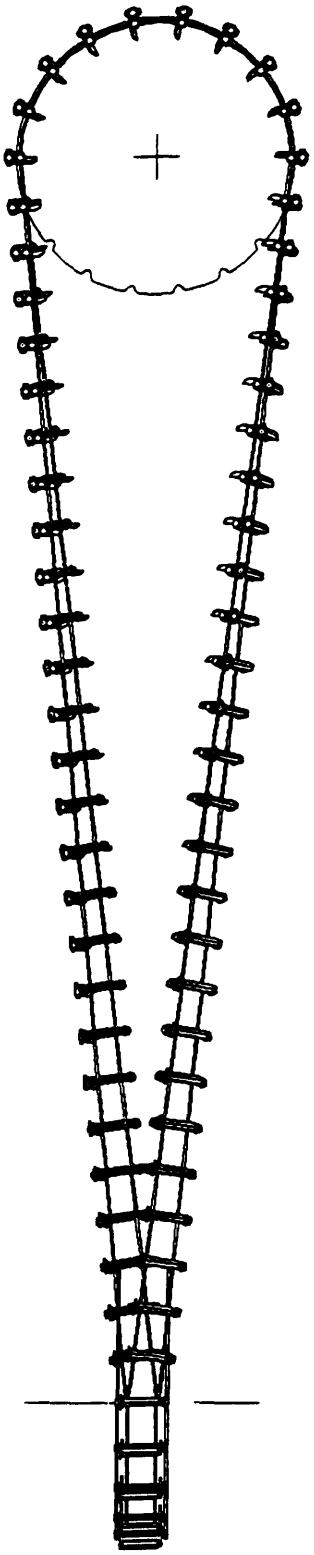

Figure 4: Demonstration of cable/carrier mechanism's ability to orient parts and carriers by turning the sprockets.

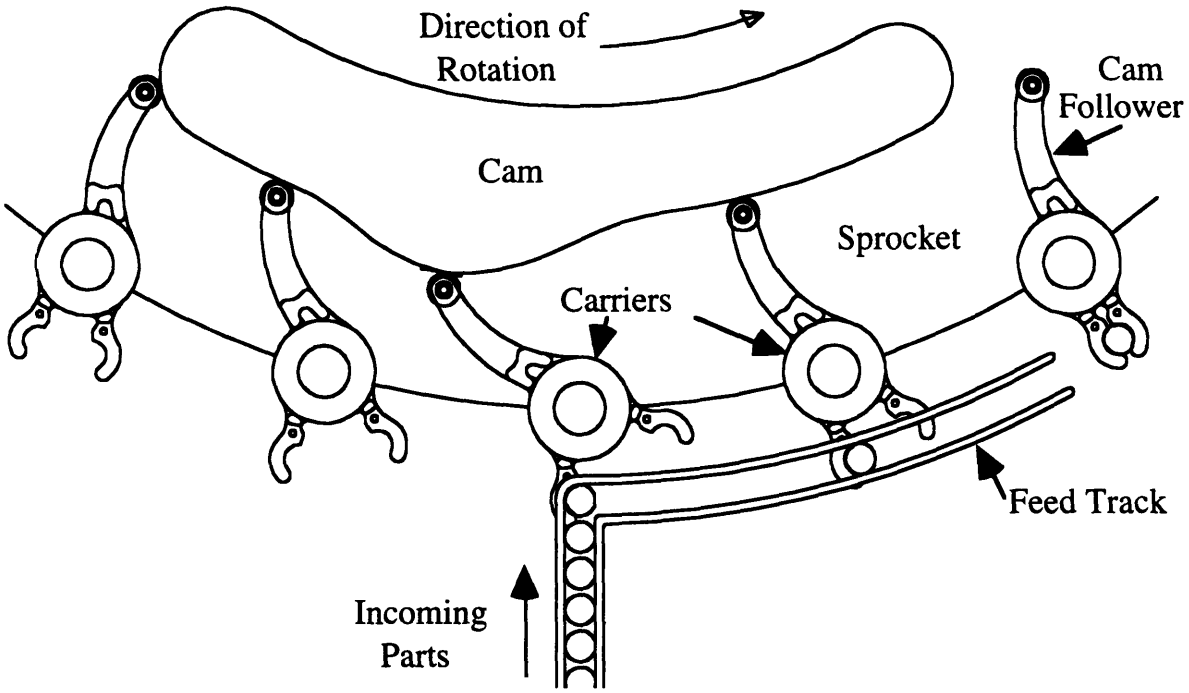

Figure 5: A possible means of feeding parts into the mechanism.

The assembly line is driven, oriented, and guided by pairs of sprockets. Figure 6 illustrates how this line concept may be applied to the pen manufacturing layout described earlier. Beginning near the upper left corner of Figure 6, the pens and carriers pass under an offset printer, then into an oven to dry. Following the line, the carriers then twist ninety degrees about their direction of travel to engage with the orientation sprockets. They reverse back toward the oven as they approach the blowout sprockets, then reverse themselves yet again and head toward the assembly station. At the assembly station, parts from another line (not shown) are inserted into the pen bodies and the assembled pens are inspected. Note that some operations were removed to increase visual clarity (for example, the testing stage). The pens then orient themselves ninety

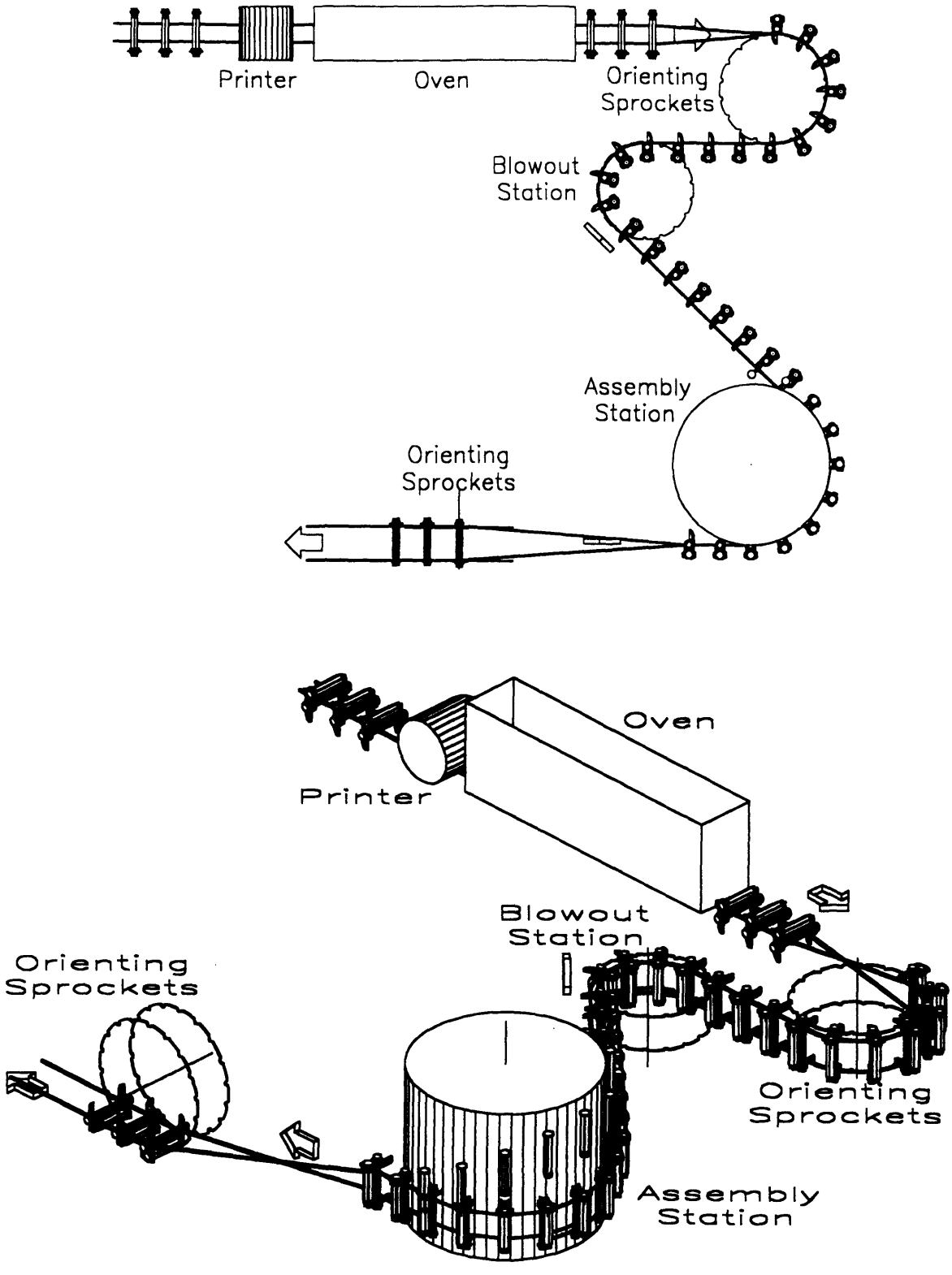

Figure 6: Possible plant layout incorporating the cable/carrier mechanism.

degrees by the constraint of the third and final pair of sprockets shown, and head off to packaging.

Many previous line concepts employed this principle to a degree, but none presented simple means for offering the part in a multiplicity of orientations for manufacture, and hence only shifted the problem from the parts to the carriers. U. S. Patent number 4,533,038 [7] describes a line similar to the one envisioned herein, but it does not possess the ability to orient its parts (Figure 7). As shown in a schematic top view of this line, a part is held in a carrier (3) attached to a transport member (2), typically a roller chain. Sprockets (4) drive and guide the parts throughout the line, where manufacturing stations such as 1 and 1' perform various operations on them. The machine can accommodate only one orientation, vertical. Operations such as assembly often work best when gravity aids the process. While this is useful for many simple parts that require few operations, many parts require more than one manufacturing operation. In operations such as printing, however, the part is best presented to the machine horizontally with respect to this page, perpendicular to the direction of travel. This patent's line cannot orient the part from one operation to the next.

Other line concepts have attempted to solve this problem typically by either 1) transferring the part in one orientation to a feeder, which then transfers it (by way of a feed track) to another line of a different orientation, or 2) rotating the part about another axis. The first "remedy" is insufficient, since it decreases the line's efficiency by adding transfer points. The second technique avoids introducing new transfer points, but convolutes the orientation

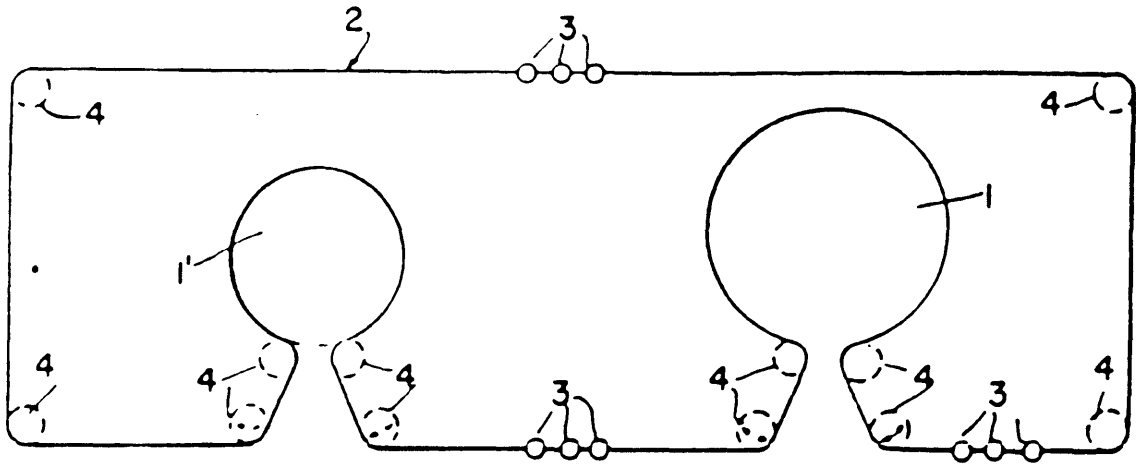

Figure 7: Schematic view of a positively displacing (but not orienting) manufacturing line. U. S. Patent #4,533,038.

process by employing complex mechanisms and guides to turn the part about an axis perpendicular to its direction of travel. An example of this can be found in U. S. Patent number 3,837,474 [8] (Figure 8), in which the method accomplishes the desired orientations by running up the machine's part count and using guides to turn the carriers, thereby increasing the complexity.

Another class of patents also tries (unsuccessfully) to mimic the cable/carrier concept. U. S. Patent number 4,320,827's [9] conveyor mechanism, among others, employs pairs of link chains or ball and socket chains in methods similar to the concept described herein. Unlike roller chains, these chains are flexible in more than just one plane. However, both of the chains suffer from significant backlash, and do not have the strength-to-weight capacities that cables do. Carriers securely attached to cables, not chains, are both flexible in all directions and capable of resisting excessive tension and backlash.

A final item that deserves mentioning is Berg's Pow-R-Tow® chain [10], depicted in Figure 9. This chain uses a single cable to drive sprockets in the same way as the cable/carrier system with the important feature of being able to twist and accommodate out of plane sprocket drives. If a stronger, longer chain were used on the Pow-R-Tow® with carriers attached to each link, this chain could be extrapolated out to a manufacturing line similar to the one herein. Some of this thesis's design ideas were modeled after the Pow-R-Tow®. However, this chain fails to provide the rotational stability that the second cable gives to the cable/carrier transport mechanism, and the space limitations on the Pow-R-Tow® chain prohibit the addition of carriers.

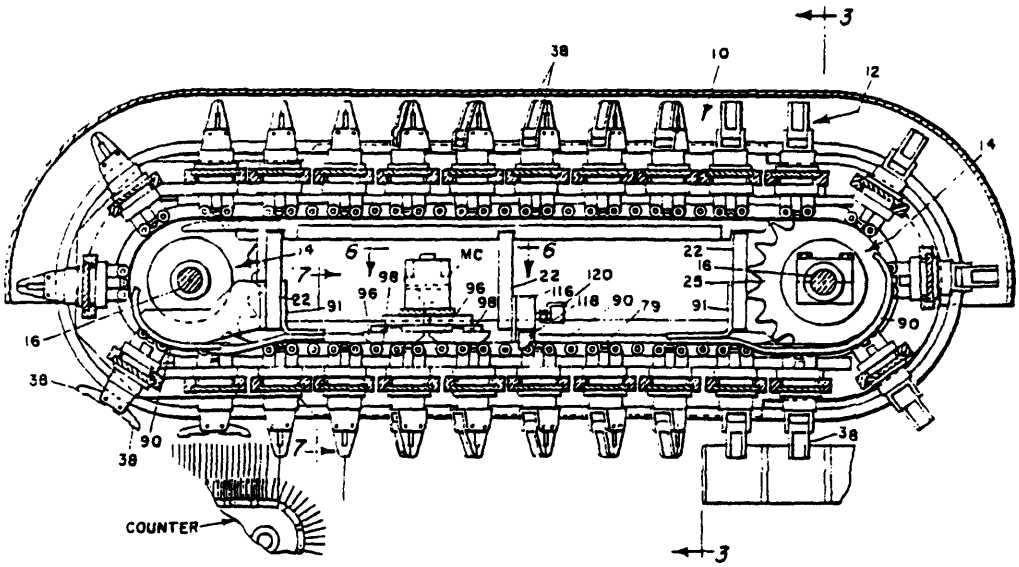

Figure 8: Top view of a system that rotates its parts about another axis. U. S. Patent #3,837,474

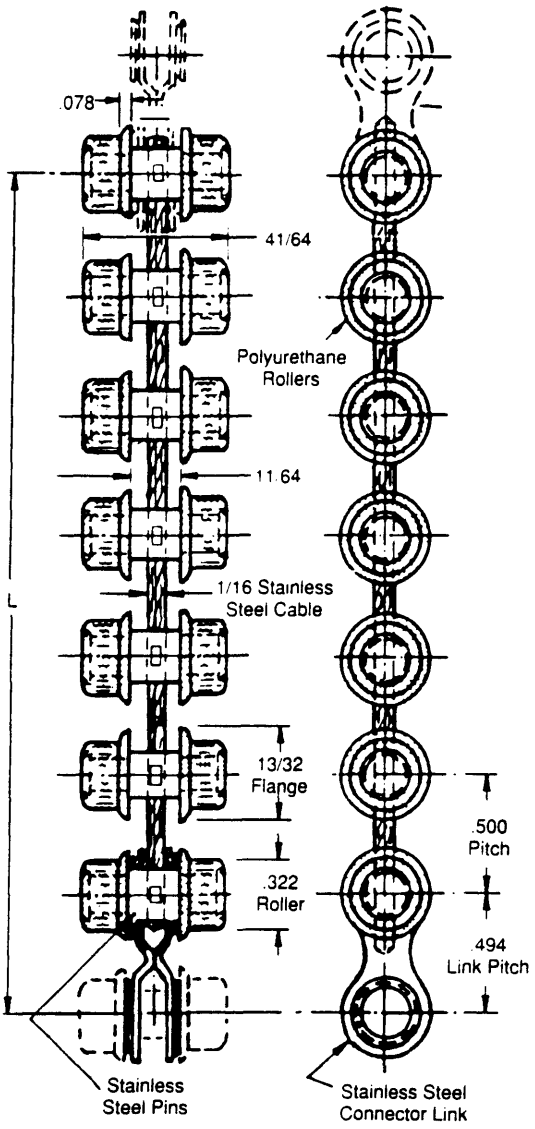

Figure 9: Berg's Pow-R-Tow® power transmission belt.

This section was laid out to describe the advantages of the cable/carrier system over current systems. However, additional questions about the proposed concept arose: Where should the carriers be placed, on the top or the sides? How can the line run around the sprockets on both sides if the carriers are side mounted? How unobtrusive should the carriers be concerning the sprocket and the part? How should the carriers be shaped? Where do the buffers go? How will the parts enter the carriers?

All of these questions deserved consideration before actual design could begin. The carriers of Figure 6 are placed on the side of the shaft connecting the sprockets because the part of interest is long and axially symmetric. Holding the pen at two ends from the carrier's top in any orientation would require a long projection from the carrier's shaft in some direction, creating serious carrier asymmetry and possible carrier/sprocket engagement problems. To decrease the asymmetry the most, side holding was chosen; however, a different part geometry may merit a different method of holding.

It was decided that the carriers and sprockets would be spaced in such a way to allow the line to wrap around the sprockets on either side. In doing so, the sprockets required movement apart axially so that the pen and carriers could fit completely between them. If a part geometry is exceptionally long or would protrude radially from the carriers so as to hit the sprocket centers, then the carriers and sprockets should be designed to accommodate this, whether by a different holding technique or by resizing them.

Another question that deserved attention regarded the buffers. As can be seen in Figure 6, buffers within this new line have been

eliminated. Buffers are useful if the actual machines performing the operations are the main contributors to downtime. However, in high-volume operations, where jams and feeding mechanisms are the main cause of inefficiency, buffers actually further decrease the efficiency. Buffers act to stockpile parts. If a machine shuts down, buffers can continue supplying a few minutes worth of parts to the remaining machines in the line by filling bowl feeders with additional parts. Buffers, however, do not increase efficiency: adding them to decouple the machines introduces additional feeders and tracks into the line, and therefore more transfer points that decrease efficiency at a faster rate than the buffers increase it. Therefore, buffers should be removed from the line unless a transfer-free technique can be devised.

Even if the buffers have been removed, one feeding method is still required: transfer from the raw materials forming machine into the cable/carrier line. Figure 5 shows a schematic view of how this can be accomplished. Each pair of carrier jaws, one stationary and one mobile, is joined by a spring-loaded hinge. As the carriers rotate between the sprocket teeth, the carriers' cam followers (located toward the radial center of the sprocket and attached to the mobile jaw) approach a cam, which is struck by the followers, opening the jaws and accepting a part from a part feed track. The feed track can be supplied by any feeding means known to the art. The cam then lets up on the follower, closing the spring-loaded jaws and sending off the part to be processed.

In review, the concept of high efficiency can be best realized by reducing the transfer points by as many as possible. The best

way to accomplish this is by establishing part registration early in the manufacturing process and by not losing it through any part orientations or operations. To orient a part through all its necessary positions without letting go, a continuous flexible system must be instituted. This system cannot suffer from backlash or require additional transfers when orienting parts. The resulting system is a series of part carriers attached to a pair of cables. These cables are driven by a pair of sprockets that engage the line at the carrier's ends, or caps. The orientation of the sprocket determines the part's orientation, which may twist along with the cables to obtain numerous positions. Parts can be fed into this system by several means, provided they are reliable. The following section will explore whether this concept of high efficiency is feasible and will present the design of a system to prove it.

CHAPTER 4: DESIGN

Within this chapter, the concept described above will be physically and analytically verified through a mock-up and calculations. After verifying that various aspects of the project are feasible, a full scale prototype is designed and constructed.

4.1 Feasibility

This section will present the calculations necessary to estimate the precision to which the cable/carrier system can position parts and determines whether this precision is sufficiently high to apply toward a class of high-volume manufacturing that includes pens.

The following procedure determined the loosest allowable tolerance that the machine could supply, assuming that the pen's critical (i.e., tightest) tolerance requirement was in the assembly operation. It was also assumed that the pen and cartridge measured approximately 0.3 inches in diameter and were designed to fit within class 2 interference locational fit (LN2) tolerances. According to LN2 standards, the maximum radial interference s_{min} equals 0.0005 inches. Mating parts are also frequently produced with chamfers to guide and align the parts into one another. It is often recommended to size part chamfers at roughly one-eighth the outer diameter. Parts having a 0.3-inch diameter would therefore be molded with a chamfer length c equal to 0.0375 inches. For simplicity, the chamfer angle was assumed to be forty-five degrees.

Figure 10 illustrates the chamfer above and τ_{max} (in.), the maximum radial misalignment a part can endure before missed assemblies may occur. As can be seen,

$$\tau_{max} = c - s_{min}. \quad (2)$$

For the example in this thesis, τ_{max} = 0.0370 inches.

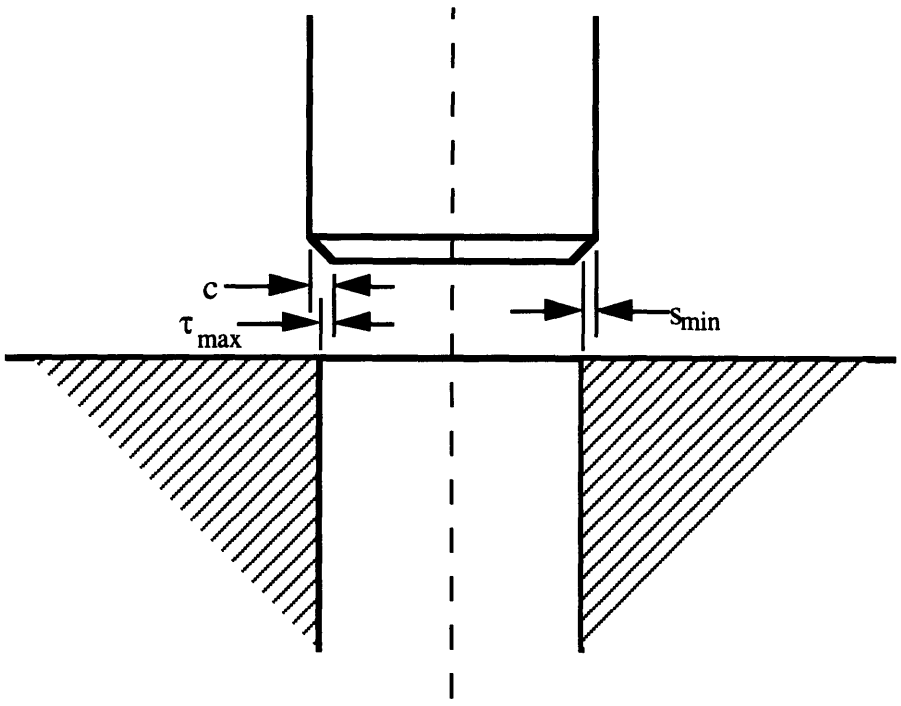

Figure 10: Graphical illustration of maximum allowable tolerance.

If the potential misalignment between axes, τ (in.), does exceed τ_{max}, the machine may still assemble parts. Although not strictly necessary for this design, this analysis is included because parts made from other processes may exceed designated tolerances. Korsakov [11], among others, has provided a formula for the probability of non-assemblibility p_{NA} of a part B being slipped over or inserted into another fixed part A. He assumes that the tolerance distributions of each part are Gaussian and centered about δ_A and δ_B, as shown in Figure 11. If τ does not exceed τ_{max}, $p_{NA} = 0$. If τ exceeds τ_{max} by some amount b (in.),

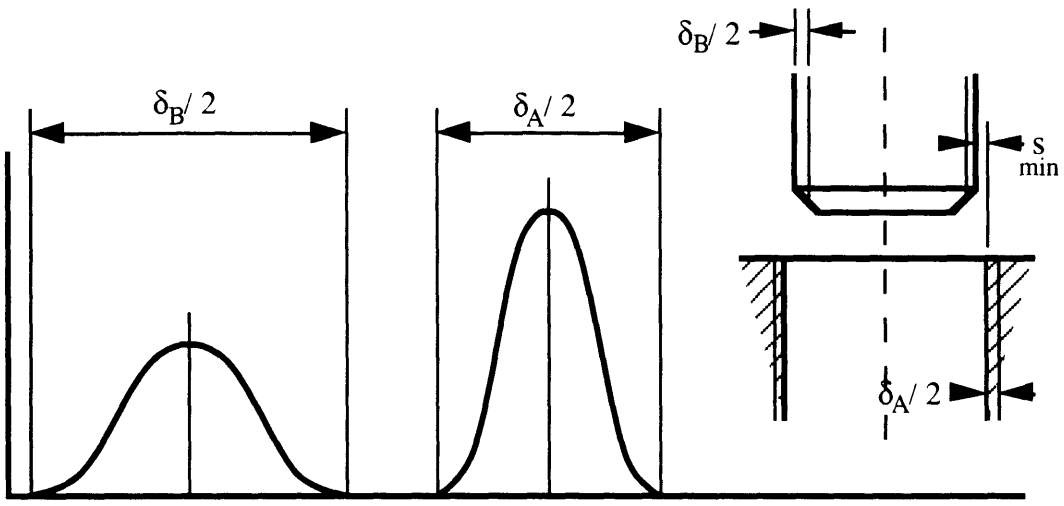

Case (a): Misalignment $= \theta$.

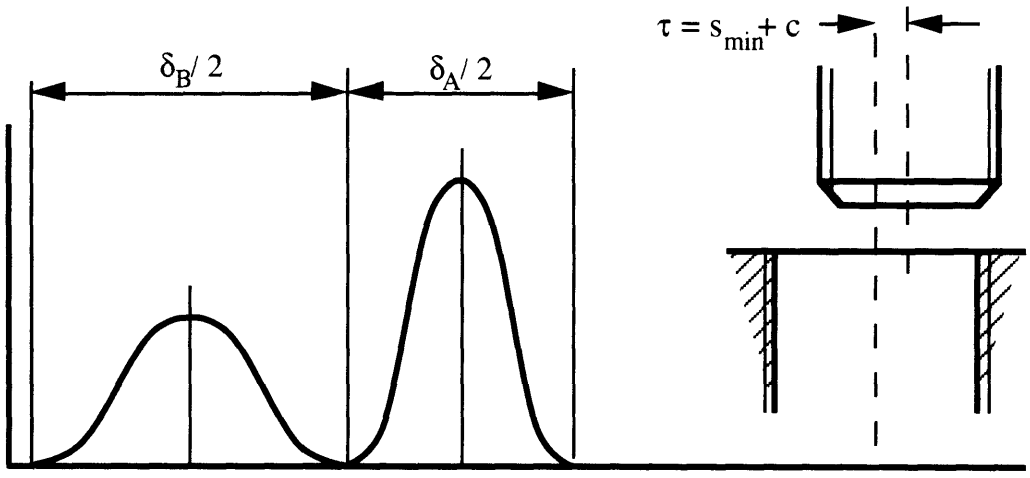

Case (b): $\tau = s_{min} + c$

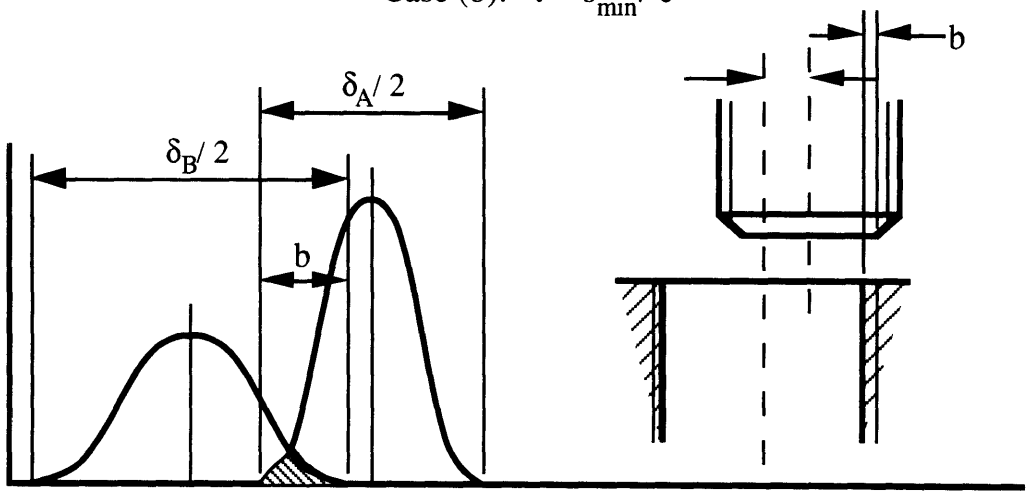

Case (c): $\tau = s_{min} + c + b$

Figure 11: Tolerance distributions for various amounts of clearance.

$$p_{NA} = 0.5 - \frac{1}{\sigma_A \sqrt{2\pi}} \int_0^{\frac{\delta_A}{2}-b} e^{\frac{(\delta_A/2-b)^2}{\delta_A^2/2}} dx. \qquad (3)$$

This formula represents the shaded area in part (c) of Figure 11. Above, σ_A is the standard deviation of the tolerance distribution of part A. For cases where $\delta_A > \delta_B$, use σ_B.

The calculations below will illustrate that Equation (3) will be unnecessary for this particular analysis. It should also be noted that the dimensional tolerances used in this analysis may not accurately represent the final dimensions of the designed system because many assumptions used below were quite conservative.

Calculation of τ was performed with the use of an error budget. Error budgets begin at one point and systematically account for sources of error through a device, propagating the error by statistical techniques. In this analysis, errors in the radial and tangential directions of the sprocket were considered. Figure 12 defines the necessary terminology.

In the radial direction, the analysis began at the center of the main shaft and propagated through the bearing, into the flange, then into the sprocket, then the cap, into the carrier shaft and carrier, then into the part, where the error was transformed into translational part tolerance. Analysis was necessary on only one half of the (basically) symmetric apparatus; any error occurring in the lower half may, at worst, cause the part to orient itself at an angle to the sprocket's axis of rotation. This angle can easily be calculated after performing the translational analysis.

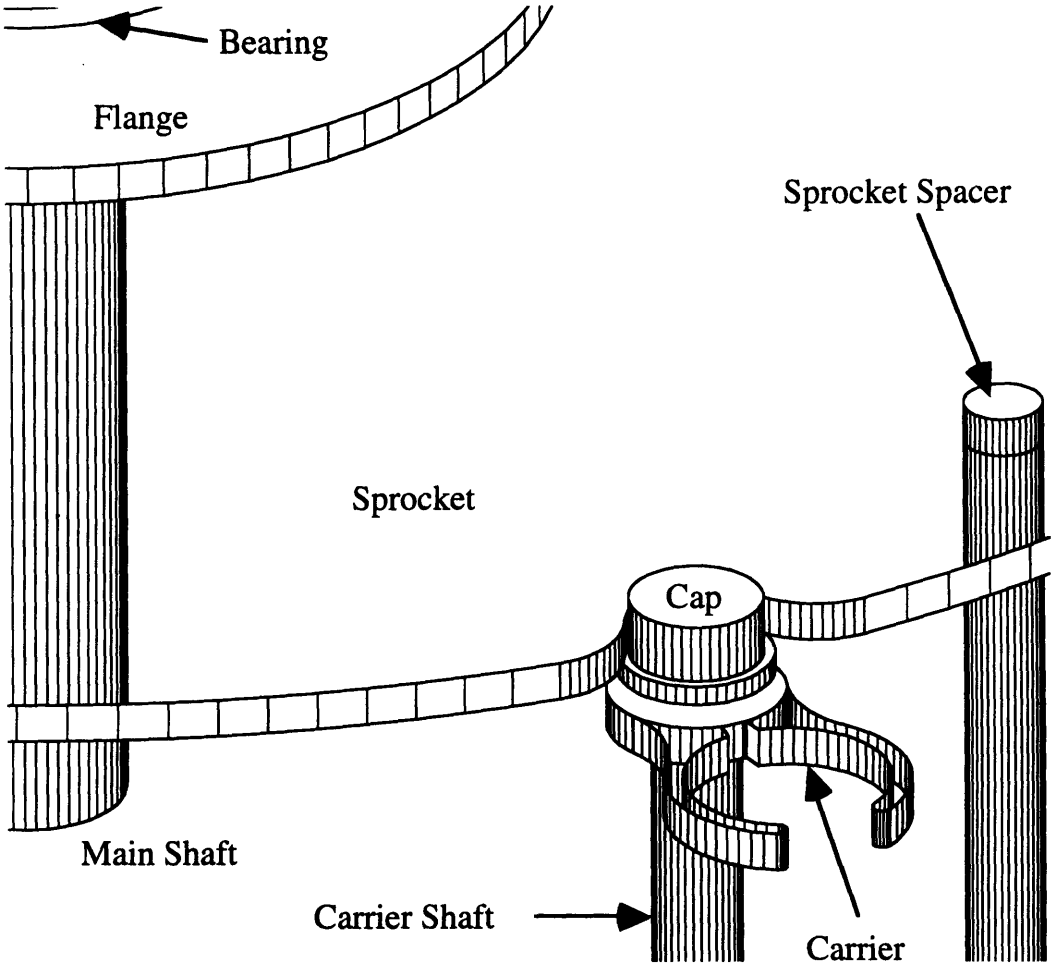

Figure 12: Definitions of terms for tolerance analysis.

Two types of translation had to be considered: play from clearance fits and play from part tolerances. Clearance fits produce a known amount of play between mating parts. Sizing tolerances account for the variability within the system. To be conservative, tolerances that generated maximum play were always used. The mean radial clearances between all the mating parts are listed below.

Main shaft/bearing clearance = 0.0002 in.
Bearing/flange clearance = 0.0002 in.
Flange/sprocket clearance = 0.0005 in.
Sprocket/cap clearance = 0.0015 in.

Cap/carrier shaft clearance = 0.0046 in.
Carrier shaft/carrier clearance = 0.0027 in.

A rough estimate of the carrier shaft's and mechanism's dimensions (Figure 13) was used in conjunction with standard clearances to arrive at the numbers above. The clearance standards used were, in order of appearance: Torrington standard [12], Torrington standard, LC4, modified ACA standard (discussed later), class 2A Unified thread standard, and LC9. Since the carrier was spring loaded, no clearance existed between the carrier and the part. The total radial tolerances between the mating surfaces of the assembly's pieces were as follows:

Main shaft/bearing tolerance = 0.0003 in.
Bearing/flange tolerance = 0.0004 in.
Flange/sprocket tolerance = 0.001 in.
Sprocket/cap tolerance = 0.001 in.
Cap/carrier shaft tolerance = 0.0049 in.
Carrier shaft/carrier tolerance = 0.0012 in.
Carrier/part tolerance = 0.0005 in.

Note that no Abbe error (the additional error incurred by rotating a part on a lever arm) existed in the radial direction. The tolerances were obtained from the same standards listed above. Additional tolerances assumed that computerized numerically controlled (CNC) mills held 0.0005 inches and that CNC lathes held 0.001 inches.

The resulting radial tolerance was calculated by combining the above errors. To attain a statistical combination (or optimistic estimate, τ_{best}) of the tolerances, the formula

$$\tau_{best} = \Sigma(\text{systematic errors}) + [\Sigma(\text{random errors})^2]^{1/2} = 0.0150 \text{ in.}$$

was used. The worst case was calculated by adding all the errors according to the formula

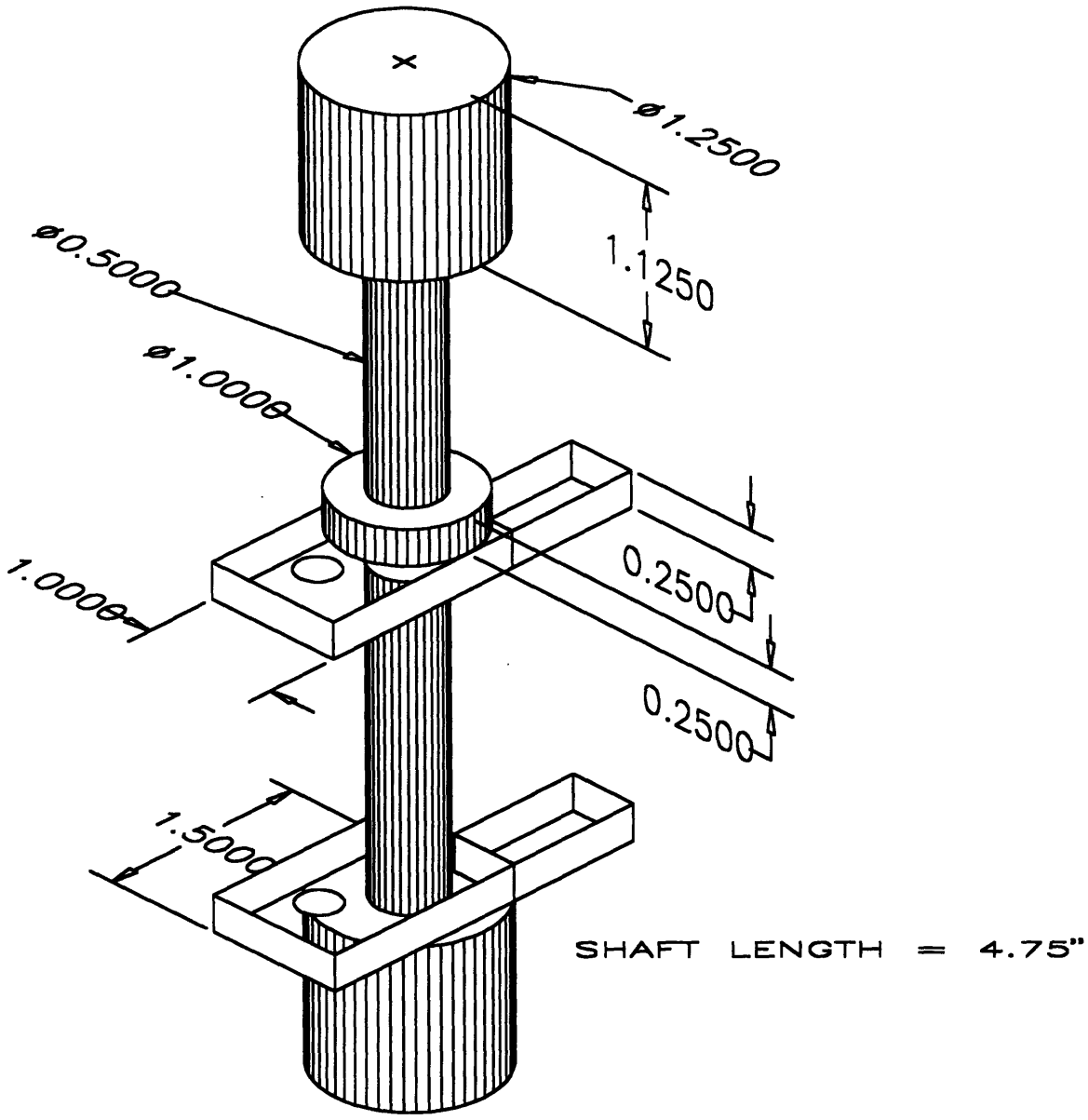

Figure 13: Approximate carrier dimensions for tolerance, weight analyses.

$$\tau_{worst} = \Sigma(\text{systematic errors}) + \Sigma(\text{random errors}) = 0.0190 \text{ in.}$$

In each of the above cases, clearance was considered systematic (unchanging) error, and tolerances were considered to be random errors. The expected tolerance value was calculated by averaging the two values above:

$$\tau = 0.5(\tau_{best} + \tau_{worst}) = 0.0170 \text{ in.}$$

Although this averaging strategy lacked a statistical basis, it has been best shown to represent engineering practice [13].

This was a somewhat conservative estimate: hand machined threads between the carrier shaft and cap could reduce the tolerance by 0.0070 inches.

Misalignment in the tangential direction was calculated in a manner similar to the radial analysis, with the following differences: 1) Abbe error had to be accounted for, 2) the error budget began at the sprocket spacers instead of the main shaft, and 3) the error budget had to account for error in the keyway connecting the carrier to the carrier shaft. In accounting for the Abbe error, some of the tolerances within the system had to be amplified by a lever arm factor F. Tangential errors due to clearance were:

Sprocket spacer/sprocket clearance = $0.0046F_1$ = 0.0048 in.
Sprocket/cap clearance = 0.0015 in.
Cap/carrier shaft clearance = 0.0046 in.
Carrier shaft/keyway clearance = 0.0027 in.
Keyway/carrier clearance = $0.001F_2$ = 0.0035 in.

F_1 was the ratio of the sprocket's pitch radius to the sprocket spacer circle radius, and equaled 1.038. F_2 equaled 3.5--the center-to-center hole distance on the carrier divided by the radius of the carrier's shaft hole. Tolerance errors are listed below:

Sprocket spacer/sprocket tolerance = $0.0059F_1$ = 0.0061 in.
Sprocket/cap tolerance = 0.001 in.
Cap/carrier shaft tolerance = 0.0049 in.
Carrier shaft/keyway tolerance = 0.0012 in.
Keyway/carrier tolerance = $0.001F_2$ = 0.0035 in.
Carrier/part tolerance = 0.0005 in.

Using the same techniques as in the radial analysis,

$$\tau_{best} = 0.0258 \text{ in.},$$

$$\tau_{worst} = 0.0343 \text{ in.},$$

and

$$\tau = 0.0300 \text{ in.}$$

The radial and tangential tolerance figures can be combined to give two important results: 1) the total possible misalignment of the system, and 2) the amount of rotation from the vertical axis these tolerances can produce. Adding the radial and tangential tolerances in quadrature gave

$$\tau = 0.0345 \text{ in.}$$

This figure is lower than τ_{max} calculated previously. Therefore the proposed system can hold most 0.3-inch diameter parts to their required tolerances through any operation, provided that the standards and assumptions above are met or exceeded. The second interpretation of these results stemmed from the need to know the offset (in degrees) from true vertical, which was easily calculated with the results above and with simple trigonometry. By assuming the part was pushed to full tolerance in one direction at the top, and to full tolerance limits in the other direction at the bottom, a formula can be set up to calculate the angular offset (given the part length L). This formula is

$$(\text{Angle}) = \sin^{-1}(2\tau/L).$$

For an L equal to 6 inches, the resulting angle was 0.66°.

4.2 Mock-Up

A detailed mock-up was created to ascertain many of the necessary considerations of the cable/carrier setup. The mock-up was created to verify the feeding concepts and to gain insight about the assembly and manufacture of the chain and its supporting structure.

4.2.1 Description

The mock-up consisted of one set of carriers attached to a carrier shaft (Figure 14), which was part of an open chain containing four shafts, three of which had no carriers. The chain was affixed to two half sprockets, each bearing five teeth. The half sprockets were attached to a main shaft. Two cams resided between the half sprockets, one for each carrier's cam follower. The shaft was press fit into a wooden base and located near a part feeding track. When the half sprockets were turned, the cam followers struck the cam and opened the carriers' jaws. Upon impacting the part, the jaws began to close and push the piece along the feed track. The jaws eventually snapped shut, finished the path through the feed track, and continued along their rotary path, holding the part.

Many of the mock-up's parts were designed to: 1) minimize weight and part count, and 2) create a setup similar in appearance to traditional manufacturing lines. Minimizing the weight reduces tensile forces and increases the line's safety. Reducing the part count not only reduces the part's weight (usually), but also reduces the part's complexity. This is a simple rule of designing for manufacture and assembly. If the line appears similar to a line currently in use, a manufacturer will be less hesitant to switch over. A line having

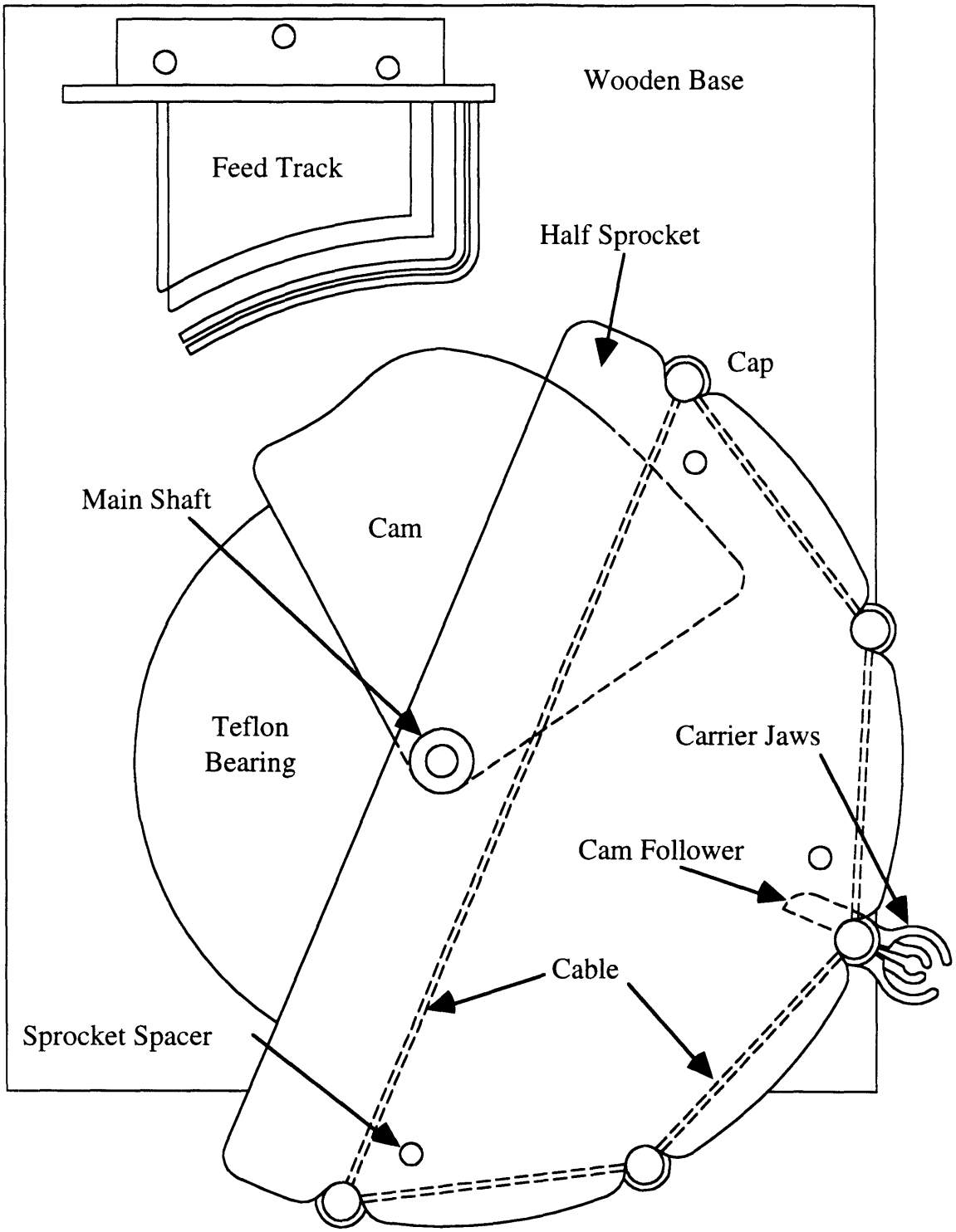

Figure 14: Schematic top view of mock-up.

many of the same dimensions as current plant layouts may reduce costs by requiring fewer replacement machines; some older machines could be retrofit with new parts.

The above principles were applied toward the creation of a lightweight, easy-to-assemble set of carriers. Figure 15 displays the carriers as conceptualized in Chapter 3. These carriers were to be originally produced from stainless steel because of its resistance to corrosion and wear. However, stainless steel is not only heavy, but difficult to machine. It was then decided that aluminum anodized with a Teflon™ impregnated ceramic would reduce not only weight, but also reduce wear and assembling complexity.

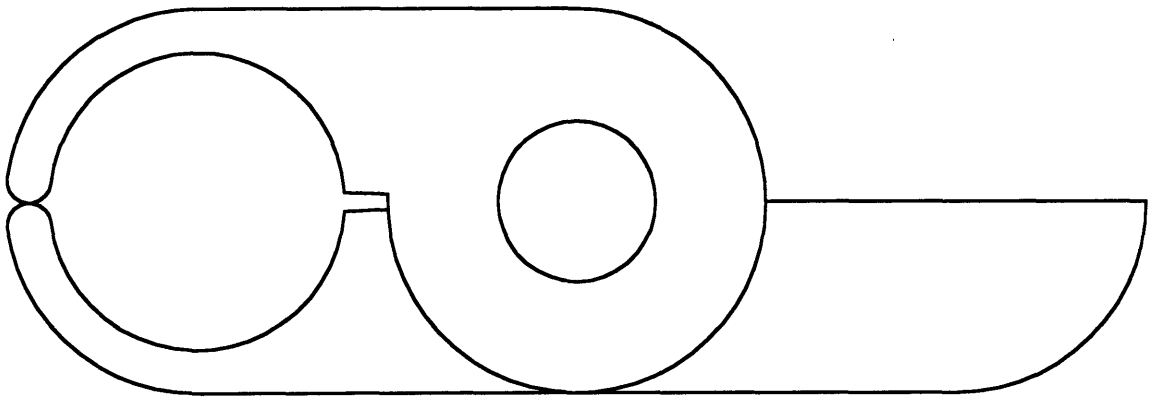

Figure 15: Carrier design concept.

To reduce additional weight, many unnecessary areas within the carrier were eliminated. For example, the jaws were shortened as demonstrated in Figure 16. Parts (a) and (b) of this figure show carriers grabbing parts with jaw length corresponding to zero and one-hundred-eighty-degree gripping angles. The shaded region beneath each figure shows the amount of area being effectively

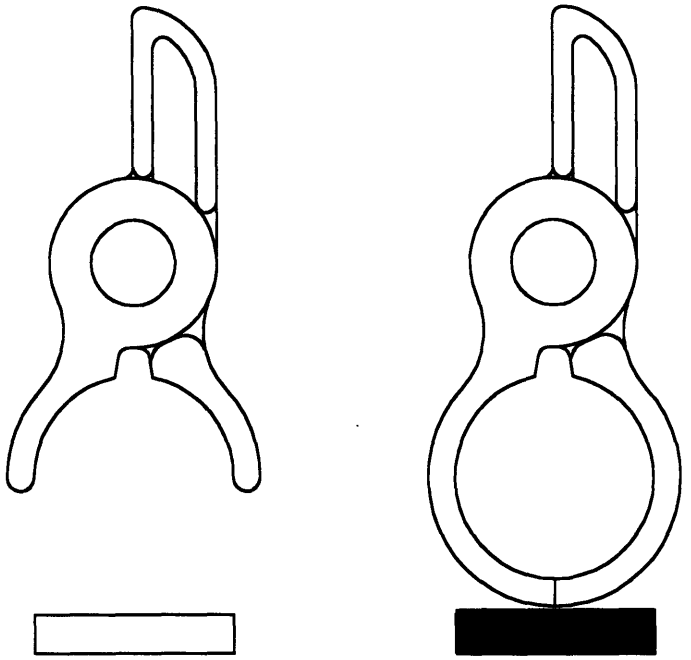

(a): 0 degrees,
0.0% grabbed

(b): 180 degrees,
100% grabbed

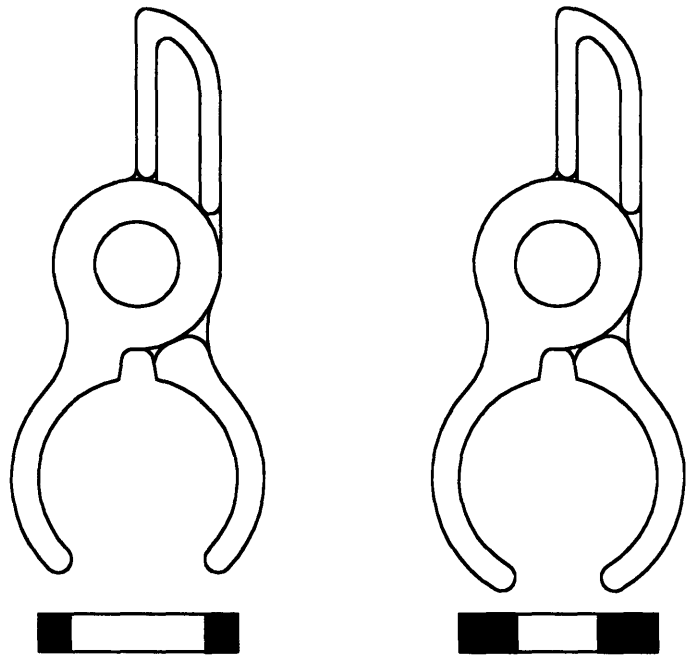

(c): 90 degrees,
29.3% grabbed

(d): 120 degrees,
50.0% grabbed

Figure 16: Demonstration of carrier weight reduction methods.

restrained by the jaws. In part (c), the jaw lengths correspond to an effective gripping angle of ninety degrees (forty-five on each side). At least half of the part's projected area must be in contact with the jaws to maintain a stable resistance to pullout forces. It can be seen that the shaded region restrains less than half of the part's projected area. To assure this and to minimize weight, the carrier in part (d) was chosen. Note that additional areas were also removed if they provided little or no carrier strength.

Figure 17 shows the disassembled carrier halves. Each half had a small (0.0625-inch) stainless steel dowel pin pressed into the reamed holes on their top surfaces. A rubber band made from slices of surgical tubing and placed on the pins pulled the carrier halves closed. The stationary carrier half (top of Figure 17) was affixed to an aluminum tube by another stainless steel dowel pin. The moving carrier half mated with the stationary half, and the two parts were closed together by press fitting an aluminum cap over the shaft, both of which were hand turned on a lathe.

Each carrier shaft was drilled radially in two places. A pair of solid 0.0625-inch diameter polyethylene rods flexible enough to act as cables were threaded through the shafts. The shafts were secured to the cable by crimping modified wire end attachments on either end of the shaft. The appropriate pitch under tension was achieved by crimping the wire ends while the carrier assemblies were fitted between the sprocket teeth and the cable was under tension. Two turnbuckles attached to the cables' ends provided the tension.

As mentioned previously, only half sprockets were used both to save material and to permit easier access to the mock-up's inner

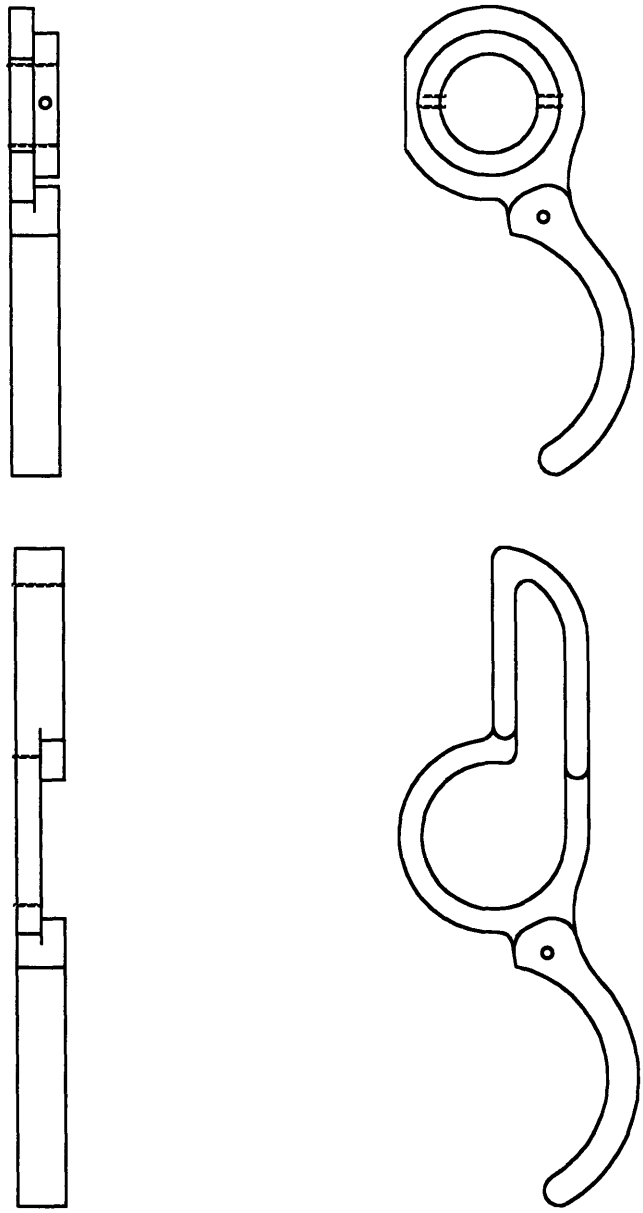

Figure 17: Disassembled carrier halves.

workings. The sprockets were created simultaneously from two 0.25-inch polyvinyl chloride (PVC) sheets fastened together. The sprocket was drawn using AutoCAD® and printed full scale, then taped to the PVC sheets. The outline was roughly cut with a bandsaw, then belt sanded to closer tolerances. The area between the teeth was cleared using a 0.75-inch dowel sander. Teflon™

spacers and bearings on either side of both sprockets permitted the sprockets to rotate freely about an aluminum shaft placed through their center. A cap screw secured the entire assembly to the shaft. To assure that the sprockets both rotated in synchronization and remained a fixed distance apart, three sprocket spacing rods were machined and press fit into holes in each sprocket. These rods had precisely spaced shoulders upon which the sprockets rested. Not only did the rods have to clear both the cams and the cables, but also they could not interfere with the carrier as it opened.

The cams were constructed in much the same way as the sprockets. First, the cam was drawn on AutoCAD®. The carrier opened over a seventy-five degree span, and closed over thirty degrees. This was done to compare the effects of engagement lengths. A spline curve interpolated through the initial carrier position, the final desired position, and three desired positions in between for both the approach and the departure to generate the cam shape. In addition, 0.5-inch radius fillets smoothed both corners. The cams were machined together from two sheets of 0.75-inch plywood, roughly outlined on the bandsaw, then belt sanded to their final shape. Two flanges bolted into the cams and secured themselves to the main shaft by four set screws. Aluminum spacers and steel washers separated the sprockets, cams, and flanges by the appropriate distances.

This entire assembly mounted into a wooden base that also housed the part's feed track. The track looked very similar to the one in Figure 5, except that it was made from Plexiglas™ and bolted to an angle mounted to the base.

4.2.2 Recommendations

The mock-up successfully proved that parts could be fed into a cable/carrier system at relatively high speeds. In addition, it assisted in formulating a series of recommendations that would further improve the design. Many of these recommendations are addressed in more detail in later sections. However, some design changes can be easily intuited, and are categorized by part below.

Carriers. As suggested by their level of detail, these devices require the greatest attention. For example, moving the springs to the carriers' undersides (the sides opposite the caps) would eliminate the need to design the feed track and caps so as to not interfere with the springs. However, further clearance analyses should be performed. Another variable to be considered further is the distance between the cap and the jaws' centers. As will be discussed later, keeping the part close to the center increases its probability of a successful feed. On the other hand, sufficient space for both a rigid feed track and for axial part asymmetries is also required. Next, the stationary carrier half should be designed a few thousandths of an inch higher than the mobile carrier half to allow for the cap to contact a surface directly, axially locating both carriers and caps; also, the mobile half can rotate without significant interference from the cap. Additionally, increasing the length of the carriers' cam followers will allow for a shorter cam and give more space to the sprocket spacers. Yet another improvement can be seen by adding a key to the stationary carrier half to prevent rotation without using a dowel pin.

Carrier Shafts. Clearly a simple tube no longer suffices for a carrier shaft. First, the dowel pin can be replaced by a shaft shoulder and keyway, both of which locate the part axially and prevent rotation, along with reducing the part count and facilitating assembly. If the shoulders are machined into the shaft accurately with appropriate fillets on the mating parts, axial accuracy will also increase. Second, threading each end and screwing on the caps will be easier to assemble.

Caps. Along with tapping the caps' centers, the cap should be reshaped to 1) reduce friction on the moving carrier half while continuing to hold it in place, and 2) center the carrier shaft between the sprockets despite conditions that attempt to misalign it. Further analysis is required.

Cams. A smaller cam radius would allow the sprocket spacers more positioning room to clear the cables, carriers, and cams. Also, the cam opening and closing pattern should be rethought to make the transitions smoother.

Sprockets. Flanges and roller bearings installed on the sprockets would provide less rotation resistance. The sprocket should also be thicker or made from a different material to stiffen it.

Cable. The cable's design requires rethinking to increase flexibility, modulus, yield strength, and creep resistance.

After the mock-up, more detailed design calculations went into creating the prototype.

4.3 Calculations

Several factors had to be accounted for before design began. Techniques for minimizing part impact when feeding are addressed in the first subsection. Subsection 4.3.2 calculates the magnitude and direction ranges of the cable's tension. Subsection 4.3.3 addresses how this tension heavily influences the system's dynamic response to forced vibrations. Subsection 4.3.4 examines how the same phenomenon that forces the system to vibrate also increases impact energy. Fatigue is addressed in subsection 4.3.5. High speed galling is mentioned briefly in subsection 4.3.6. Lastly, subsection 4.3.7 summarizes the major conclusions from each of the previous subsections.

4.3.1 Feeding

Simulation of feeding the parts into the transfer mechanism was difficult to determine analytically since several pieces and their interactions had to be accounted for, including the sprocket, the cam, the carrier, the part, and the part guide. Most of the concept's proof was best handled by the detailed mock-up; however, some simple calculations produced additional limitations and recommendations.

The main concern in part feeding was the part's reaction when speeds began to increase and impact forces tended to propel the parts out of control. A simple, conservative constraint was placed on the maximum feed rate. This was done by modeling the pen and carrier as a round surface and a wall, respectively, impacting. The carriers, propelled by the motor driven sprockets, impact the pens at a linear velocity $d_P\omega/2$ (d_P is the pitch diameter, in., and ω is the angular velocity, rad/s). The pens were considered to be initially

horizontal, resting on stops, and were struck vertically. Since the carrier was driven by a motor, it was modeled as an infinite mass, or wall. In the case of a perfectly elastic collision, a reference frame on this moving "wall" would see a pen moving toward it at a velocity $d_P\omega/2$, colliding, then moving away from it at the same velocity. Reverting to a stationary reference frame, the final pen velocity would be $d_P\omega$.

The collision, however, is not perfectly elastic, and is most easily modeled using a coefficient of restitution e, defined as

$$e = \frac{(v_{2f})_n - (v_{1f})_n}{(v_{1i})_n - (v_{2i})_n}. \tag{4}$$

In the equation above, v represents velocities, the subscripts i and f represent the initial (before collision) and final (after collision) states, respectively, the subscript n signifies the normal component (the line drawn between two impacting sphere centers) of the impact, and the numbers identify the two impacting bodies. This coefficient varies with the relative impact velocity, yet typically tapers off to a minimum at high velocities. For aluminum impacting aluminum, e = 0.6; for plastics on plastics, e = 0.7. When two bodies of differing materials collide, a new coefficient of restitution arose, defined by the formula

$$e = \frac{e_1E_2 + e_2E_1}{E_1 + E_2}. \tag{5}$$

E is the elastic modulus of the colliding materials (E_{Al} = 10.3 Msi, $E_{Plastic}$ = 3.77 Msi). For an aluminum carrier hitting a plastic pen, e = 0.67. The coefficient of restitution, when applied to the collision, reduces the final impact velocity to $0.84d_P\omega$.

If the pen is struck vertically and no track exists to slow its progress, it will rise a certain height h before gravity reverses its direction. Conservation of energy equations combined with the final impact velocity reveal h to be

$$h = 0.35(d_P\omega)^2 / g, \qquad (6)$$

where g is the acceleration of gravity (in./s^2). For a pitch diameter of eighteen inches, similar to the mock-up, the following table emerges:

Table II: Resulting Unconstrained Pen Travel vs. rpm

rpm	ω (rad/s)	h (in.)
10	1.05	0.321
25	2.62	2.01
50	5.24	8.02
100	10.5	32.1
200	20.9	128.
500	52.4	802.

Clearly, any appreciable sprocket velocity requires some means of restraining the pen after impact.

Directly after impact, the part wishes to travel tangentially from the sprocket. A track placed along the circular path followed by the carrier would constrain the part to trace the same path as the carrier because the part would hit the outer edge of the track, rebound, then continue toward the inner edge. This cycle repeats itself until a) the part leaves the track, or b) the part slows enough to be grabbed.

The reliability of feeding depended on several factors: the sprocket speed and diameter, the radius of the track's (and the carrier's) path, the track to part clearance, and the track's material, among others. At high velocities, it was desirable to slow the part's

speed to the point where the carrier half's spring could close on it. (A strong spring would obviously increase reliability.) In addition, it was desirable to create a track that maximized the number of impacts and slowed the part substantially with each impact, which would be achieved by minimizing the carrier path's radius and reducing track to part clearance--these changes would force the part to impact the track's sides more frequently. In typical high-volume manufacturing lines, feed tracks are either made from a non-rigid material or spring loaded so that part jams from track friction do not occur. Also, track materials with low coefficients of restitution, such as brass, cast iron, lead, or plastic should be used to decrease the part's final velocities.

4.3.2 Tension

ACA sprocket design standards, discussed later, allow for proper cap engagement into the sprocket with chain pitch misalignments as high as eight percent. Chain standards, however, can only be applied to misalignments in the sprocket's tangential direction. As discussed before, roller chains travel in only one plane, the plane of rotation; in the system discussed herein, the cables allowed movement out of the plane of rotation. By adding this convenience, additional cap engagement problems inevitably arose. Figure 4 presented earlier showed a plan view of the cable/carrier system with sprockets whose axes of rotation are perpendicular. As can be seen, the chain travels in a direction skewed from the sprocket's plane of rotation, and as a result, axial forces, axial displacements, and higher radial forces affect the engaged cap as it enters and leaves the sprocket. As the distance between sprockets

decreases, the cables have to travel more and more out of plane to engage properly with the sprocket teeth.

The design of the cap, and perhaps the entire carrier mechanism, depended on the magnitude and direction of the cables' tensile force as they engaged and disengaged the sprocket. An estimate of the tension was calculated by beginning with a roller chain of the approximate dimensions of the cable/carrier mechanism. The chain's weight per unit length w (lbm/in.), recommended sprocket span S (in.), and recommended tension were used to obtain rough sag-to-span ratios for chains. This ratio, along with the same span and new w, provided enough information to back out a recommended tension for the cable/carrier system. Then, using approximate sprocket and carrier geometries and a conservative (small) sprocket span, the tension's direction was calculated for later use.

Magnitude. The recommended tension T (lbf) for a roller chain follows the formula

$$T = 125P^2, \tag{7}$$

where P is the chain pitch (in.). Recommended optimal sprocket spans range from thirty to fifty pitches. Spans below thirty pitches overexpose the chain's rollers to sprocket tooth forces; and spans exceeding fifty pitches develop chain whip, poor sag to span ratios, and other dynamically malevolent properties. To minimize sag to span, a span of thirty pitches was chosen.

Literature covering catenary curve shapes [14] states that the sag y (in.) divided by 0.5S, half the span, can be plugged into the formula

$$2y/S = (\cosh z - 1) / z \quad (8)$$

to create a useful dimensionless variable z. Z is useful because it can be converted to and from the dimensionless variable wS/2T (where w is the chain's weight per unit length, lbm/in.) via the equation

$$wS/2T = z / \cosh z. \quad (9)$$

Equations (7) through (9) can be used in conjunction with a chain whose weight per unit length is similar to that of the cable/carrier chain to arrive at a recommended tension. W for the system was calculated from dimensional assumptions in Figure 13. Also, each carrier was assumed to be connected by two 0.125-inch diameter 7 × 7 steel aircraft cables, each weighing 0.00221 pounds per inch. Below are the remaining weights:

Cap weight = 0.135 lbm
Shaft weight = 0.0768 lbm
Carrier weight = 0.0472 lbm
Collar weight = 0.0192 lbm

The total weight per unit length (calculated assuming a two-inch pitch) equaled the sum of the cap weight, the carrier weight, the cable weight, and half the shaft and collar weights. The assumed system weighed 0.232 pounds per inch, which roughly equaled that of a roller chain with a 1.25-inch pitch.

A 1.25-inch pitch roller chain has a recommended tension of 195 pounds and a weight per unit length equal to 0.209 pounds per inch. For a span of sixty inches (derived from thirty pitches of a two-inch pitch cable chain), wS/2T = 0.0321. Inserting this number into Equations (8) and (9) gave z = 0.0321 and 2y/S = 0.0160. The tolerable sag to span ratio, y/S, equaled 0.00803.

Using the y/S above and w for the cable/carrier chain (and sparing the additional calculations), the recommended tension for the cable/carrier system became 217 pounds, i.e.,

$$T = 217 \text{ pounds.} \tag{10}$$

Direction. The direction of the tension was crucial in determining the components in the axial and radial directions. Figure 18 shows each of the three components of the tension acting in the directions assumed to be positive. Figure 19 zooms in on this force vector and defines the angles used in locating the tension's direction. Any two angles listed, combined with the magnitude, can define the remaining two angles by the relations

$$\tan \theta_3 = \tan \theta_2 \sec \theta_1 \tag{11}$$

and

$$\tan \theta_4 = \tan \theta_1 \cos \theta_3. \tag{12}$$

As demonstrated below, all four angles had significant reasons for being calculated.

Figure 4 is repeated again in Figures 20 and 21 with labels. Figures 22 and 23 break the polygon of interest out of each view and show the labels more clearly. Here, d_P is the pitch diameter (in.), S is the sprocket span (in.), and a is the separation between sprockets (in.). Additionally, two dummy variables u and v were included to facilitate calculations. It should be noted that all the Figures 20 through 23 are projections of the system onto the plane of the paper. This explains the need for using the angles θ_1 and θ_3 instead of θ_2 and θ_4. Beginning with the polygon of Figure 22, the equations

$$\tan \theta_1 = 2u/a, \tag{13}$$

$$\sin \theta_1 = 2u / [(1 - v)d_P], \tag{14}$$

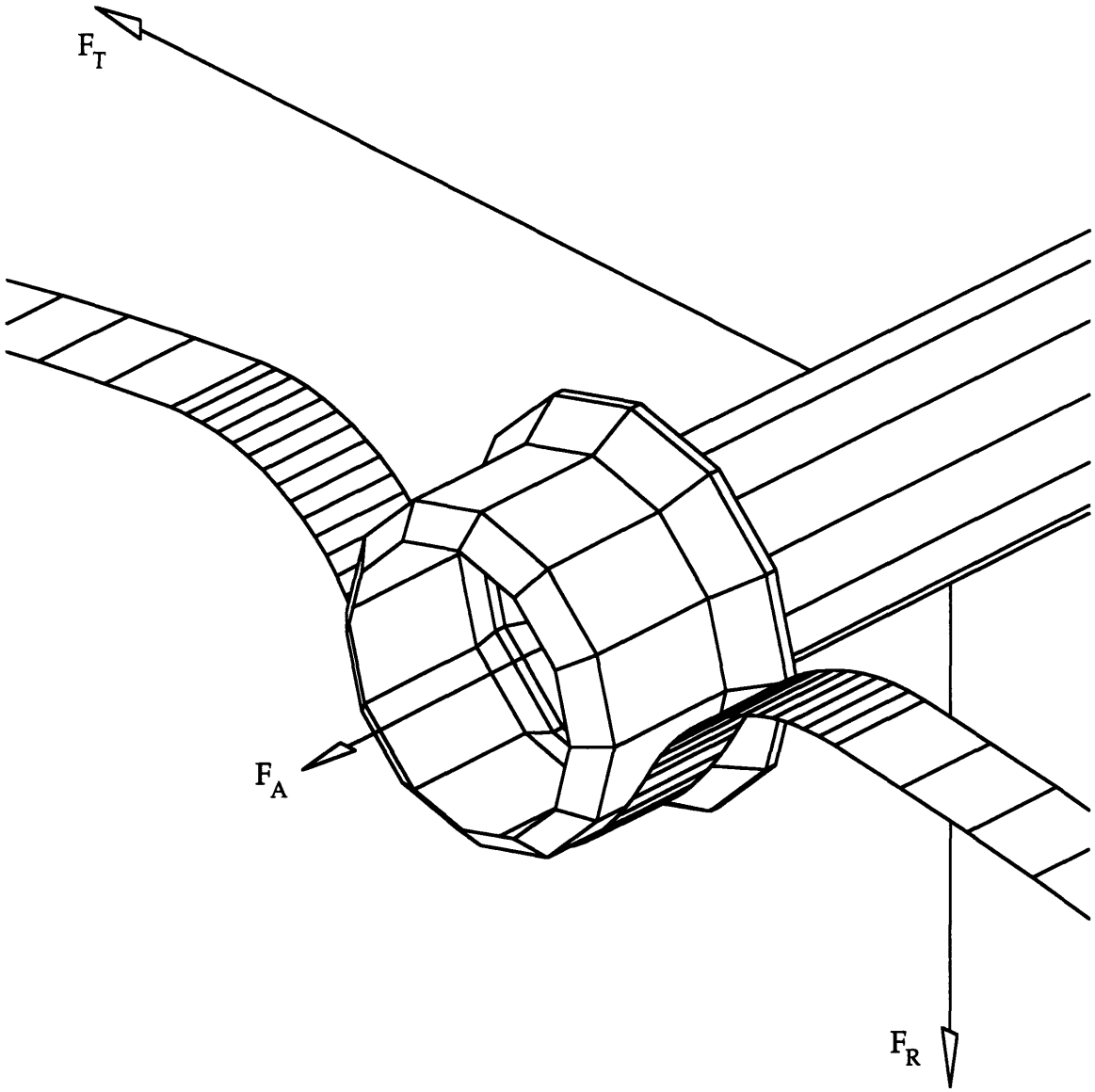

Figure 18: Definitions of the positive radial, tangential, and axial net forces imposed on the carrier by cable tension.

and

$$2(S - u)\sin\theta_1 = vd_P \qquad (15)$$

were derived. Combining these equations eliminated u and v to produce

$$\cos\theta_1 - (2S/d_P)\tan\theta_1 + \tan\theta_1\sin\theta_1 - a/d_P = 0, \qquad (16)$$

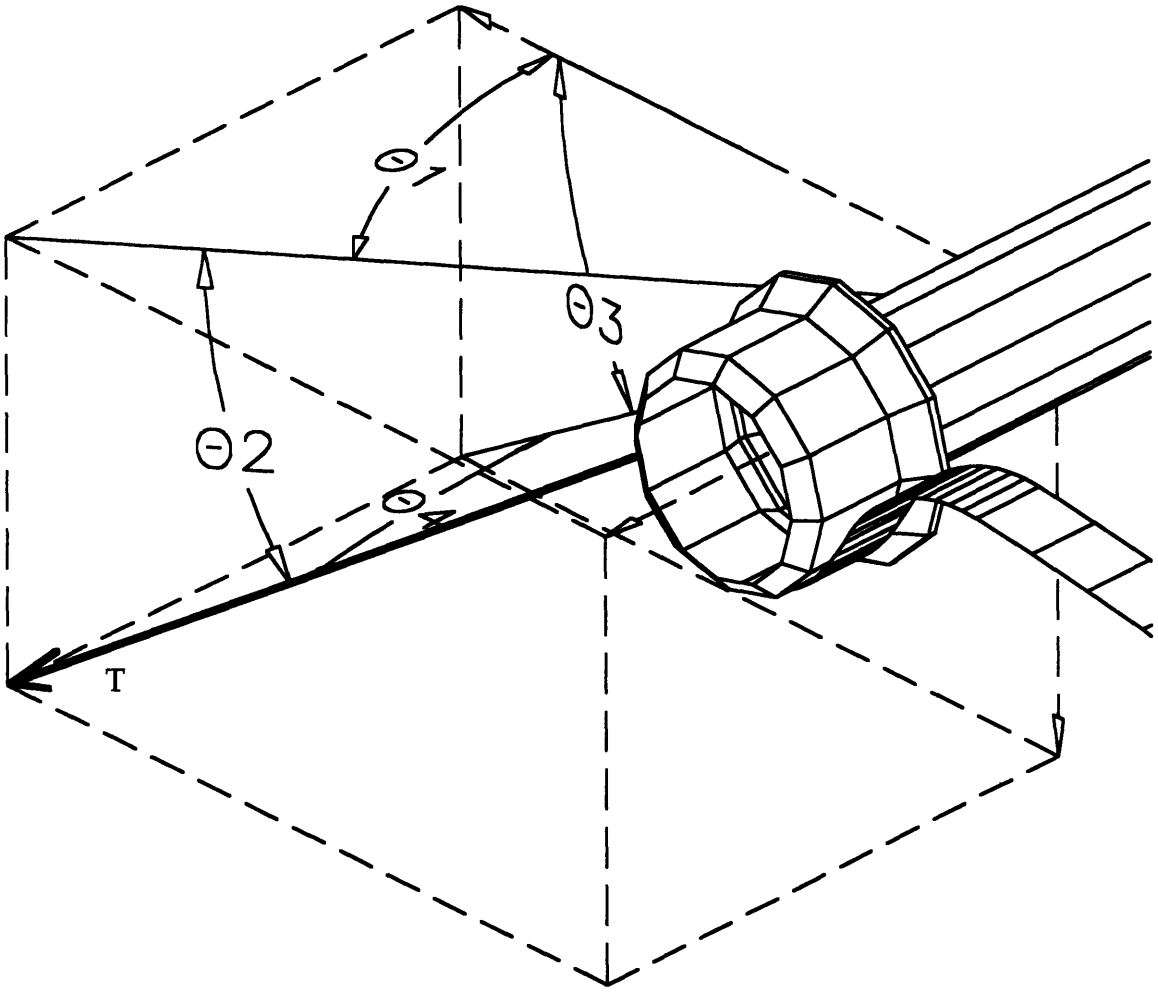

Figure 19: Definitions of θ_1 through θ_4, used in various analyses.

from which root finding techniques produced θ_1. This same technique yielded θ_3 of Figure 19. However, the side view of the system failed to account for any sag within the cable, so θ_3 had to be corrected.

Within the vertical plane of the cable, it was assumed that the cable's endpoints were of equal height, that an origin existed at the lowest (middle) point of the cable, and that y and x were defined as in Figure 24, within the plane of the cable. The equation describing the cable's shape was

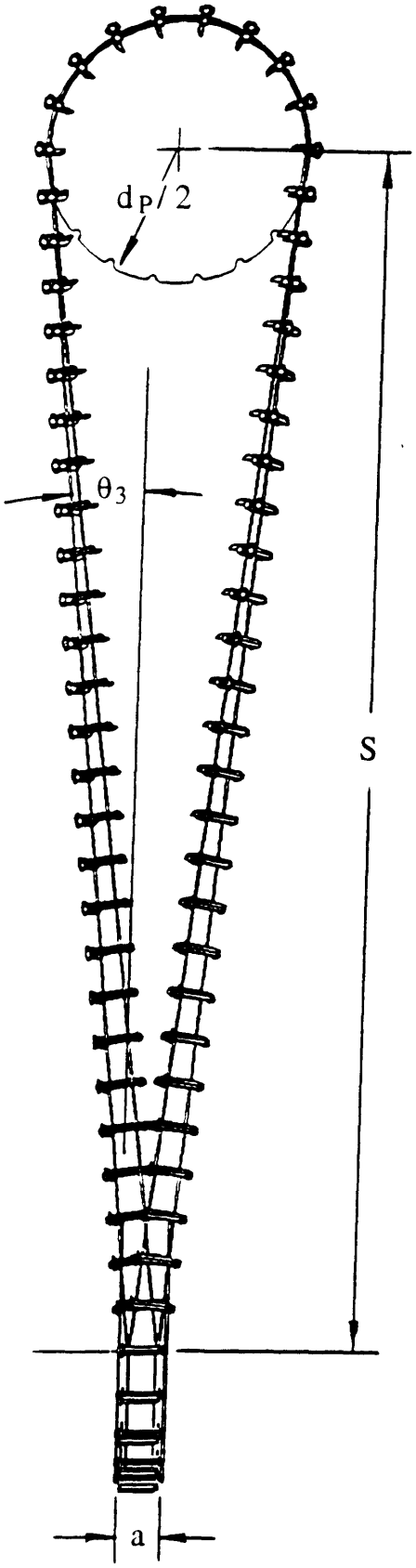

Figure 20: Side view of perpendicularly oriented sprockets.

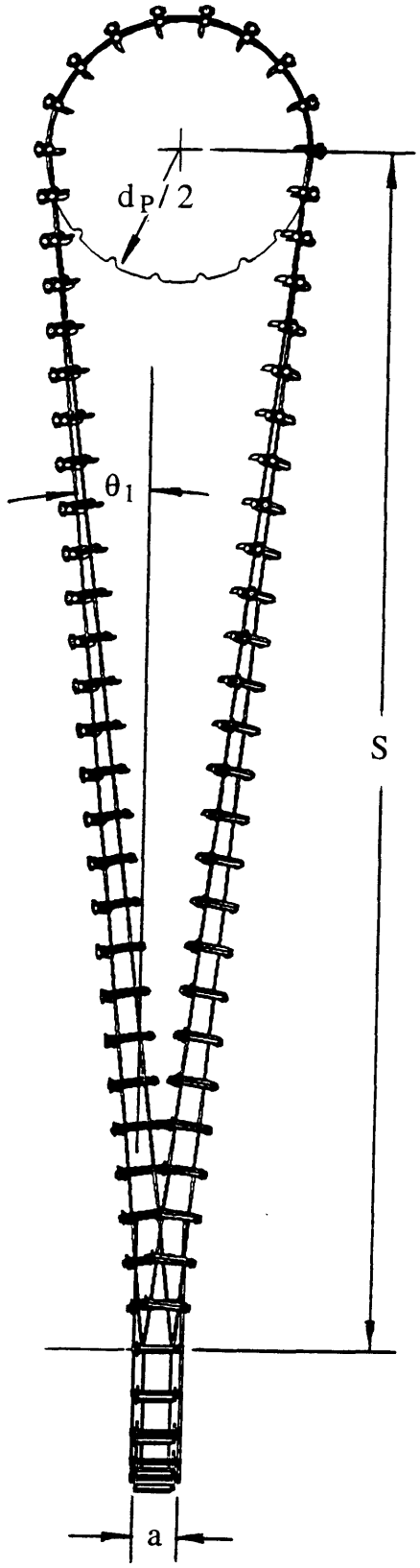

Figure 21: Top view of perpendicularly oriented sprockets.

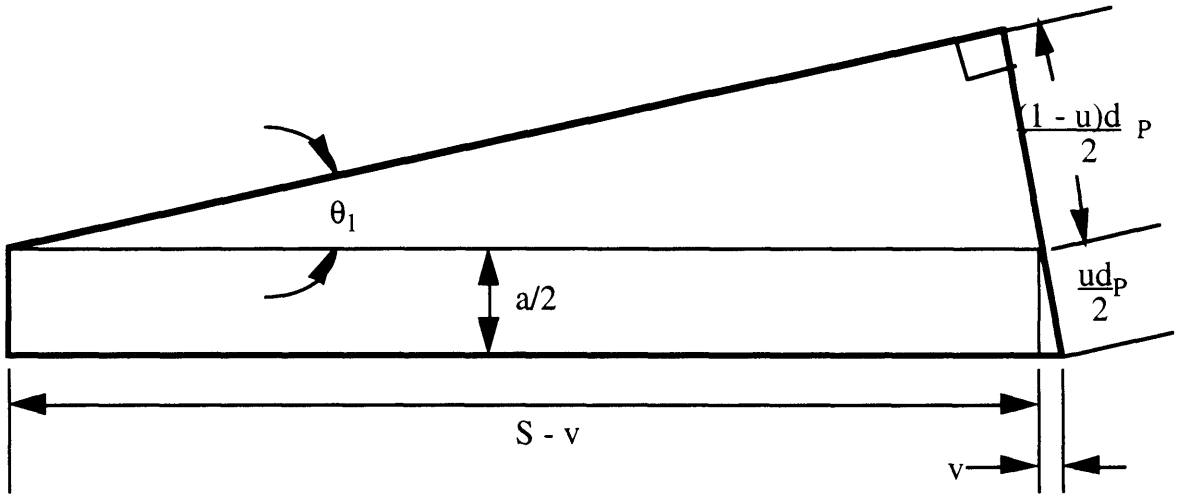

Figure 22: Isolated polygon from Figure 20, used to calculate θ_1.

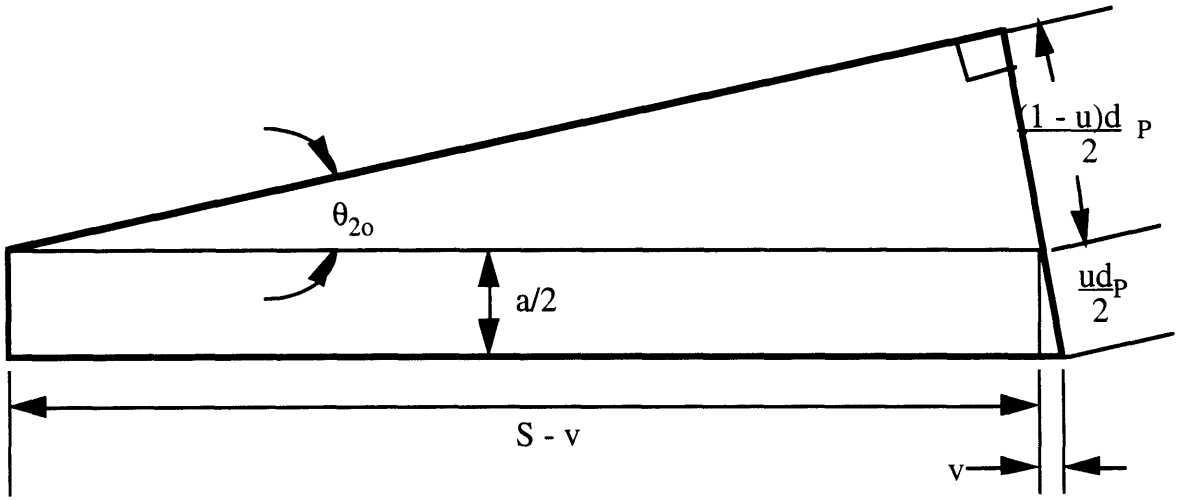

Figure 23: Isolated polygon from Figure 21, used to calculate θ_{2o}.

$$y = (x/z)\cosh z, \tag{17}$$

where z maintained its previous definition. β was defined as the angle from the horizontal to the cable, represented by

$$[\beta = \tan^{-1}(\Delta y/\Delta x)]_{x = S/2}. \tag{18}$$

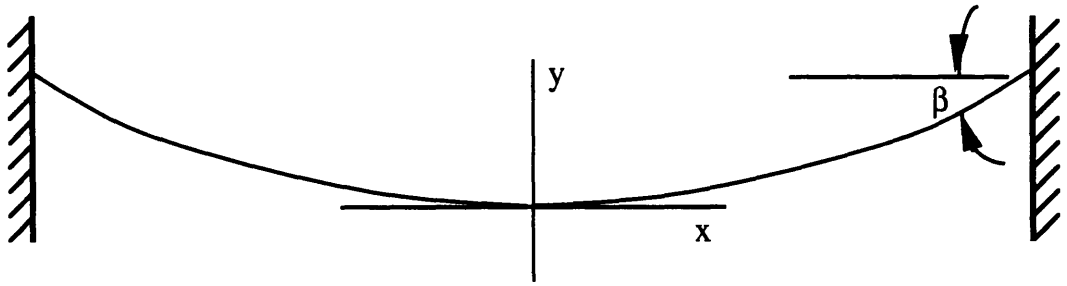

Figure 24: Definitions of x, y, β for determining cable sag.

The approximate derivative is shown since numerical methods were used to calculate this angle.

Since β was defined within the plane of the cable, geometry showed that

$$\theta_2 = \theta_{2o} + \beta, \tag{19}$$

where θ_{2o} was calculated from θ_1 and θ_3 assuming no cable sag, and using Equation (11). Note that the true θ_3 had to be recalculated after θ_2 had been derived.

With each of the four angles of Figure 19 then available, the tension was broken into its radial (F_R), tangential (F_T), and axial (F_A) components. Force balances derived from Figure 25 yielded the components:

$$F_R = T[\cos \theta_4 \sin \theta_3 + \sin (180/N)] \tag{20}$$

$$F_T = T[\cos \theta_3 \cos \theta_4 - \cos (180/N)] \tag{21}$$

$$F_A = T \sin \theta_4. \tag{22}$$

N was the number of sprocket teeth. These numbers became very useful, especially when designing the caps.

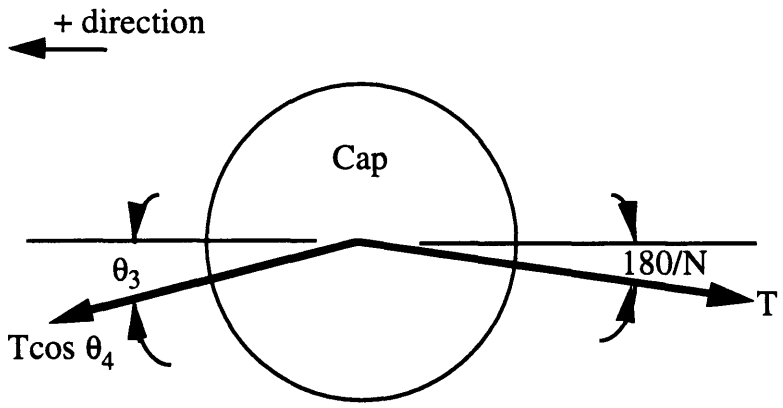

Figure 25: Projections of the tension forces onto the cap.

4.3.3 Dynamics

Past analyses [15] of rotating chain paths have concluded that a chain link can travel two different ways: at a low speed periodic rate or at a high speed straight rate (Figure 26). The low speed rate is more prone to periodic motion, resulting in resonance and possible chain jumping; therefore it is necessary to establish whether the system must occasionally operate in the low speed regime. The term differentiating low speeds from high speeds is the highest natural frequency the chain can obtain; for this reason an analysis of the chain's natural frequency is required.

Binder and Mize [16] derive a set of relations that approximate the natural frequencies for a simplified roller chain. As it turns out, the simplifying assumptions better approximate the cable/carrier chain than a roller chain. The chain is replaced with a massless cable in tension between two parallel sprockets; n masses located P feet apart lie along the cable's length. The number n does not include the carriers within the sprockets. The cable tension T (lbf) is assumed constant throughout the chain. Vibrations within the cable are not

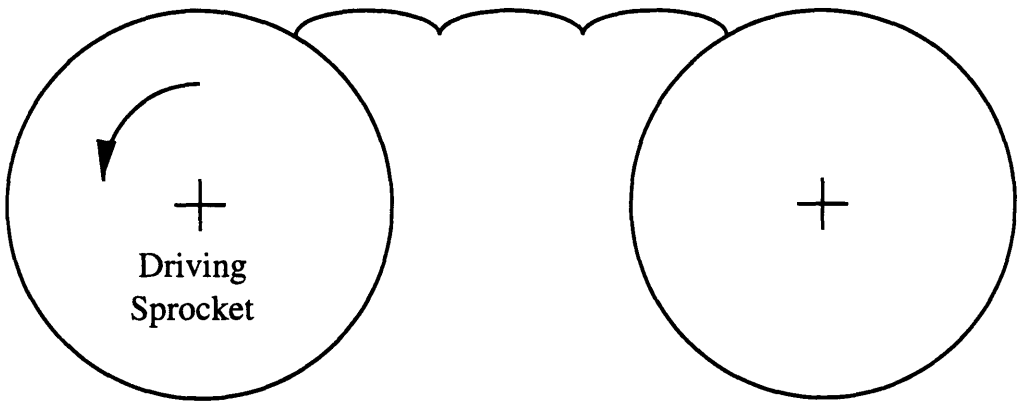

(a) Low speed carrier path.

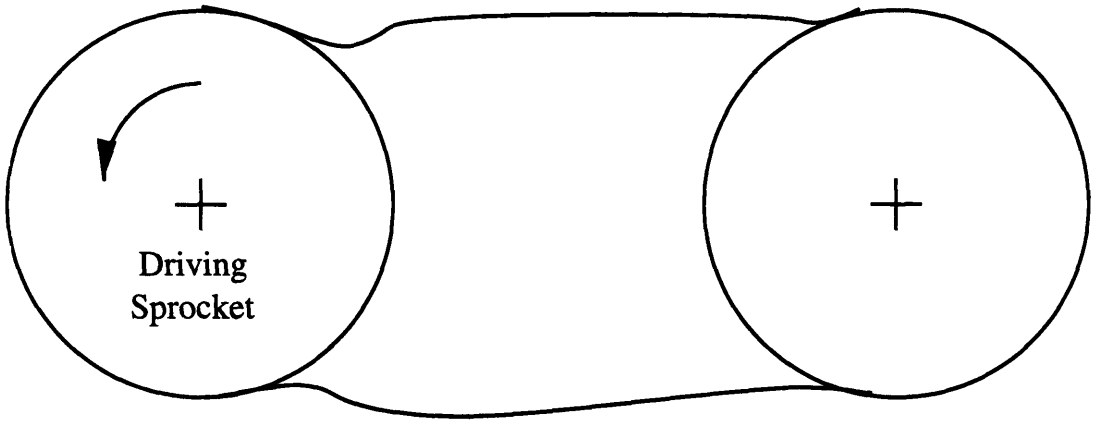

(b) High speed carrier path

Figure 26: Low and high speed carrier paths between sprockets.

damped and occur only within the plane parallel to the plane of the sprockets. Sparing the derivations, the natural frequency of vibration f_s is:

$$f_s = \frac{1}{\pi}\sqrt{\frac{T}{Pm_c}}\sin\frac{s\pi}{2(n+1)}, \qquad (23)$$

where m_c is the mass of each carrier assembly and its neighboring cable in slugs. Here, s is any integer from 1 to n, representing the

first (fundamental), second, etc., natural frequencies of the cable. Of course, in a real system, there are an infinite number of harmonics, but to a close approximation only n harmonics are of importance. The highest natural frequency, f_n, occurs when s = n, and equals:

$$f_n = \frac{1}{\pi}\sqrt{\frac{T}{Pm_C}}\sin\frac{n\pi}{2(n+1)} \approx \frac{1}{\pi}\sqrt{\frac{T}{Pm_C}}. \qquad (24)$$

The final term in the equation can be used when n is large.

Even if conditions existed to minimize this frequency, such as low tension (200 pounds) and a high pitch (6 inches), the highest natural frequency occurs at roughly 53 Hz. A thirty-toothed sprocket that forces vibrations at every tooth must exceed 110 rpm to damp out this frequency. With carriers between every tooth, a sprocket spinning at 110 rpm would pick up approximately 3200 parts per minute; ten-toothed sprockets would have to spin at 320 rpm, again corresponding to approximately 3200 parts per minute. Since it is likely that the system will operate below this frequency, the low speed chain path described above should be conservatively assumed for any possible system configuration.

The low speed path a carrier would follow is depicted in Figures 26 and 27. In the second of the two figures, the shaded carrier at the center, point A, is attached to the other shaded carriers. The sprocket is assumed to be turning from right to left. As it turns, the line connecting the carrier at point A to the one at point B remains horizontal, and drops with the carriers until point C is reached. From here, the rightmost carrier engages with the sprocket and rotates to point A, where the cycle repeats itself. This periodic

carrier motion is known as chordal action. Its amplitude A_C is defined by the equation

$$A_C = \frac{P[1-\cos(180/N)]}{2\sin(180/N)}, \tag{25}$$

and its frequency equals (Nn/60) Hz, where all the variables above hold their previous definitions. Chordal action not only induces a forced vibration on the chain, but is also responsible for excessive sprocket noise during operation. Consideration of these effects is addressed in subsection 4.3.7.

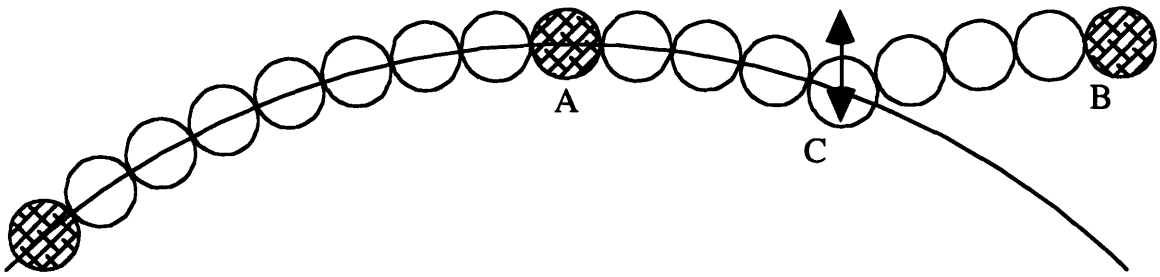

Figure 27: Graphical explanation of the carrier's path.

4.3.4 Impact

The noise produced by a rotating sprocket is caused mainly by the sprocket's chordal action creating successive impacts between the carrier caps and sprocket. Besides noise, these impacts damage the caps and sprocket, adversely affecting how smoothly the sprocket can effectively engage, which may also lead to other undesirable conditions such as breakage, heating, and wear.

Analytical work on the study of impact between chains and sprockets has been presented by Binder and Covert [17], who state that correlation between impact and chain life is only empirical so far, but the damaging aspects of impact appear to be related to the

impact's kinetic energy. If this is the case, it becomes necessary to determine the relative velocity and effective mass of impact.

Figure 28 shows the roller positions used in calculating two possible relative velocities. This relative velocity occurs between the carrier cap's center and the point of impact on the sprocket. In the first analysis, this point is assumed to be the point on the sprocket's pitch circle that is coincident with the cap center after impact. The second analysis' point of impact lies at the base of the sprocket seat, along the radial line connecting the cap center and the sprocket center after impact. In the instant before cap A hits the sprocket, its velocity vector V's magnitude equals that of cap B, specifically,

$$V = \pi d_P n \tag{26}$$

in the direction shown. On the sprocket, the (first) point mentioned above has a velocity magnitude V' equal to the same as V, but in the upward direction shown. Adding these two vectors would produce a rough estimate of the relative impact velocity $V_{I,1}$. It is equal to

$$V_{I,1} = 2V\sin(\alpha/2) = 2\pi d_P n \sin(180/N). \tag{27}$$

Combining this equation with Equation (35), discussed later, gives

$$V_{I,1} = 2\pi n P, \tag{28}$$

independent of the pitch diameter.

Figure 29 shows the velocity vectors represented when impact occurs at point x, the second assumed point. The relative velocity of the carrier center remains the same, but now the velocity of point x equals

$$V_x = \pi(d_P - d_R)n, \tag{29}$$

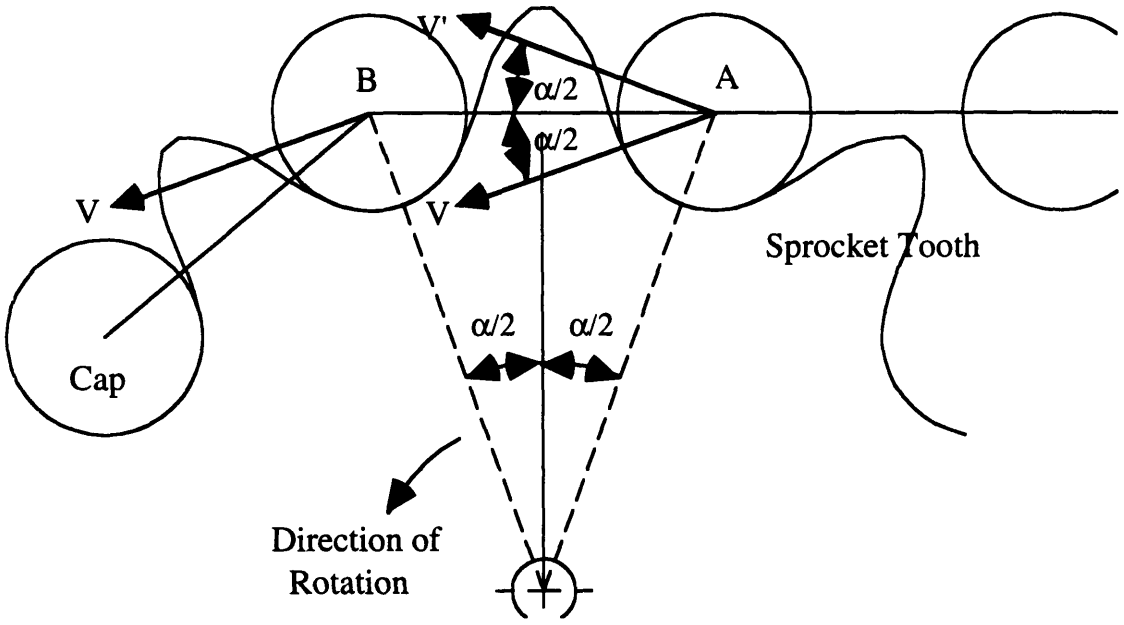

Figure 28: Cap positions for relative impact velocity calculations.

where d_R is the sprocket's seating curve diameter, roughly equal to the carrier cap diameter. Sparing the geometry, the relative impact velocity $V_{I,2}$ becomes

$$V_{I,2} = \pi n \sqrt{d_R^2 + 4(d_P^2 - d_P d_R)\sin^2 \frac{180}{N}}. \qquad (30)$$

For purposes of simplicity, however, Equation (28) will be used for the relative impact velocity.

As stated earlier, damage due to impact is suspected to be related to the kinetic energy of impact. As a first approximation, the effective mass can be assumed to be some fraction of the mass of one carrier assembly, m_C. Using this assumption, the impact energy KE_I is proportional to

$$KE_I \propto m_C n^2 P^2. \qquad (31)$$

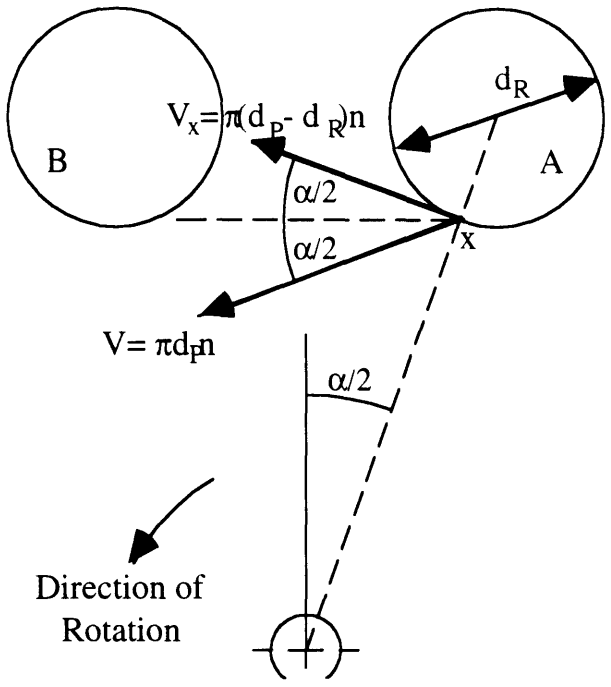

Figure 29: Velocity vectors for determining another definition of relative impact velocity.

Impact energy currently cannot be directly translated to limiting equations, however, and can only be used as a guideline for design. For more specific results, it is still necessary to rely on empirical formulas. Faulkner and Menkes [18] relate a roller chain's horsepower rating (hp, limited by impact at high speeds), to speed, pitch, and number of sprocket teeth by the following equation:

$$hp \propto (N)^{1.5}(P)^{0.8}(n)^{-1.5}. \quad (32)$$

By studying Equations (25), (31), and (32), the means for minimizing chordal action and its resulting impact can be determined. The equation describing the chordal amplitude suggests that designing a sprocket with a large number of teeth and a small pitch would prevent excessive forced vibrations. The second and third equations, describing various properties of impact, recommend

slow operating speeds and a large number of teeth. They conflict regarding an appropriate pitch; in this case, the analytical result would earn precedence since the empirical equation was derived specifically for roller chains.

4.3.5 Fatigue

A reliable cable/carrier transport mechanism would require replacement at very lengthy intervals, so choosing a pitch that extends the chain's fatigue life is essential. As a chain's pitch increases, the mass per unit length of chain decreases, allowing for lower tension; however, the tension within the chain is distributed over fewer carriers within the sprocket for higher pitches. The question arises: which of these contradicting forces prevails?

The answer can be found by observing the qualitative trends of the design equations against fatigue in roller chains. A chain's maximum horsepower rating (hp), which is limited by fatigue at low speeds, is proportional to the following empirically derived equation [18]:

$$hp \propto (N^{1.08})(n^{0.9})(P^{3.0-0.07P}). \qquad (33)$$

For P = 2 inches, the exponent of the third term equals 2.86; for P = 6 inches, it equals 2.58. This equation shows that a high pitch increases a chain's fatigue resistance the most between the variables pitch, number of teeth, and sprocket speed. It is believed that higher sprocket speeds slightly reduce roller fatigue because centrifugal effects reduce the contact stresses.

4.3.6 Galling

Chain failure due to galling is rare and only occurs at very high speeds. In fact, researchers state that a chain can operate (albeit

with a reduced life) at speeds above their maximum recommended value against galling. Consideration of galling was included the design, however, to assure that all factors had been taken into account and to form additional recommendations for the design. Faulkner and Menkes [18] report that the maximum recommended speed that avoids galling emerges from the equation

$$\left(\frac{n}{1000}\right)^{1.59\log P+1.873} = \frac{82.5}{(7.95)^{P}(1.0278)^{N}(1.323)^{T/1000}}. \qquad (34)$$

This implies that very small pitches and somewhat small tensions and numbers of teeth prevent galling most effectively.

4.3.7 Summary

The subsections above laid out a number of prerequisites and recommendations for the prototype's design that included:

- Impact between the carriers and part during feeding is significant, and may cause the part to be ejected from the feed track. This effect can be reduced by dropping the sprocket diameter, providing the carriers with tight springs, and minimizing clearance in the feed tracks.
- Tension within the cable should be in the order of 220 pounds. Closely spaced sprockets oriented ninety degrees with respect to each other will introduce significant tensile components into the system. These components may tend to pull the carrier out of the sprockets. Sprockets that force a twist in the chain should have a center distance no less than 60 inches.
- High numbers of teeth on sprockets are beneficial in overcoming the system's highest natural frequency. This is because the amount of teeth the sprocket possesses increases the chordal

frequency at a faster rate than the decreased pitch resulting from additional teeth raises the natural frequency.

- Small pitches and large numbers of teeth decrease the amplitude of forcing vibrations caused by chordal action.
- Studies of impact show that low speeds, lightweight carriers, numerous sprocket teeth, and small pitches reduce noise and damage caused by impacts between the carriers and sprockets.
- Empirical correlations between fatigue and roller chain parameters show that small pitches, large numbers of teeth, and high speeds reduce fatigue.
- Galling can be prevented best with a small pitch, low operating speeds, light tensions, and fewer sprocket teeth.

4.4 Prototype

Many suggestions for improvement and design ideas from the creation of the mock-up carried over to the prototype design. However, detailed analyses of each part were necessary to promote optimal performance and prevent against operational failure. The first subsection begins the process by selecting the design parameter that alters the system's response the most--the chain's and sprocket's pitch, or carrier separation. After choosing the appropriate pitch, the remaining parts were easier to design. The remaining subsections outline the part-by-part analyses performed.

4.4.1 Pitch Selection

The pitch of the chain and sprocket are perhaps the most important variables to determine. Selecting an appropriate pitch will not only provide clearance between the carriers and allow for

sufficient clearance for manufacturing machinery, but will also influence the dynamic and long-term performance of the system. The chain's pitch plays a vital role in determining wearing forces, misalignments due to tension, and fatigue life, each of which are the factors that influenced the pitch and had to be accounted for. Some of these were determined above. The remainder are studied below.

Study of Industry. Observations of various manufacturing lines already functioning provide important starting points for machine dimensions and clearances. For example, besides esthetics, an assembly machine with a large pitch may be necessary to accommodate the automated assembly equipment inside it. Two types of sprockets, or dials, appear prominent in high-volume assembly plants: preparation dials and operation dials. Preparation dials usually hold a part during cleaning or inspection, whereas operation dials perform an action on the part, such as assembly, and usually contain internal machinery. Preparation dials are typically twelve inches in diameter and have from five to eight teeth; operation dials often measure closer to thirty-six inches across and work on fifteen to twenty parts at a time. The formula common to chain and sprocket design literature [14]

$$d_P = Pcsc\ (180/N) \tag{35}$$

was used to calculate the pitch. (All the variables above maintain their same definitions as before.) Plugging the numbers above into this formula yielded pitches of approximately 6.25 and 7.00 inches for operational and preparational dials. It seemed then that a somewhat large pitch was necessary to house the necessary manufacturing equipment and to allow for easier, more reliable

inspection. Also, jams within the dials may be easier to clear if other nearby parts did not impede access.

Clearance. To facilitate obtaining accurate results for clearances, the carriers were drawn and moved about with AutoCAD®. This eliminated the need for crippling geometric equations and simple assumptions that reduced accuracy. Figures 30 through 33 show the carrier designs spaced along their hypothetical pitch diameters. These carriers were the final versions developed; the process of choosing the pitch and altering the carriers was iterative. The iterations were spared from this document. The pitches were 1.25, 1.5, 2, and 2.5 inches. Each was selected to match ACA standard chains [18]. The sprocket diameter in these figures was chosen to be approximately eighteen inches to accommodate manufacturing machinery while not excessively increasing rotational inertia. Each carrier was opened to its maximum position, in other words, so that the moving jaw rotated clear of the part upon pickup. Figure 30 shows that extremely small pitches (1.25 inches and smaller) could not accommodate carriers on every section, only caps and shafts. The figures are conservative, however, because in practice the jaws to either side of the center jaw would not be opened to their full maxima. In Figure 31, the carriers on every shaft lie on a 1.5-inch pitch chain and are separated from each other by at least 0.02 inches. Although this chain would suffice, an even safer pitch, such as the 2- and 2.5-inch pitched carriers shown in Figures 32 and 33 would allow for additional clearance between the carriers. In summary, clearance between moving parts of the carriers determines the minimum pitch the chain can have.

Depending on how conservative the designer is and the shape of the carriers, a value from 1.5 to 2.5 inches can be adopted.

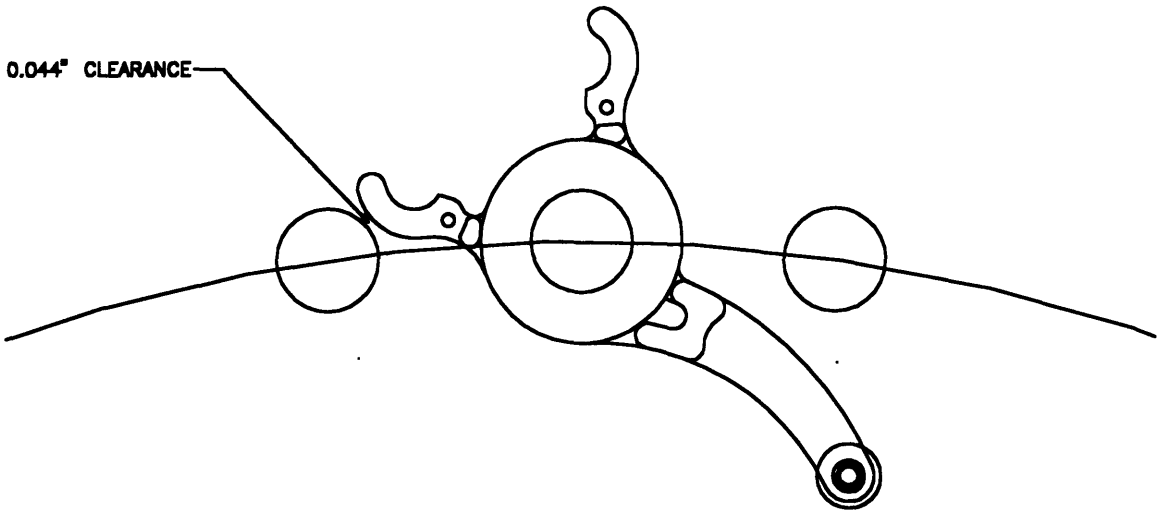

Figure 30: Graphical clearance analysis for a 1.25 inch pitch chain.

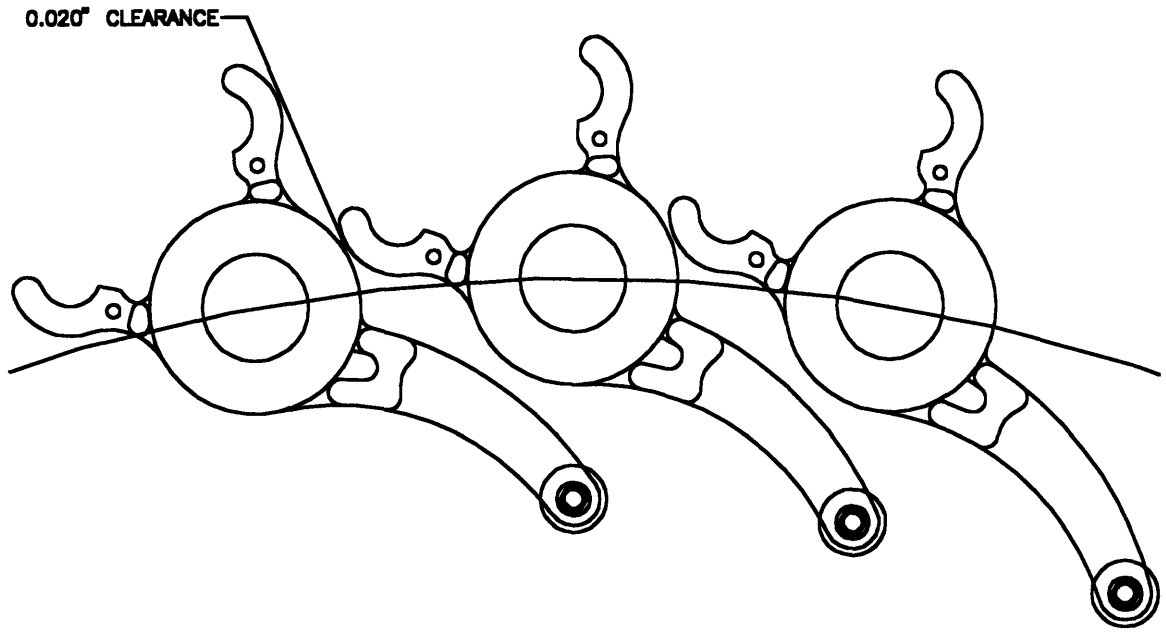

Figure 31: Graphical clearance analysis for a 1.50 inch pitch chain.

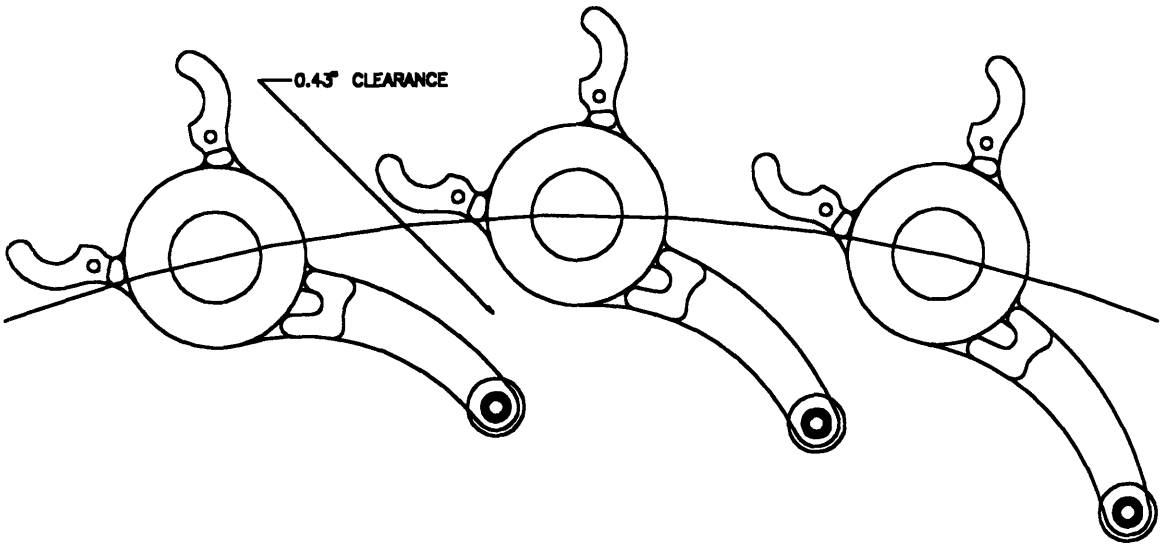

Figure 32: Graphical clearance analysis for a 2.00 inch pitch chain.

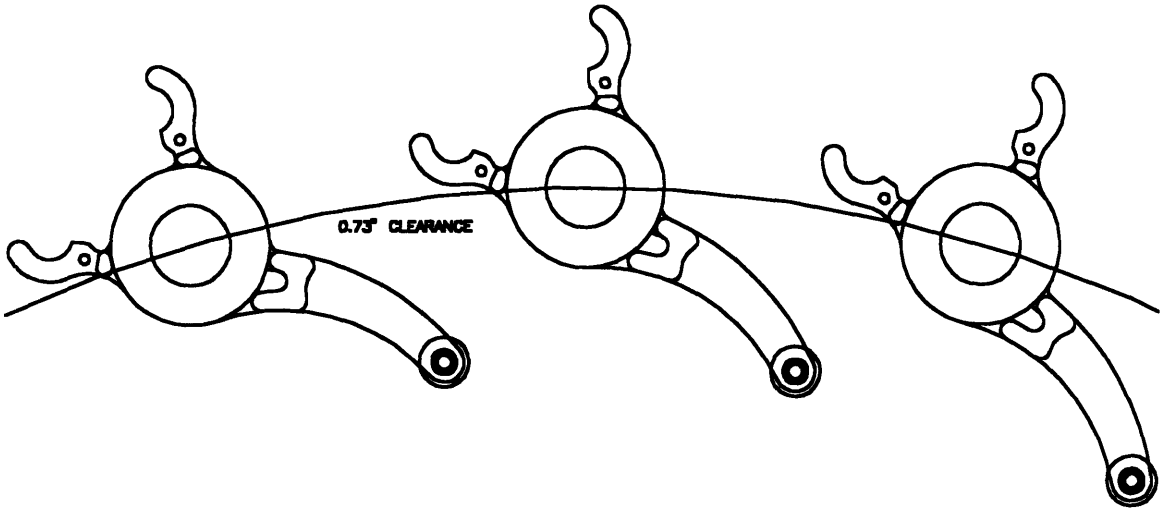

Figure 33: Graphical clearance analysis for a 2.50 inch pitch chain.

Centrifugal Effects and Resistance to Twist. Another factor that required attention in choosing the pitch was the carrier shaft's resistance to twisting from spring forces. A twisting carrier would nullify the tolerance analysis performed earlier by introducing large

amounts of Abbe error. Furthermore, the resistance decreased even more when the system rotated at high speeds. As will be discussed, this was attributed to centrifugal effects.

Figure 34 shows a free body diagram of the stationary portion of a carrier engaged in a sprocket that is rotating with an angular velocity ω; the cam is assumed to be forcing the carrier to its fully opened position. This action creates a moment about the stationary portion of the carrier equal to the spring force F_S times its perpendicular distance from the shaft center, approximately 0.66 inches. A moment created by the friction force f between the cap and sprocket counteracts the former. If, however, f is not large enough to cancel the spring moment, the carrier will rotate. The resulting misalignment could decrease the system's precision, and possibly damage both the parts and the system. The maximum frictive moment must therefore always surpass the spring moment to remain reliable.

Though few pitch decisions were confirmed, it was clear that a somewhat large sprocket was necessary to accommodate the necessary equipment that arises in the manufacturing environment. To balance out this need with a demand for minimal sprocket inertia, a tentative d_P was (again) chosen to be eighteen inches. For a fixed diameter, the pitch P varies with N, the number of teeth, by Equation (35). The maximum frictive moment the cap can endure was calculated by summing the forces in the vertical direction to produce the cap's normal force, N_C:

$$N_C = 2T \sin (180/N) - F_C, \qquad (36)$$

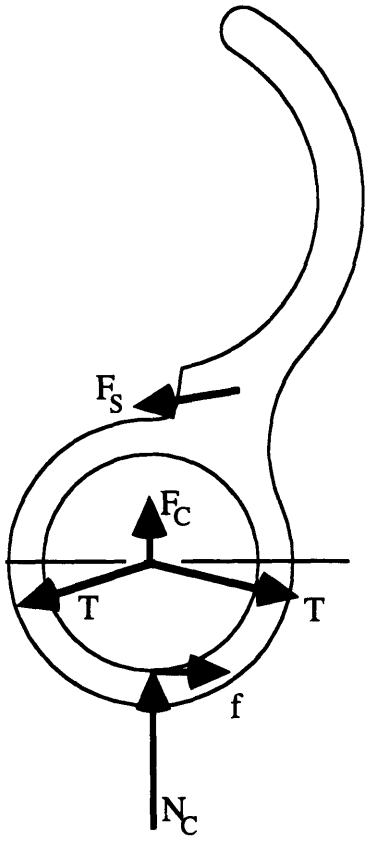

Figure 34: Free body diagram of the stationary carrier half.

where F_C is the centrifugal force. Multiplying the normal force by the friction coefficient μ between the cap and the sprocket, and the tentative cap diameter d_R gives

$$M_f = d_R \mu T \sin (180/N), \qquad (37)$$

where M_f is the maximum moment due to friction, neglecting centrifugal effects. The cap diameter was increased with the pitch in keeping with ACA standards. Expanding the cap's outside diameter changed neither the relative velocity of sprocket impact nor the probability of successful sprocket to cap engagement. It did, however, reduce contact stress and increase the carrier's resistance to rotation caused by the spring.

To determine the spring moment, the spring was assumed to be linear and at its rest length when the jaws were closed without a part. According to recommendations of manufacturing engineers, the spring applied two to three pounds (2.5 was used) of gripping force to the part when it rested within the carrier's jaws. When the jaws were opened eighty-six degrees from rest (their maximum), the spring was displaced 0.67 inches from its rest length. A sixteen-degree, 0.16-inch displacement was assumed to occur when the part was within the jaws. The distance separating the cap center and jaws was assumed constant for conservatism; 0.875 inches separated the part's and the cap's centers.

The spring needed to pull with 3.3 pounds to apply 2.5 pounds of gripping force, which corresponded to a spring constant of 21 pounds per inch. When fully opened, the spring force equaled 14 pounds, and the applied moment was 9.2 pound inches. Given that T = 217 pounds and μ was roughly 0.5 (conservatively low for aluminum), Table III shows the resulting variables for different pitches:

Table III: Sprocket and Moment Information

P (in.)	d_R (in.)	N	d_P (in.)	f (lbf)	M_f (lbf-in.)
1.25	0.750	44	17.52	15	5.8
1.5	0.875	36	17.21	19	8.3
2	1.125	28	17.86	24	14
2.5	1.562	22	17.57	31	24
3	1.875	18	17.28	38	35

It can be seen from this information, too, that a larger pitch is favorable. However, it should be noted that in practice, 1) the tension will probably be higher, 2) the friction coefficient will be

larger, 3) the spring setup may differ, and 4) the spring may be non-linear. Most of these differences would result in more favorable resisting moments. Conservatively, pitches equal to two inches and larger would provide enough resistance to rotation.

Centrifugal forces affect the above results significantly at high speeds. Binder [17] states that the centrifugal force acting on each link (carrier) of a chain is equal to

$$F_C = m_C d_P \omega^2 / 24g \qquad (38)$$

where m_C is the carrier mass (pounds) and g is the acceleration of gravity (ft./s^2). At speeds greater than roughly 100 rpm, the reduction of moment becomes significant, as illustrated in Table IV (assuming a carrier mass of 0.46 pounds, a sprocket diameter of 18 inches, and a cap diameter of 1.1 inches).

Table IV: Reduction of Normal, Friction Forces by Centrifugal Action

n (rpm)	ω (rad/s)	$-F_C$ (lbf)	-f (lbf)	$-M_f$ (lbf-in.)
10	1.05	0.012	0.0059	0.0033
50	5.24	0.29	0.15	0.083
100	10.5	1.2	0.59	0.33
150	15.7	2.6	1.3	0.74
200	20.9	4.7	2.4	1.3
500	52.4	29	15	8.3

Comparison of Facts. The two subsections above provided analyses that established a minimum pitch, and clearance analyses showed that carriers spaced at least 1.25 inches apart would not interfere with one another. At this pitch, however, elimination of the carriers from every other carrier shaft was necessary. When the carrier shafts were spaced 1.5 inches apart, carriers could be placed on all of them, but this was not necessary. Placing carriers on only a

fraction of the carrier shafts had the advantages of costing less to machine fewer carriers, allowing the feed rate to depend less on the number of sprocket teeth and the sprocket's speed, and giving manufacturing machinery the room it required to perform operations on each part. If these advantages proved insufficient or unnecessary, the carrier-free shafts could be replaced with working mechanisms.

Unfortunately, the calculations of Table III showed that carriers spaced less than or equal to 1.5 inches did not have the necessary 9.2 pound inches of resisting moment that the carriers with larger pitches provided. Pitches two inches and larger not only provided sufficient clearance, but also had a sufficiently high radial tension component to resist carrier rotation. No calculations mandated a maximum pitch; consequently, industry's average pitch of six inches was selected as a maximum.

Varying the chain's pitch between two and six inches affects severely the system's performance. The following table compares the effects of these pitches on each of the responses discussed in this section and the previous one. Below, a four-inch pitch was assumed to be the norm. The numbers represent ratios of each of property's values; the higher the number, the better the response corresponding to that pitch.

Table V: Comparison of Pitches

P (in.)	N	A_C	Impact Energy	Fatigue	Galling	M_C
2	28	4.1	4.0	0.4	3.6	0.2
3	18	1.8	1.8	0.7	1.9	0.6
4	14	1.0	1.0	1.0	1.0	1.0
6	9	0.4	0.4	1.5	0.3	2.3

The evidence above favors a low pitch. The chordal amplitude, impact energy, and galling susceptibility decrease with the pitch, yet the fatigue life dwindles as the pitch drops. Fatigue life, however, drops at a slower rate than the other properties' rates of increase. For example, while fatigue life in the two-inch pitch chain is nearly four times lower than that of the six-inch pitch chain, the latter chain sees roughly ten times more impact energy than the former. The additional increases in properties other than fatigue resistance better the overall performance of the chain as well as, if not better than, fatigue resistance. It is believed that as long as the resistance to carrier rotation is above a certain value and will not be compromised through centrifugal effects, it need not be maximized.

The following table shows that the system's dynamic response is also improved with a lower pitch:

Table VI: Comparison of Pitches for Dynamic Response

	Fundamental		Highest	
P (in.)	Frequency (Hz)	rpm	Frequency (Hz)	rpm
2	4.8	10	95.6	205
3	4.0	13	78.1	260
4	3.4	15	67.6	290
6	2.8	19	55.2	368

It can be seen in Table VI that the range of potentially harmful harmonics shrinks with the pitch. As noted before, larger pitches decrease the highest natural frequency. However, they fail to keep up with the higher frequency of chordal action that excites the natural frequencies. Faster chordal action is realized from the increase in sprocket teeth that accompanies lower pitches.

The facts above demonstrate that a pitch of two inches should be chosen in conjunction with an 18-inch, 28-tooth sprocket to optimize performance.

4.4.2 Carrier/Shaft Design

Fortunately, many of the design changes to the carrier were realized through assembly of the mock-up. Modifications decreased the weight, reduced the part count and complexity, eliminated or decreased interference with other parts, and stiffened the means by which one half rotated. Below is a list reviewing the remaining tasks:

- Increase cam follower length.
- Determine optimal spot to place spring posts.
- Allow sufficient clearance for part and feed track.
- Produce a working re-designed carrier shaft.
- Evaluate alternative springs.
- Create specifications for CNC machining production.

Cam Follower. Figures 35 and 36 illustrate the complications involved in creating the new cam follower. Here, the cam followers have been upgraded from solid pieces of material to tails housing roller bearings at their ends. The roller bearings could not be too large; they were made from steel, and large bearings would drastically increase both the weight and the cost of the line. In the figures, the bearing's outer diameter equaled 0.3125 inches.

The ideal configuration for the system designed would have a follower that traced a path similar to A in Figure 35: it would extend to the right, then down. This follower would always interact with the cam in such a way as to produce smooth and reliable opening and closing. The following technique illustrates why. A straight line

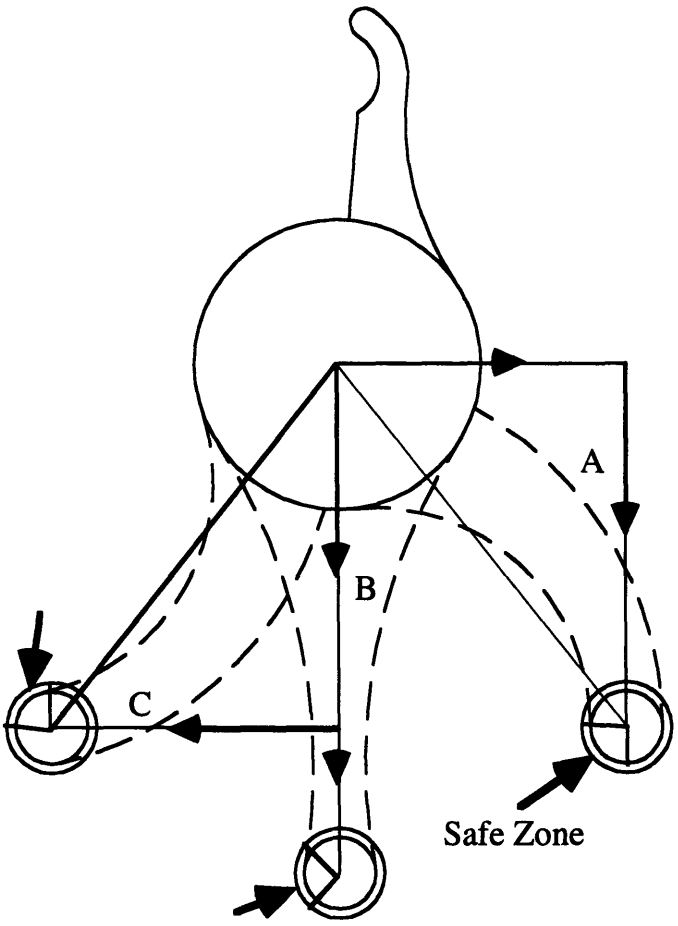

Figure 35: Definitions of possible cam follower paths.

drawn from the carrier shaft center to the bearing center represents a lever arm. Forces acting on the bearing can be broken into two components: those perpendicular to the lever arm line, and those that are parallel to it. Forces acting perpendicular to the lever arm would impose a pure moment on the jaw, causing the carrier's jaws to open. On the contrary, forces acting in the same direction as this line will attempt to push or pull the carrier out of its seat between sprocket teeth. Common sense dictates that the component of force acting to rotate the carrier open should be greater than the one pushing the carrier out. Therefore, the realm of "safe" operation, that

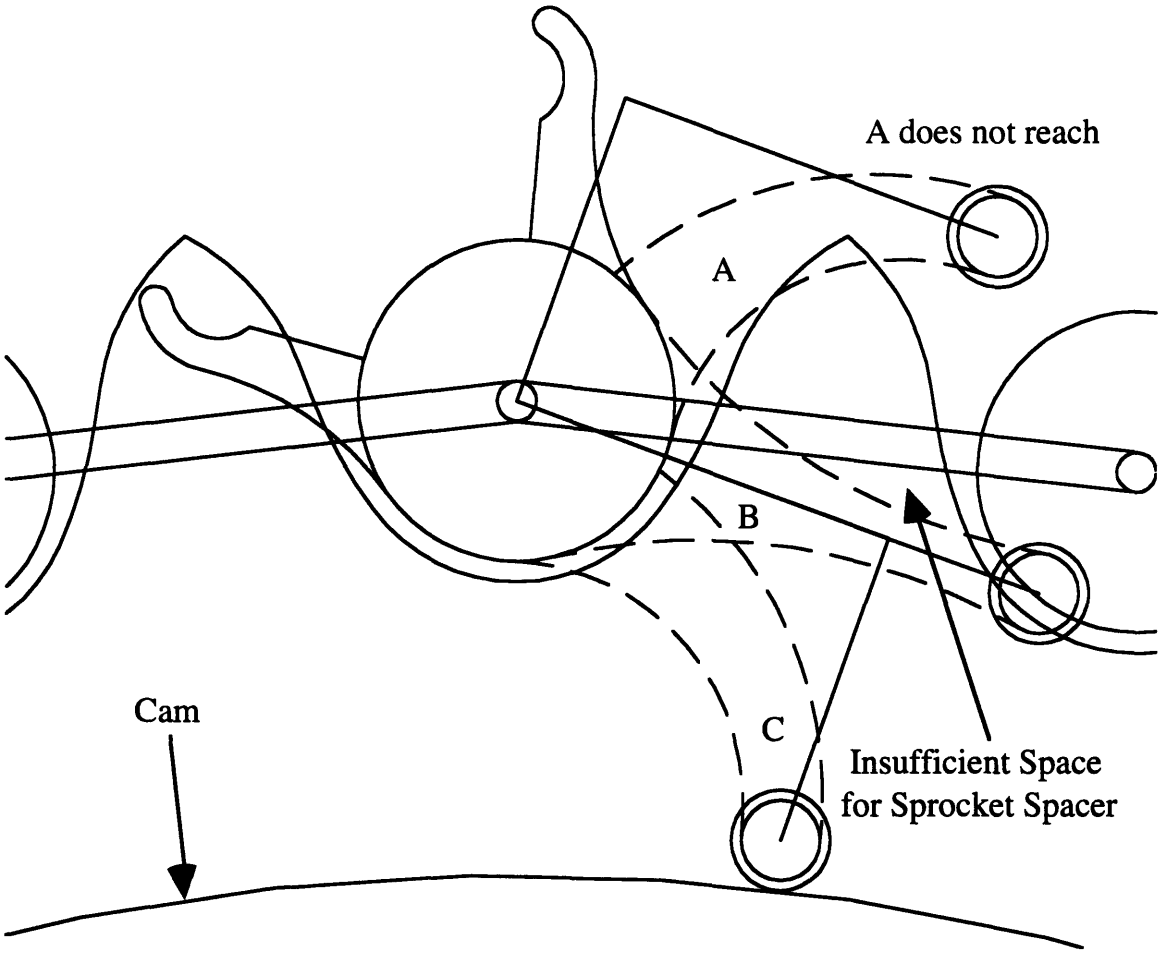

Figure 36: Complications involved in selecting cam follower paths A or B.

is, smooth and reliable motion, should lie within forty-five degrees in either direction from the line's perpendicular (Figure 35).

Shifting this line to the left as it is in paths B and C will rotate this "safe area" farther up the bearing, making smooth and reliable operation more difficult. For example, if a vertical surface moving from left to right were to hit cam follower A of Figure 35, it would result in a different effect than if it struck cam follower C of the same figure. The resulting forces on cam follower A would rotate the carrier jaws and a pull the carrier in toward the sprocket. Cam

follower C, however, would be pushed out from between the sprocket's teeth by the parallel component of force, and it is possible that it would not open. This aspect will be discussed further in the cam design section--it should suffice to say here that the center-to-center line should deviate as far from left as possible.

Unfortunately, a competing factor tempers the above argument. Figure 36 shows the carrier and its three possible cam followers in the fully opened position. As can be seen, cam followers A or B would have to stretch over extremely long distances to open the jaws to their desired position. This would increase weight and production costs, as well as decrease the esthetic value (the carriers would appear disproportional). Disproportional carriers may induce undesirable dynamic effects. In addition, carrier path B does not allow sufficient space to locate a sprocket spacer.

To account for each of these factors, a compromise between B and C was adopted. The design changes to the carrier remained simple so as to not require excessive analyses. The cam follower was designed to be twice the length of the jaw and half as thick, maintaining a reasonable balance. The carrier was then moved to the left, under the length restriction above, until the bearing reached the cam, resulting in the follower of Figure 37.

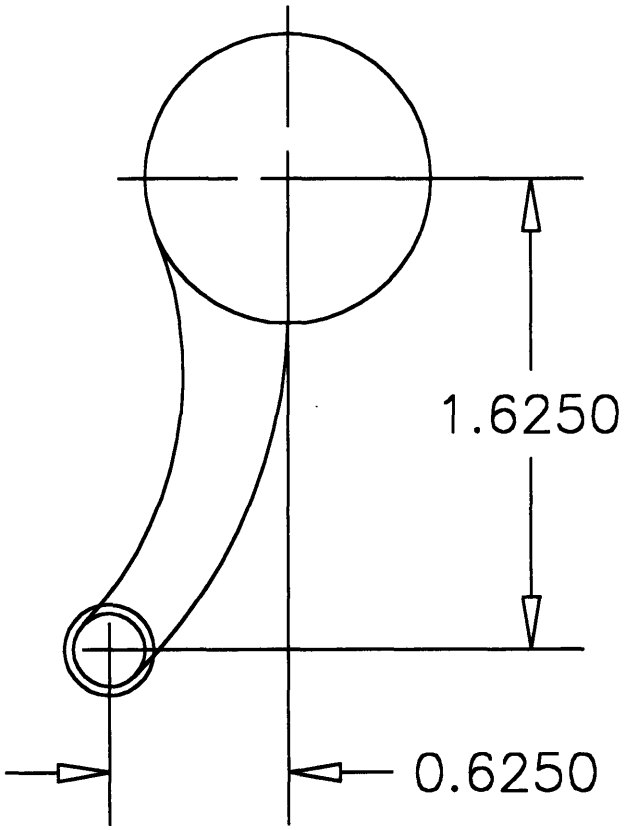

Figure 37: Resulting cam follower and its dimensions.

Spring Post Location. When the cam follower forced the jaws to their fully opened position, the springs on the mock-up began to interfere with other parts. Therefore the clearance between the spring, spring posts, and everything else had to be maximized. Moving the springs to the underside greatly helped this problem since the part rack and the cap no longer brushed with the spring. The part rack, however, could still potentially interfere with the posts and spring, so the posts had to be located in such a way as to maximize the distance from all possible obstacles on the carrier.

The goal was to maximize the total distance from each of the lines drawn while remaining within the constraints of the jaw's

geometry. In other words, the post had to lie between the jaw's walls, below the "part interference" arc, and above both the "mating area" and "shoulder interference" line. These five constraints trace out a polyline made up of lines and arcs, shown in Figure 38. It was clear, however, that the small region constrained by the "mating area" fell far too close to the left wall. Therefore, the "mating area" constraint was essentially considered unnecessary, and eliminated.

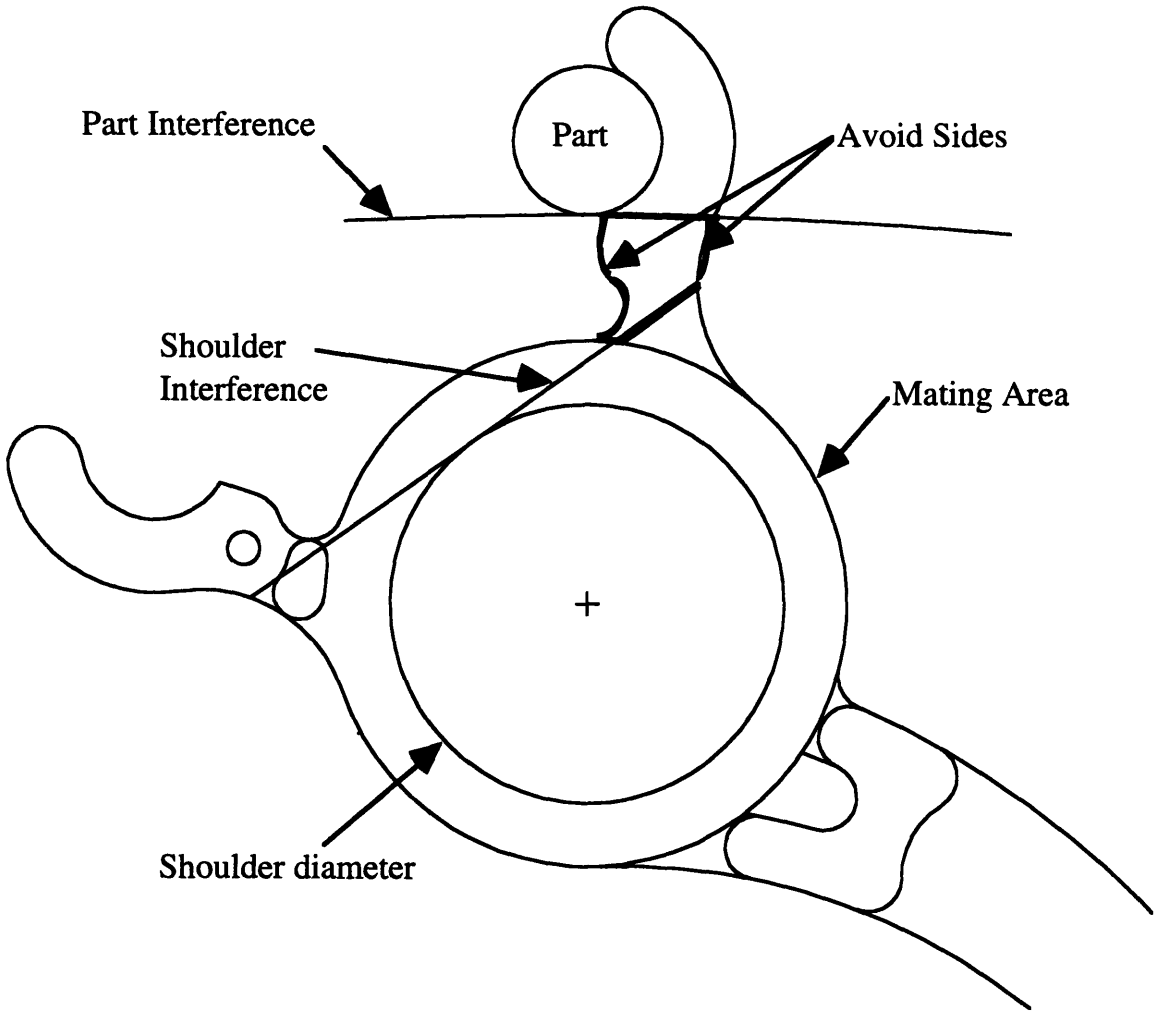

Figure 38: Graphical calculation of optimal spring post location: definition of constraints.

The obvious restrictions were each of the jaw's sides, and the main circular area where each of the carrier halves mated (identified by the arrows labeled "avoid sides" and "mating area" on Figure 38). Locating the pin too close to the part would result in the part's contacting the spring when the jaws were closed. A limiting arc is constructed by drawing the path that the closest radial point on the pen would take (labeled "part interference"). Next, in the open position, the pins cannot be pushed too far back toward the engagement region, since the center of the opening spring traveled radially inward. This would continue until the jaws were completely open, or until something prevented the spring from continuing. In the mock-up, the cap was this obstacle. With springs now on the underside, the obstacle became the shoulder on the carrier shaft, assumed to be 0.75 inches in diameter. The line labeled with the arrow "shoulder interference" shows how the spring would appear directly before hitting the shaft's shoulder. This line represents the closest distance the spring can come before contacting the carrier shaft.

With the obstacles established, it became necessary to maximize the remaining distances, a procedure different from maximizing the sum of the distances from each constraint, since very large distances from one constraint may offset a near zero clearance of another. Figure 39 shows the method used. It was assumed that if the post was equidistant from three of the constraints and a longer distance from the fourth, the post was located in a nearly optimal spot. Following this logic, four circles were drawn, each tangent to three of the four constraints. Each circle's center represented the

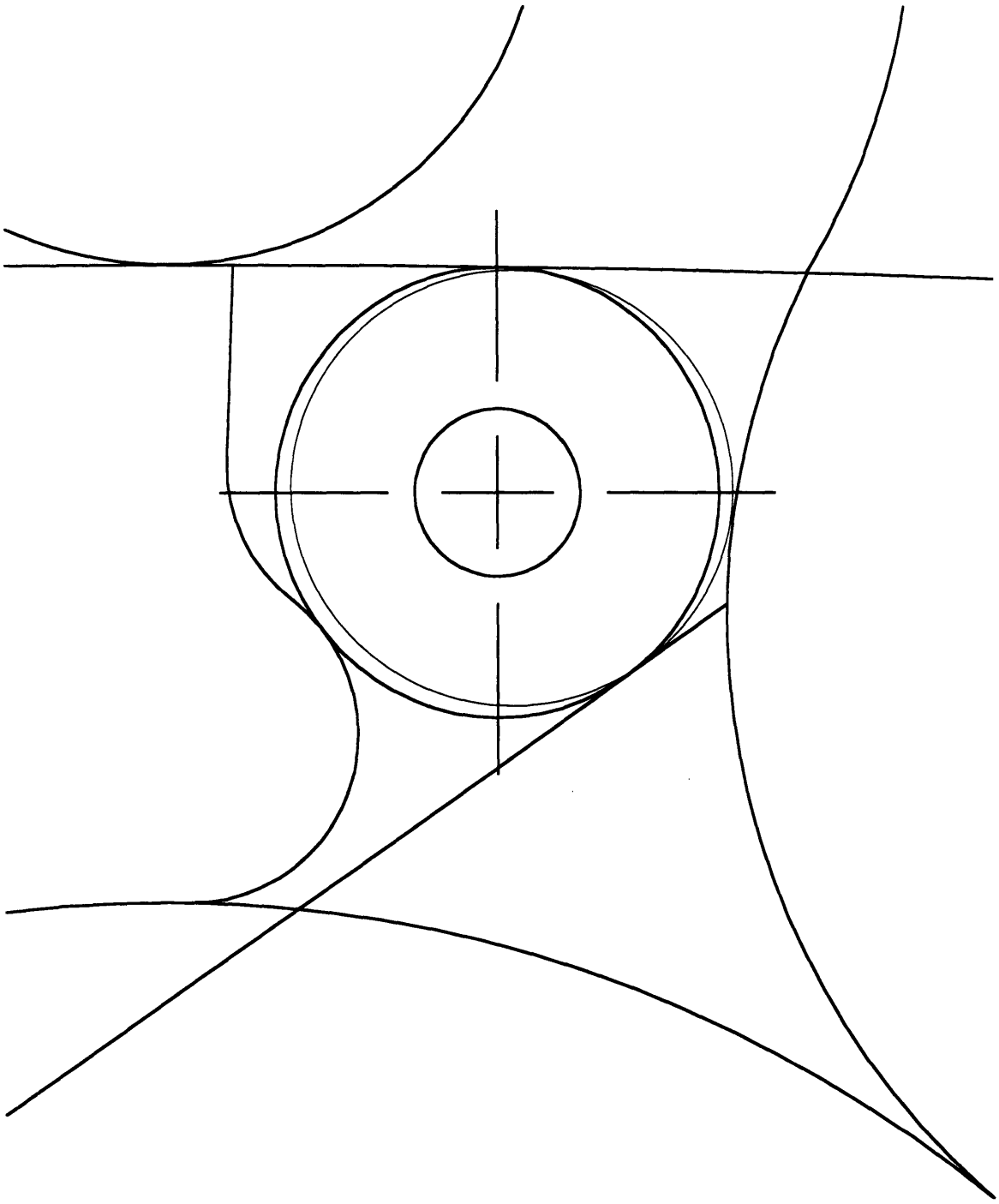

Figure 39: Graphical calculation of optimal spring post location: method employed.

point equidistant from three of the constraints. If it fell entirely within the polyline, the distance from the fourth constraint was

larger than the distance from the first three. Circles outside this polyline were eliminated. The largest remaining circle's center lay farthest from three of the constraints, and even farther from the fourth, so this point was close to the optimal location. Two of the circles went beyond the polyline of Figures 38 and 39; the remaining two are shown in Figure 39. The larger of the two circles was chosen, drawn as a solid line in Figure 39. The smallest circle and the crosshairs represent the spring post location.

Part and track clearance. The new carrier design required thinking about how much rotational freedom a gripped part would have. For a ball point pen, this freedom required minimal design changes. It was assumed that the carrier should provide clearance for a lid in any rotation about the pen's long axis. For the pen of Figure 1, the maximum radius of the lid was 0.33 inches. Therefore, the carrier was designed without any interfering parts within a radius of 0.33 inches around the part's center. This was accomplished by extending the distance from the carrier shaft center to the jaw center until sufficient part and feed track clearance was reached.

Carrier shafts. After implementing the suggestions for improvement emerging from the mock-up, design of the carrier shaft became a simple matter of calculating appropriate clearances and tolerances. Shoulders and keyways replaced a locating hole for proper positioning of the carriers; reversible threads became substitutes for permanent press fits. The cap held down the bottom carrier jaws, and a nylon collar held down the jaws located in the center. Finally, the shaft was hollowed out and tapped at the ends as

a means for fastening the cable. (This technique will be discussed further in subsection 4.4.4, Cable Design.)

Alternative springs. Figure 40 shows the other types of springs considered for replacing the rubber bands. Analyses were conducted on each type of spring in an attempt to supplant the rubber bands' properties. Each spring was constrained by the following criteria: 1) its makeup had to fit within the geometry of the carrier and/or shaft, 2) it required a spring constant stiff enough to supply two to three pounds of force to the jaws when opened roughly sixteen degrees, and 3) it had to be capable of opening to eighty-six degrees under repeated cycling without yielding or fatiguing. Unfortunately, several spreadsheet analyses failed to produce a spring of any kind (other than rubber bands) that satisfied all the above conditions. However, the author firmly believes that a spring, most likely a torsion spring, would exist within these boundaries if minor additional changes to the carriers were made. The equations and data used in creating these spreadsheets are included in Appendix A. The rubber bands proved to be effective under cyclic loading for several months; to date, none of the bands have failed.

CNC Production. Each carrier was designed to be machined from a solid block of aluminum without repositioning the part within the machine; for this reason one side of each carrier half is detailed in the axial direction.

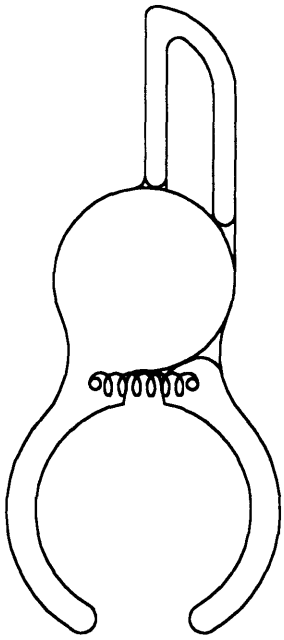

(a) Linear Spring

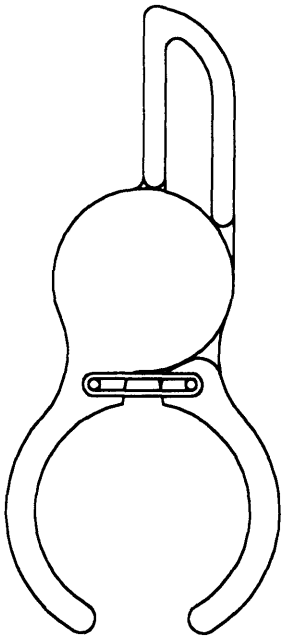

(b) Elastic Band

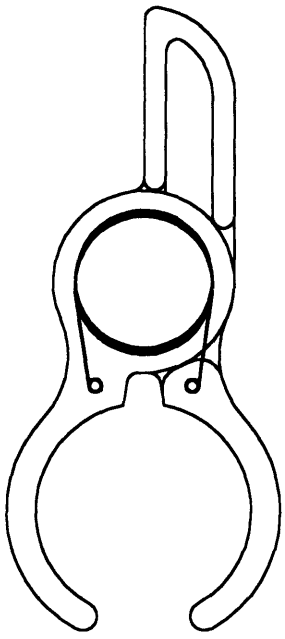

(c) Torsion Spring

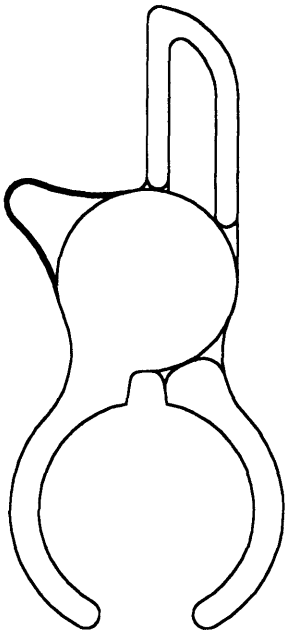

(d) Leaf Spring

Figure 40: Alternative springs.

4.4.3 Cap Design

By this stage in the design, much of the tedious geometric analysis required to design an appropriate cap had been completed. The pitch had been selected to prevent unwanted twisting, and the magnitude and direction of the tension had been calculated. Aluminum was the preferred material because of its high friction coefficient and modulus of elasticity. Two remaining factors had to be accounted for: 1) cap resizing to reduce wearing and friction from the new carriers (and to reduce weight), and 2) self-centering tapers--which would serve to correct minor misalignments within the system--to combat chain twist and displacement.

The bottom diameter of the cap determined the amount of surface that each half of the carrier was exposed to. It was chosen to be 0.875 inches. This diameter covered all the stationary carrier half's top surface (locking it axially in place) and approximately fifty percent of the mobile carrier half. The cap's top diameter (the section that engages the sprocket) was already determined to be 1.125 inches as specified in ACA standards.

The remaining variable to be determined was the angle the taper made with the plane of the sprocket, ϕ. Measurements of the Pow-R-Tow® chain described in Chapter 3 gave a starting point of sixty-one degrees, which was analyzed against pullout due to friction, reanalyzed at 72.6 degrees, then implemented. Below is a brief description of the calculations involved in the pullout analysis.

As described in the Section 4.2.2, the tension of a chain between two perpendicularly aligned sprockets can be broken down into a radial, tangential, and axial component as it leaves or enters

the sprocket. These forces were quantified in Equations (20) through (22). A concern in determining the cap angle was that axial forces on the tapered area of the cap were sufficient, under poor conditions, to pull the cap out of the sprocket prematurely. Of course, this could be corrected by designing the cap with a small ϕ that would act almost like a wall against these forces. To design a generous taper that self centers large misalignments, however, the cap's diameter change across the taper would have to be very large. This could foster new problems with excessive weight and smaller clearances. A proper balance was reached through the analysis below.

The tension's components were assumed to act entirely on the tapered surface of the cap, as shown in the views of Figure 41. If, under conditions of excessive tension, short spans, and varying cable weights, the resultant friction force f exceeded (or approached) μN (the maximum friction force), the cap angle was changed until a safe limit was reached. The calculations were relatively straightforward--for this reason they were spared from this document. The cap angle of sixty-one degrees never came within more than ten percent of the maximum pullout force, i.e., a cap with this angle would not slip out under most conditions. When a sixty-one degree taper was applied, however, across the necessary length (calculated below), the resulting outside diameter pushed the cap weight up too high.

A cap angle $\phi = 72.6$ was chosen and analyzed (see *Cap Design*). This bigger angle was necessary to keep the larger diameter of the cap from growing so big (due to a large tapered area) that it would interfere with the parts and add excessive weight.

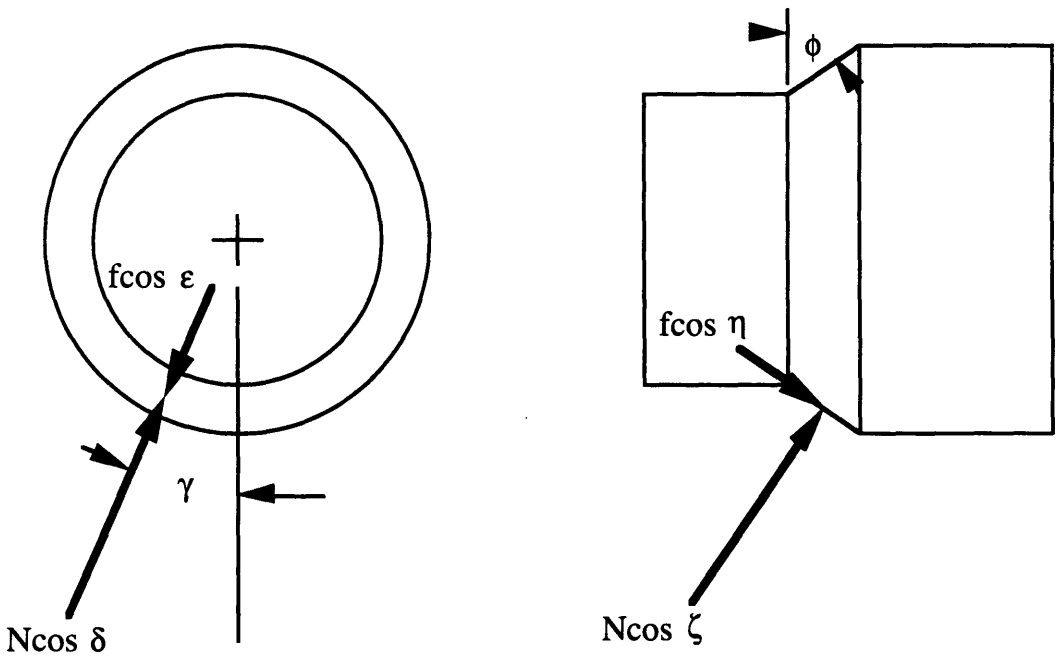

Figure 41: Free body diagram of the forces acting on the cap.

The length of the tapered area was determined by combining safeguarding against chordal action with resistance to axial pullout forces. First, the vertical movement from chordal action was conservatively assumed to push the cap entirely horizontally; in other words, misalignment due to chordal action was assumed to equal the magnitude of the chordal amplitude itself. For a two-inch pitch, twenty-eight tooth sprocket, the chordal amplitude equaled 0.056 inches. Second, when the sprocket center distance is conservatively short (sixty inches), the angle θ_1, defined in Figure 19 and Equation (16), grows to the point where sideways misalignment is expected. The total possible misalignment that can occur equaled θ_1 multiplied by the pitch. For a sixty-inch span, $\theta_1 = 5.4$. For a two-inch pitch, this misalignment would be equal to 0.19 inches. Both the first and second values described above were added in

quadrature to arrive at the total length of the self-centering taper--0.20 inches.

4.4.4 Cable Design

Proper selection of the cable was crucial to the machine's success. A number of problems could arise if the cable failed to meet any of the following requirements: a high strength-to-weight ratio, high stiffness-to-weight ratio, excellent creep resistance, small minimum bend radius, resistance to abrasion and wear, and limited corrosion resistance. Many twisted fibers fit the description above. Below are some of the fibers worth considering, in tabular form:

Table VII: Mechanical Properties of Fibers

	ρ (lbm/in.^{3})	S_y (ksi)	S_y/ρ ($\times 10^3$)	E (Msi)	E/ρ ($\times 10^5$)
Polyethylene	0.0350	377.	10.8	17.0	4.85
Kevlar™ 49	0.0520	464.	8.93	16.4	3.15
Carbon	0.0625	450.	7.19	32.9	5.27
Nylon-66	0.0412	139.	3.38	0.928	0.225
S-Glass	0.0900	667.	7.41	12.9	1.43
Steel	0.282	100.	0.354	30.0	1.06

Minimum bend radii depend principally on the fiber's tensile strength and elastic modulus; higher strength fibers can be made smaller, giving them lower moments of inertia. The product of the elastic modulus and the moment of inertia determine the fiber's stiffness and minimum bend radius.

Other fibers, such as alumina, boron, silicon carbide, and polyethylene terephthalate (PETE) could also be used, but at an increased cost. Gel-spun polyethylene fibers were best for the job, but were also costly. Aramid fibers, specifically Kevlar™ 49, were

tried because the benefits nearly matched those of gel-spun polyethylene at a significantly lower cost.

Aramid fibers alone, however, were insufficient since the fiber bundles tended to fray and tangle if left exposed and were difficult to grab. The bundles can only be effectively grabbed by tying knots around the area of interest; failure to do so would cause the fibers to spread out among the grabbing surface. The fibers would then either move as if not held, or break. However, the wearing and tangling properties of the fiber could be reduced by enclosing the fibers in a sleeve. It was assumed that constricting the fibers into a small enclosure, in this case a polyethylene sleeve, would allow for them to be grabbed without spreading out.

Under this assumption, a means for attaching the encased fibers to the carrier shafts was developed. The following constraints had to be met: 1) the method had to maintain accurately the chain's pitch (ACA standards [18] recommend a tolerance of 0.015 inches per foot), 2) under tension, the cable could not create any rotational moments that could not be completely canceled by the second cable in the carrier shaft, and 3) the cable could not be crimped or compressed against sharp corners. Solutions falling within these conditions were sparse. The method used in the mock-up--crimped modifications of wire ends--failed to hold the pitch accurately and was difficult to implement. Attempts to wrap or tie the cable around the carrier often created a moment, while other wrapping attempts forced the cable to bend over sharp edges. It was decided to rely instead on the constrictive abilities of the polyethylene sleeve, and to grab the cable tightly using two adjustable flattened surfaces. One

surface was a flat-tipped set screw; the other was a turned rod held in place by the cables, as shown in Figure 42.

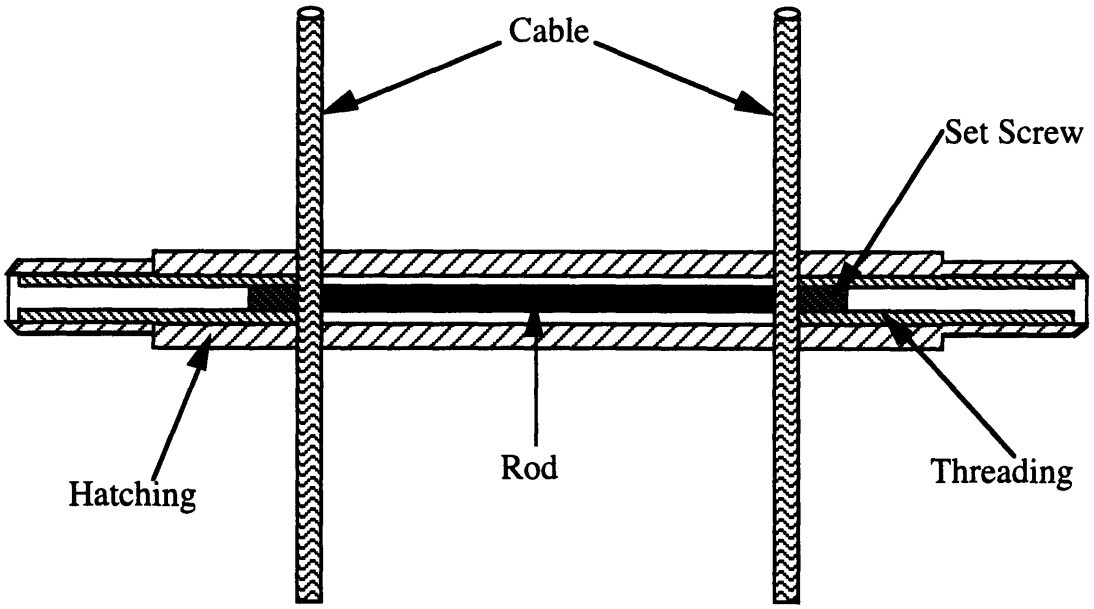

Figure 42: Employed method of attaching cables to carrier shafts.

The mechanical properties of the chosen cable's core, Kevlar™ 49, include high creep resistance. Although the polyethylene sleeve encasing the aramid fibers had extremely poor creep resistance, it was assumed that a strong gripping mechanism on the composite cable would take advantage of the core's inherent resistance to creep. Conversations with the cable's vendor helped to confirm these assumptions--the potential benefits of a cable that fulfilled all the mechanical requirements (and then some) seemed to justify risking the investment.

As it turned out, the gripping method works in principle, but not in this case since the fibers within the cable provided by the vendors failed to adhere to the sleeve. In fact, the sleeve produced

had an inner diameter much greater than the outer diameter of the fibers. Because of these properties, the following problems arose: 1) the fibers slipped within the sleeve due to the low friction coefficient between polyethylene and Kevlar™ and the lack of adhesion, and 2) the fibers spread out within the spacious confines of the sleeve, creating the gripping problems mentioned earlier. The result of these problems was excessive creep within the cable. This occurred because the grips failed to seize, and therefore take advantage of, the creep resistant Kevlar™ interior. It was then decided that the cost effective way of proving the orientation and feeding concepts would be to replace the cable with two 0.125-inch diameter 7 × 7 steel aircraft cables. These cables were fully functional, however not optimal.

4.4.5 Sprocket Design

The function of this sprocket was threefold: 1) to absorb smoothly and reliably the tension within the cable chain; 2) to accommodate successfully a certain amount of wear and/or creep, whether it existed in the form of wear within the tooth/cap form or in the form of pitch elongation; and 3) to position accurately the carriers and parts within rotary automated equipment for manufacturing.

Chain and sprocket interaction theory is extremely complex, especially when factors such as wear and elastic deformation are taken into account. Binder [17] provides a broad overview of these interactions, and cites several references for more detailed analyses. Fortunately, sprocket tooth forms for precision roller chains have evolved to the point of having a standard for their design--ANSI

B29--which lays out dimensions and recommended manufacturers' practices for sprocket design and construction. A brief summary of the tooth layout has been taken from Faulkner and Menkes' book [15] and placed in Appendix B.

The caps of the carrier shafts measured 1.125 inches at the point of engagement with the sprocket. These caps rested in the gaps between the teeth in an area known as the seating curve. The diameter of this curve was the only dimension designed differently from the standard (besides axial constraints that don't apply to the type of chain used here). ANSI B29 recommends that the seating curve's diameter, D_S, be

$$D_S = 1.005D_R + 0.003 \tag{39}$$

inches, where D_R is the cap (roller) diameter (in.). In the sprockets created here,

$$D_S = D_R + 0.003 \tag{40}$$

inches, which assured a tighter fit between the cap and sprocket.

Consistent with past assumptions and the mock-up, the sprocket diameter was initially chosen to measure approximately 18 inches in diameter and 0.25 inches thick. The mock-up's solutions recommended using a stiffer sprocket material, so aluminum was initially chosen. With the dimensions and materials chosen, only two things remained to be calculated: the resulting inertia and the maximum rotational stresses caused by this inertia.

For the prototype, the sprocket's inertia would only become an important issue if the resulting rotational/inertial stresses approached the yield strength of the material. Otherwise, it was more important that the system was constructed sturdily from stiff,

reasonably priced materials capable of holding tight tolerances. The larger motors and bearings necessary would only enhance the system's performance. Shigley and Mischke [19] cite the equations for the tangential (σ_t) and radial (σ_r) stresses along a rotating disk. They assume that the disk's outside radius r_o exceeds ten times the thickness, that the disk's thickness remains constant, and that stresses are constant over the thickness. The stresses are

$$\sigma_t = \rho\omega^2\left(\frac{3+\nu}{8}\right)\left(r_o^2 - \frac{1+3\nu}{3+\nu}r^2\right) \qquad (41)$$

and

$$\sigma_r = \rho\omega^2\left(\frac{3+\nu}{8}\right)\left(r_o^2 - r^2\right), \qquad (42)$$

where ρ is the sprocket density (slugs/in.^{3}), ν is Poisson's ratio for the sprocket material, and r is the radius along the sprocket (in.) where the calculated stress is desired. For aluminum, ρ = 0.00303, ν = 0.334, and the maximum stress occurs at the center, r = 0. At 1000 rpm (104.7 rad/s), the maximum tangential stress equaled the maximum radial stress. Each inflicted 93.5 psi on the rotating system, which was practically negligible.

In contrast to the mock-up, the sprocket spacing rods no longer had a place to be fastened (the spots between the teeth were covered by open cam followers). This challenge was remedied graphically in much the same way the spring posts were placed. Figure 43 shows the drawing used; only the carrier's cam followers were required on the drawing since the jaws did not interfere. The sprocket spacing rod's center had to be located in such a way to maximize the distance from the cam follower, the right edge of the sprocket tooth, and the cable. A circle tangent to these three surfaces was drawn, and its

center, marked on the figure with crosshairs, was chosen as the best point to relocate the sprocket spacing rods.

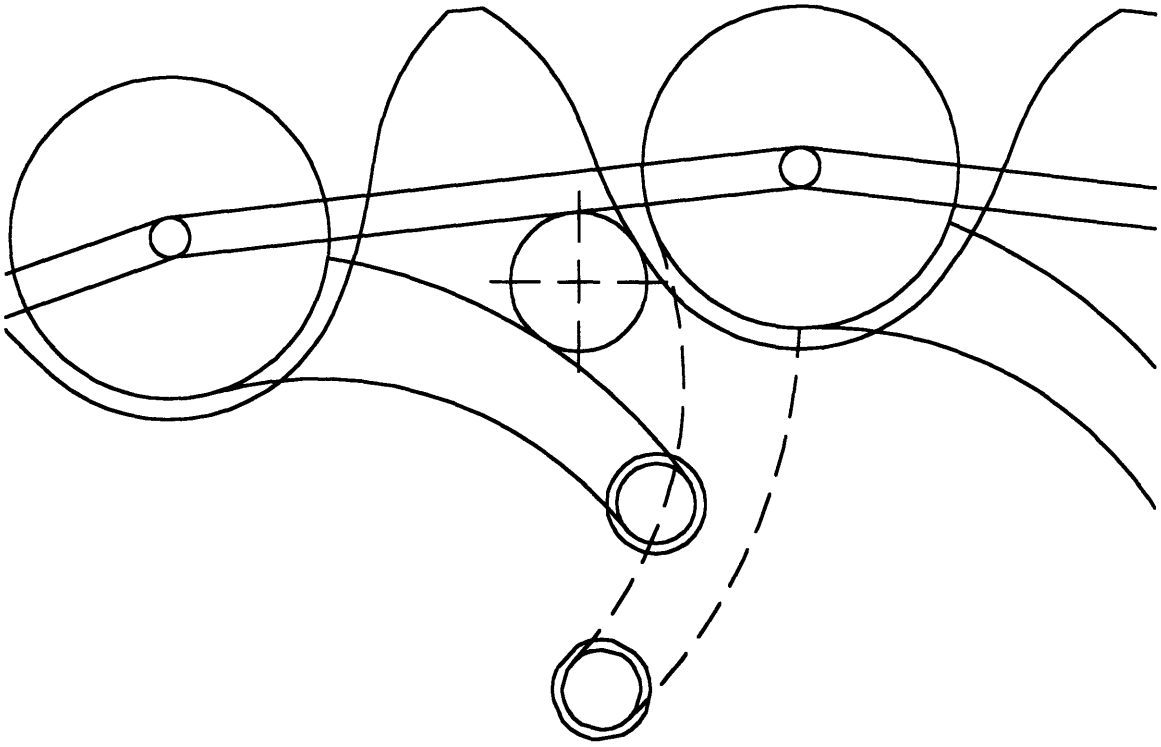

Figure 43: Graphical calculation of optimal sprocket spacing rod location.

4.4.6 Cam Design

Subsection 4.4.2 explained briefly (in its section on the cam follower) the moment arm and the optimal "safe zone" in which the cam should engage the follower. The zone's size varies with such factors as the cable's tension and the spring's constant. Higher cable tension would increase the safe zone's size; a larger component of pushing force would be required to misalign the carrier. Higher spring constants would shrink the zone because more force would be necessary to open the jaws. Ideally, each follower would engage the cam slightly higher than the center of its safe zone, then smoothly

shift toward the zone's center. The high end of the safe zone has both a component of force to open the jaws and a component that pulls the carrier into the sprocket, so engaging in this region would produce a more reliable opening.

Figure 44 shows the path the cam follower would take if it could open evenly as it traveled across the cam's length. Also shown on each follower is the safe zone described above. No cam could be constructed from this figure in such a way that each follower position was tangent to the cam within its safe zone. Consequently, the design had to go one of two ways: open the jaws evenly and adjust the tension and spring constant to allow for a larger safe zone, or sacrifice some smoothness and aim for a cam that runs tangent to each position's safe zone. The latter produced a more reliable cam. Adjusting the tension and spring constant is no easy task, and even if they were easily adjustable, the safe zone's boundary must still have a component in the opening direction. At any rate, operating on the boundaries of safe zones is an unreliable practice. If the design variables could be adjusted to increase the safe zone, the cam should still be adjusted to attain the goal of running more reliably, even if perhaps, less smoothly.

The line tangent to the far right cam follower in Figure 44 represents the end of the cam. This line allows the cam follower to engage the cam within the safe zone. Therefore, the follower should hit the cam's edge instead of risking an unreliable engagement with its bottom surface. Since the cam follower hit the cam edge near the end of the safe zone, the impact force was smaller than hitting the zone's center. The cam designed gradually decreased this slope

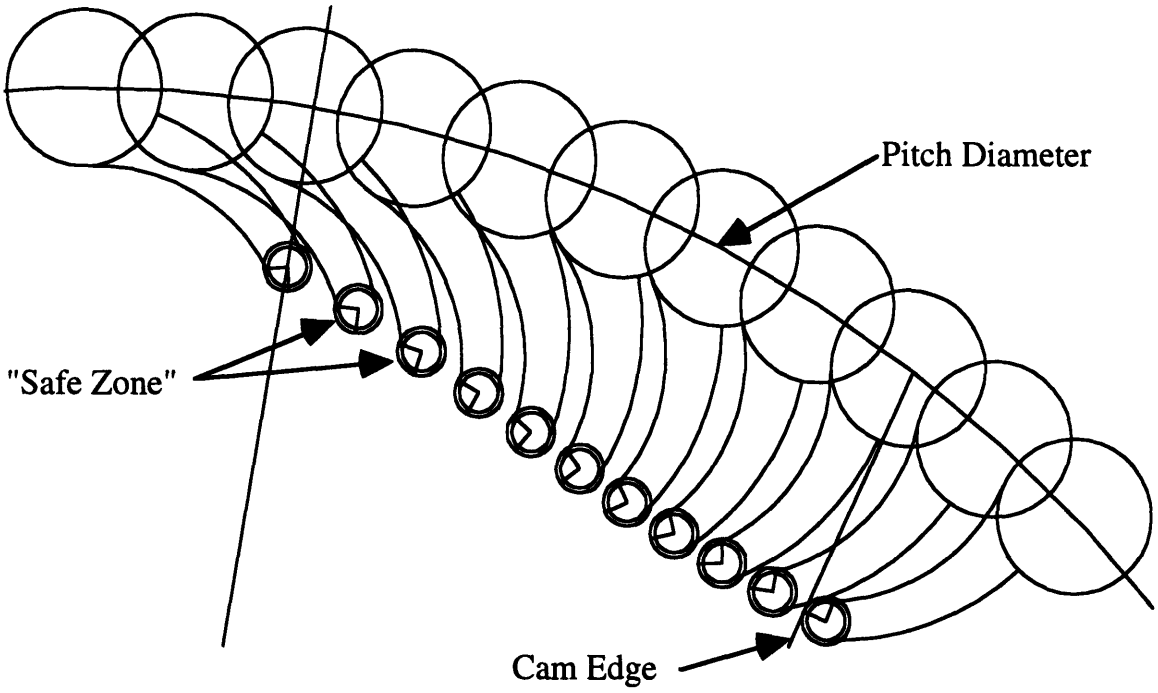

Figure 44: Ideal path of an opening cam follower.

toward the horizontal, then proceeded straight until roughly the third position from the left was reached, as represented in Figure 45, minus a few additional changes.

Closing the jaws proved to be even more difficult than opening them. Figure 46 shows a series of follower positions created in the same way as Figure 44's followers. It was again impossible to create a cam that ran tangent to each follower position within the safe zone. In fact, none of the closing follower positions lay in the realms of their safe zones. The only two alternatives were to maintain the jaws' fully open position for a time, then slam them shut by tapering immediately off (this alternative would keep the cam within the followers' safe zones), or run tangentially down the ideal path of positions, holding the jaws open until the opening force is exceeded by the other component. Since the jaws were spring loaded to

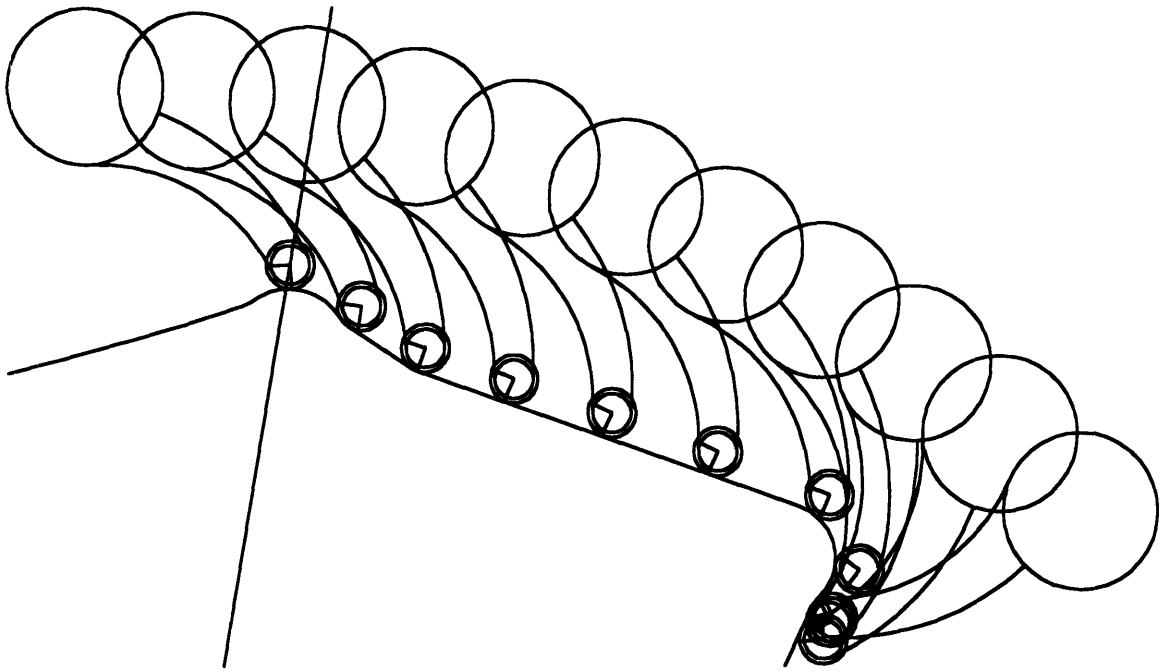

Figure 45: Final cam design and cam follower's resulting path (opening).

remain closed, reliability was less of an issue on this side of the cam. In the former alternative, the bearing would roll quickly along the cam, slamming the jaws shut. Although neither alternative was ideal, the latter case--which was the final design for the cam's left side--allowed the cam to close slightly before slamming shut, and the former did not. The path of tangents is traced in Figure 46.

4.4.7 Frame Design

The non-unique parts to the system included in this section were the motor and bearings, flanges that attached to the sprockets, which in turn attached to the main shafts, and the frame structures on either side.

Motor and bearings. Determining the proper requirements for these pieces of equipment was quite straightforward since the motor

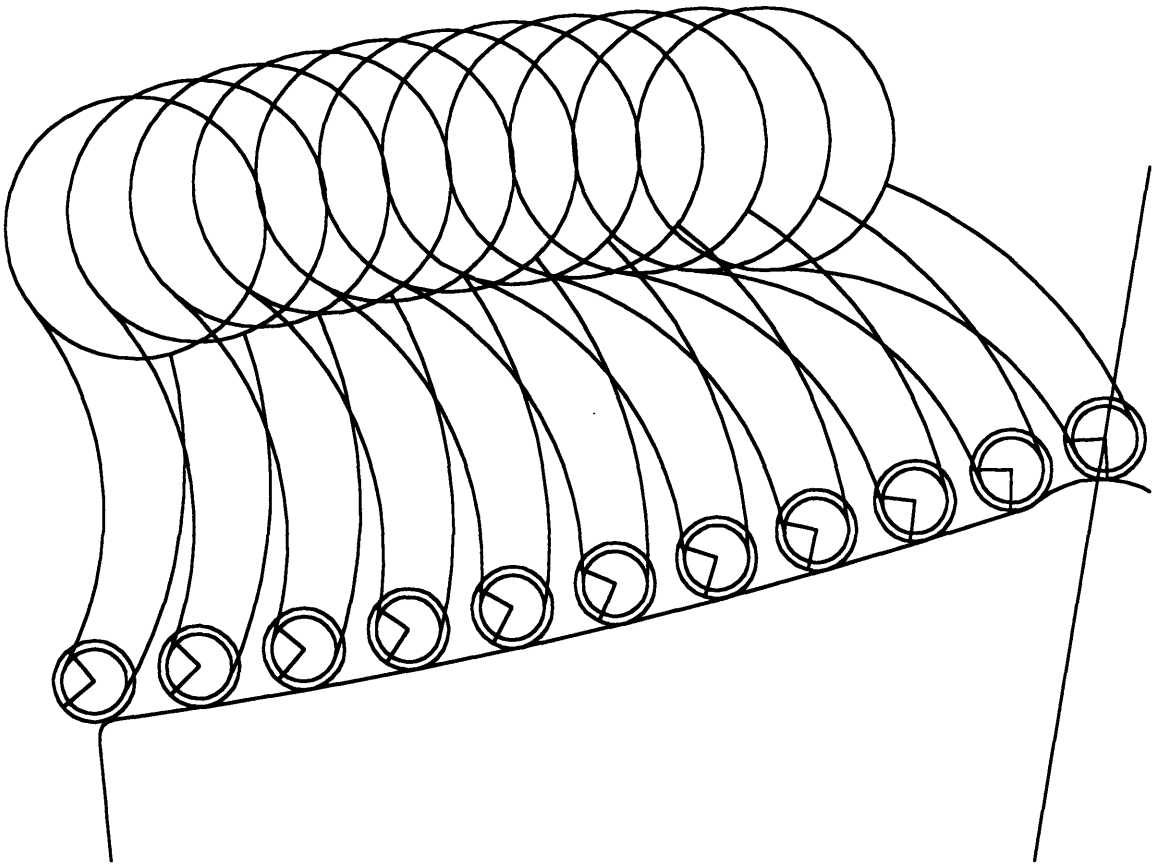

Figure 46: Closing cam path.

required minimal precision and no feedback, and the bearings did not require ABEC level precision. The motor's size was determined by multiplying the maximum torque (in.-lbf) it would see by its maximum possible speed. The design speed was 1000 rpm. The maximum torque t (in.-lbf) was the sum of the friction torque, the rotating members' inertial torque, and the chain's inertial torque, or

$$t = \mu T r_B + I\alpha + 0.25 m_C d_P^2 \alpha. \qquad (43)$$

Above, μ is the bearing's friction coefficient, T is the tension (lbf), r_B is the bearing radius (in.), I is the sprocket assembly's inertia (slugs-in.^{2}), α is the angular acceleration (rad/s^2), and m_C is the chain mass (slugs). Running torque was caused by the bearing friction. Angular

acceleration was based on 0 to 1000 rpm in 10 seconds. A Class II service factor was assumed. (This factor takes into account shock and duration of loading, and can be found in most motor manufacturers' catalogs.). Also, the following load schedule was assumed:

First month: 0-500 rpm, 8 h/day, 0.768 hp start, 0.02 hp run
Second month: 500 rpm, 24 h/day, 0.768 hp start, 0.02 hp run
Thereafter: 1000 rpm, 20-24 h/day, 1.40 hp start, 0.04 hp run.

The assumptions above and a fifty percent torque margin created the need for a two horsepower motor.

The bearings were also designed using standard formulas [19]. The desired life L was one year, 24 hours per day, at 1000 rpm. Reliability was chosen to be 0.99, and the load, i.e., tension, to be 250 lbf (500 lbf distributed over two bearings). From these figures and the formula

$$L = 16667a/n\ (C_E/T)^3, \qquad (44)$$

the effective load rating C_E was 3350 pounds. In the formula above, a--a factor based on the assumed reliability--was 0.21, based on the reliability, n was the rpm, and T was the tension (lbf). The bearing chosen was the smallest to have a C_E = 3395 pounds, and influenced future decisions on shaft and flange sizes.

Flanges and shafts. The flanges were machined from low carbon steel and housed the bearings using shoulders and retaining rings. Three $^1/_2$-13 bolts fastened the flanges to the sprockets. The bearing dimensions and appropriate wrench clearances sized the flanges. Each shaft was also made of low carbon steel according to the recommendations of the bearing catalog. The bearing bores

proved to be more than sufficient gages for shaft sizing. A series of stepped shoulders and retaining rings held all the parts in place.

Frames. Condensed assembly drawings are included as Figures 47 and 48, in which all the qualitative details of each frame stand out. However, in Figure 47, one area, the motor mounting technique, was removed for visual clarity. The mount consisted of a one-inch-thick aluminum plate containing two slots. In each slot resided a shim bolted to the motor frame and held to the mount plate by four screws. The plates in which the main shaft was mounted in Figure 48 were bolted via aluminum angles to a prefabricated movable crank/leadscrew base. This base rested on top of two aluminum box tubes with horizontal slots. Adjustment of the base within the slots and movement of the leadscrew's nut allowed for several square feet of travel in the horizontal plane.

Engineering drawings of all the prototype's pieces are enclosed in Appendix C.

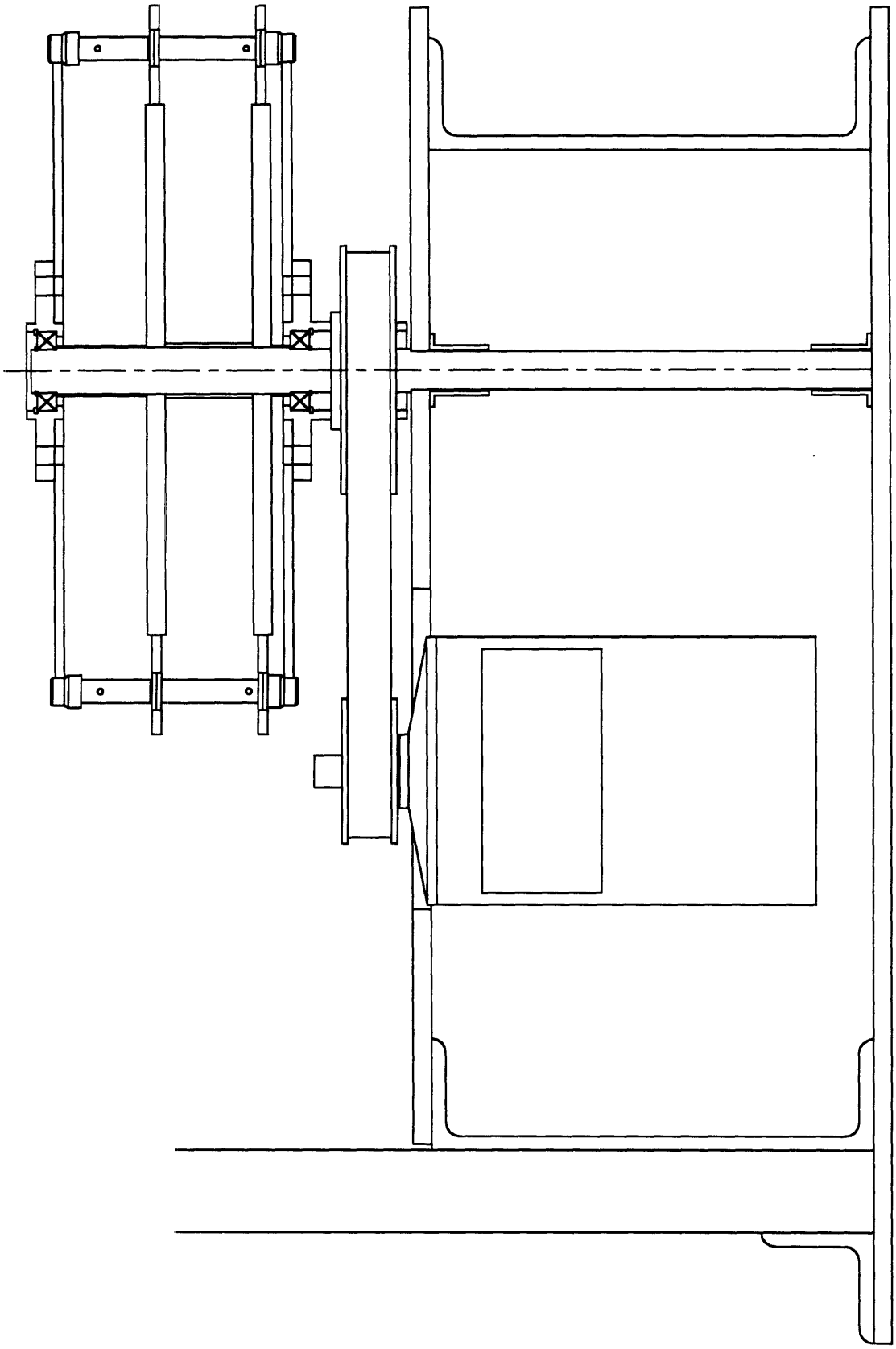

Figure 47: Assembly drawing of the design's driving unit.

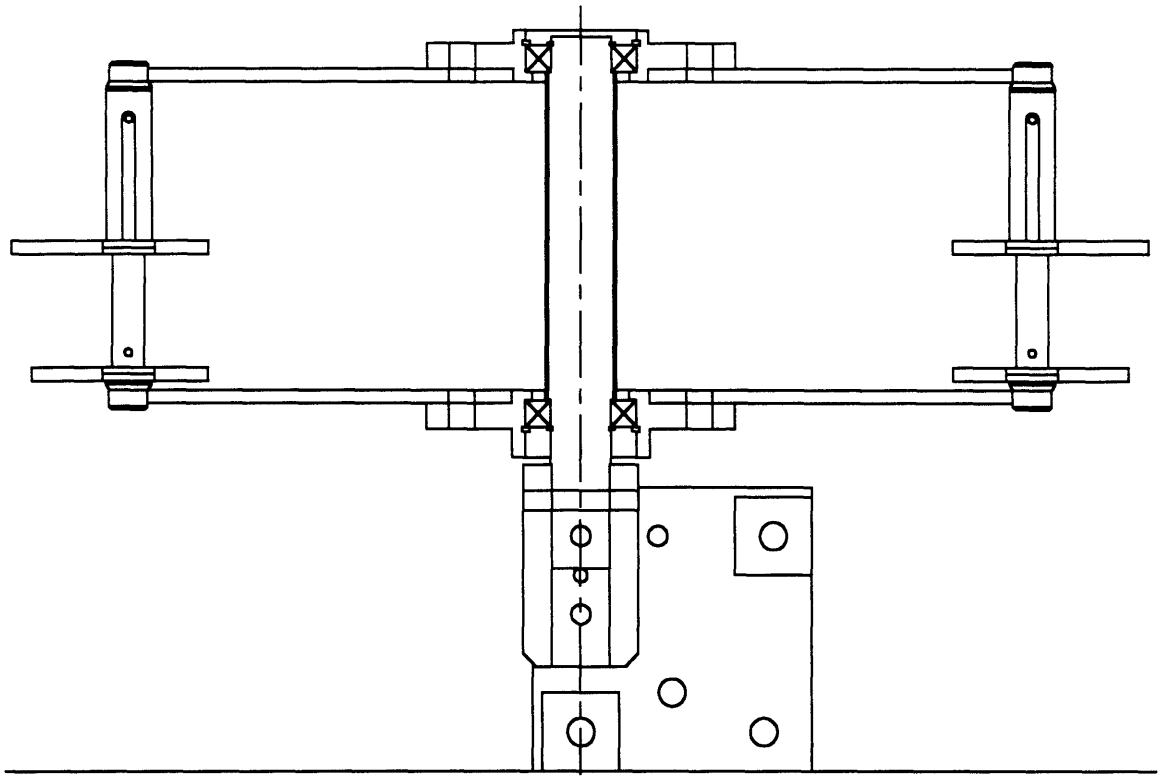

Figure 48: Assembly drawing of the design's driven unit.

CHAPTER 5: RESULTS

The cable/carrier prototype's main purpose was to evaluate whether a chain-like apparatus can effectively accept and transport parts through a series of manufacturing operations at rates comparable to or higher than current manufacturing standards. As a result, the machine exceeded expectations: it reliably took in ball point pens from a "homemade" vibratory feeder and transported them about the circumference of both sprockets. The feeder itself could not supply parts quickly enough to the apparatus--the only failed hand-offs occurred because of the feeder or feed track.

Operating speeds ranged from 5 to 90 rpm. In the prototype, the sprockets possessed 28 teeth each; 90 rpm corresponds to a feed rate of 2520 parts per minute--ten times the manufacturing norm--if each carrierless sprocket is replaced with a carrier. With the current configuration, carriers on sprockets spinning at 90 rpm were capable of picking up 840 parts per minute, well beyond the capabilities of a makeshift feeder. Conventional feed rates ranging from 50 to 300 parts per minute could be obtained at speeds as small as 10 rpm with this new device. Feeding and transporting would no longer present a potential bottleneck.

The remaining facets of the operation performed as expected. The cam followers opened and closed choppily, but consistently. Chordal action, and therefore forced vibrations, were extremely small. Low noise and smooth operation also came as benefits. The caps centered themselves more reliably than the mock-up's caps despite the angle change (this is because the caps centered

themselves from both sides of the sprocket instead of one, see Appendix C).

The system was run continuously at 82 rpm for a period of three hours. Eighty-two revolutions per minute corresponded to a feed rate of 769 parts per minute; consequently, no feeder was used in conjunction with this test. The carriers engaged with the sprockets at a rate of approximately 4610 per minute. After three hours and no missed engagements, this corresponded to a engagement reliability of 0.9999988, or no misses after over 830,000 engagements.

CHAPTER 6: CONCLUSIONS AND RECOMMENDATIONS

The goal of this thesis was to improve the disposable consumer goods manufacturing sector's competitive stance through a well thought out investment in a manufacturing line. The four most commonly increased parameters for such lines--yield, efficiency, speed, and flexibility--were compared to each other using overall cost savings as a basis; higher efficiency was found to improve best the bottom line. From there, a manufacturing line's inefficiencies were broken down into their components and analyzed individually to determine inefficiency's main cause--excessive transfer points. A single transfer point's inherent reliability may be extremely high, but when combined with both the time necessary to remedy a failed transfer and the thirty to fifty additional points that exist on typical manufacturing lines, efficiency drops severely.

A solution to the problem above, described previously, employs sprockets, carriers, and cable in a conveyor mechanism that drastically reduces the number of transfer points. The cable and carriers form a chain that resembles a rope ladder. The chain operates similarly to roller chain drive, but is capable of twisting about its direction of travel to orient its carriers (and therefore parts) without introducing additional transfers. The sprockets serve both to drive the system and to act as manufacturing stations, where operations such as assembly and printing could be performed on the parts as the carriers nest between the teeth. The line would pick up components from injection molders or stampers and not let go until the parts are complete and placed into packaging. An ideal system

can reduce the number of transfer points to only two: initial pickup and final dropoff.

To prove this concept, a prototype was designed consisting of the chain described above and two sprockets. The carriers' jaws were opened and closed by cams located between the sprockets, and accepted ball point pens as the sprockets turned. This was done to simulate some of the operations a full scale manufacturing line would have to undergo. The following conclusions can be drawn from the research described in this thesis:

1. The mock-up and prototype demonstrate that the concept of a positively controlling transport mechanism is completely feasible for both moving and orienting parts. This has been shown to work for a system employing carriers, sprockets, and cable.

2. When employed properly, this system can effectively reduce the number of transfer points to two per line. Previously, this number was approximately five times the number of manufacturing operations. Even with transfer point reliabilities as high as 0.99998, efficiency can be increased by as much as fifty percent, depending on the part's complexity and the current line's efficiency.

3. The first generation system designed here, when spinning at 100 rpm, can accept as many as 930 parts per minute, with the option of increasing to 2800 parts per minute. The rates attained by this prototype do not push this concept's limits; it is believed that a system employing guides and other safety precautions could easily

accept several thousand parts per minute. Feed rates this high virtually guarantee that part transferring and orienting would never again become a bottleneck.

4. The current system must overcome two major obstacles. At low speeds (feed rates below 1910 parts per minute), it must avoid excitation of the cable's harmonics through forced periodic (chordal) action. At higher speeds, carrier misalignment from centrifugal forces prevails; the effects of these problems and others can be minimized however, by following the recommendations below.

Several variables--chain pitch, number of sprocket teeth, cable tension, sprocket speed, carrier weight, sprocket center distance, carrier spring constant, and carrier cap angle--needed to be simultaneously weighed against one another to determine a working system that fulfilled the guidelines described in Chapter 3. Each of these had to be chosen carefully so as not to upset greatly the effects of other variables. For example, a higher pitch increased the system's fatigue life and overall clearances and decreased the highest natural frequency, but in the process it exacerbated forcing vibrations, jacked up impact velocities, and promoted galling. Table VIII, which summarizes the effects of increasing each variable on various responses of the system, can be helpful in determining changes to be implemented on future transfer lines employing cables.

In this table, an upwardly pointing arrow represents an improvement in the response; a downward arrow means a decline in

performance. Arrows in parentheses symbolize indirect changes in performance. It should be clarified that the natural frequency response variable is considered "better" at lower values. This may not be the case for lines requiring low feed rates, and should be reversed accordingly.

Table VIII: Effects of Design Variable Increases on System Response

	Carrier Positioning	Impact Velocity	Natural Frequency	Forced Vibration	Fatigue Life	Sprocket Engagement	Part Feeding	Galling	Carrier Clearance	Machine Clearance	Recommendation
Chain pitch, P	–	⇓	⇑	⇓	⇑	⇓	–	⇓	⇑	⇑	low
No. of teeth, N	⇓	⇑	–	⇑	⇑	⇑	–	⇓	(⇓)	(⇓)	high
Cable tension, T	⇑	(⇑)	⇓	–	⇓	(⇓)	(⇑)	⇓	–	–	low
Sprocket speed, n	⇓	⇓	–	–	⇑	–	⇓	⇓	–	(⇓)	low
Carrier weight, w	⇓	⇓	⇑	–	–	(⇑)	–	(⇓)	(⇓)	–	low
Cable span, S	(⇑)	(⇑)	(⇓)	–	–	⇑	–	(⇓)	–	(⇑)	depends
Spring constant, k	⇓	–	–	–	–	–	⇑	–	–	–	depends
Cap angle, phi	(⇑)	(⇑)	–	–	–	⇓	(⇓)	–	–	(⇑)	depends

Many changes that could greatly increase the system's performance are relatively simple to implement, such as replacing the carrier's springs (preferably with a torsion spring) and redesigning the carrier to accommodate it. This would decrease the part count (by eliminating the dowel pins) and increase the carrier's long term reliability. If a torsion spring does not exist within the geometric constraints that can impose a two to three pound force on

the part, experiments should be performed to determine if smaller gripping forces are sufficient.

Another simple change that would decrease cost, friction, and weight would be to investigate replacing the carrier mechanisms with injection-molded parts. A hard plastic such as phenolic, polycarbonate, polystyrene, or any reinforced polymer would suffice. Polymers are less expensive per pound to purchase and form than aluminum or other metals and allow for design detail in all three dimensions (if necessary). Also, they have higher strength-to-weight and stiffness-to-weight ratios than most metals.

In reforming the carriers, special attention should be given to the cam followers and cam. The prototype forced the sprocket spacing rods out into the sprocket teeth, allowing for a larger maximum cam radius. As shown in subsection 4.4.6, the cam followers can be shortened and modified on redesigned carriers to operate more smoothly without losing reliability. (This change was not implemented in the prototype due to the excessive time and cost of CNC machining new carriers.)

Another worthwhile change would be to replace the current cable with one that fulfilled all the requirements of the cable design section. A good starting point would be Kevlar™ or polyethylene fibers pultruded with polyethylene. Pultrusion, which involves pulling the fibers and a molten matrix material through a die, results in a cable that would create the fiber-to-sleeve adhesion necessary to give the same properties as before without the complications. The means for fastening the cable to the shaft can be modified or improved to accommodate the new cable.

The suggestions above focus primarily on reducing weight; however, another broad recommendation is to increase the system's safety. Recommendations to accomplish this include enclosing the line within a cage, installing emergency stop buttons, and incorporating a wire within the chain that stops the sprockets if the chain breaks. The sprockets' inertia can be reduced by replacing the sprocket material with a stiff polymer such as reinforced polyester or acetal and by decreasing the diameter to as small as possible without sacrificing performance.

Installing friction-free roller guides (roller tracks or low friction sliding tracks) along the path of the carriers could also improve both safety and performance. If safety is a large issue, the guides would act to restrain a broken cable within its path. Also, installing guides would practically eliminate the need for considering dynamic effects (if these prove to be a problem) and boost the system's engagement reliability by at least an order of magnitude. These tracks would guide the caps into the sprockets, through twist orientations, and through straight-line manufacturing operations.

Other recommendations for improvement--such as the idea of a third cable--are for the long term and involve more conceptual planning. This cable can act to maintain the pitch accurately and apply tension, while the other two may be axially flexible and stretch to engage with a twisted sprocket more reliably. Perhaps this cable could also be the safety wire discussed above.

Another large-scale effort that could reduce the number of transfer points to only two encompasses designing a machine that extracts the parts directly from the forming machines. To

complement the more efficient transfer line, a more efficient buffer that would be smaller and able to interact with the line if there were a machine shutdown can be designed.

These recommendations would easily boost the performance of this system to levels of efficiency and speed far beyond current manufacturing standards. The preliminary results were encouraging and should only improve. In conclusion, this technology shows great promise for the manufacturing sector's future.

REFERENCES

1. United States Bureau of Labor Statistics, *Employment and Earnings*, March 1992.

2. Schloemer, P. G. "Let's Get America Back to Business," *Industry Week*. Volume 241, issue 7 (April 6, 1992).

3. Garelli, Stéphane et. al. *The World Competitiveness Report 1992*. IMD: Lausanne, Switzerland, 1992.

4. Smith, L. and Kaden, L. B. *Rebuilding Economic Strength*. M. E. Sharpe: Armonk, New York, 1992.

5. Sutton, J. R. Untitled. *Industrial Engineering*. Volume 22, issue 5 (May 1990) pp. 14-5.

6. United States Bureau of Labor Statistics, *Report 844*, April 1993.

7. Richard, J. R. "Conveyor For Objects Treated While Continuously In Motion," United States Patent No. 4,533,038. August 6, 1985.

8. Brooke, A. A. "Article Handling Apparatus," United States Patent No. 3,837,474. September 24, 1974.

9. Puppel, A. and Dalferth, H. H. "Chain Conveyor," United States Patent No. 4,320,827. March 23, 1982.

10. W. M. Berg, Inc. Manufacturer's catalog: East Rockaway, New Jersey, 1992.

11. Korsakov, V. S. and Zamyatin, V. K. *Assembly Practice in Machine Building*. Mir Publishers: Moscow, 1987.

12. The Torrington Company. Service Catalog: Torrington, Connecticut, 1988.

13. Slocum, A. H. *Precision Machine Design*. Prentice-Hall, Inc.: Englewood Cliffs, New Jersey, 1992.

14. Baumeister, T. and Marks, L. S. *Standard Handbook for Mechanical Engineers*. McGraw-Hill: New York, 1967.

15. Binder, R. C. *Mechanics of the Roller Chain Drive.* Prentice-Hall, Inc.: Englewood Cliffs, New Jersey, 1956.

16. Binder, R. C. and Mize, G. G. "Strand Vibrations in a Roller Chain Drive," *Journal of the Franklin Institute*, Volume 247, No. 1 (1949) pp. 25-32.

17. Binder, R. C. and Covert, W. V. "Impact between Chain Roller and Sprocket in a Chain Drive," *Journal of the Franklin Institute*, Volume 245, No. 4 (1948) pp. 319-329.

18. Faulkner, L. L. and Menkes, S. B. *Chains for Power Transmission and Material Handling.* Marcel Dekker, Inc.: New York, 1982.

19. Shigley, J. E. and Mischke, C. R. *Mechanical Engineering Design.* McGraw-Hill: New York, 1989.

BIBLIOGRAPHY

Bolz, H. A. and Hagemann, G. E. *Materials Handling Handbook.* The Ronald Press Company: New York, 1958.

Goldsmith, W. *Impact: The Theory and Behaviour of Colliding Solids.* Edward Arnold Publishers: London, 1959.

Kalpakjian, S. *Manufacturing Engineering and Technology.* Addison-Wesley: Reading, Massachusetts, 1992.

Newnan, D. G. *Engineering Economic Analysis, 4th ed.* Engineering Press, Inc.: San Jose, California, 1991.

Oberg, E. et. al. *Machinery's Handbook, 24th ed.* Industrial Press, Inc.: New York, 1992.

Poli, C. "Techniques for Feeding and Orienting Small Parts," *Computer Aided Manufacturing, Part II: Recent Advances in the Automation of Discrete Product Manufacturing.* MIT Press: Cambridge, Massachusetts, 1978.

Sharon, A. and Pennisi, F. J., Jr. "Transport Apparatus Having a Flexible Member for Reorienting Articles During Processing and Method of Using Same." United States Patent Application No. 147,770 filed November 4, 1993.

Webb, R. M. *Automated Assembling, parts 2-4.* The Institution of Production Engineers: London, 1984.

APPENDIX A:
Design Considerations of Alternative Springs

Figure 40 displays the four types of springs that were studied: linear coil, elastic band, torsion coil, and leaf plate. The elastic band was chosen because it fit the system's requirements, and was sufficient to prove the concept demonstrated by the prototype. Unfortunately, insufficent time was available to research thoroughly the inifinite number of other spring configurations available. Below is a summary of the remaining three springs, and the formulas and assumptions used to design them.

Linear coil. As mentioned before, a linear coil spring would attach itself to the spring posts of each carrier half and act in much the same way as the elastic band. The linear coil spring had to satisfy three conditions: it had to 1) fit within the geometry of the carrier, 2) provide two to three pounds of gripping force to the part, and 3) not yield or fatigue when cyclically opened and closed between zero and eighty-six degrees.

These conditions were satisfied by examining the spring constant and spring stress at two points of rotation: closed with a part and completely open. The spring constant k (lbf/in.) was determined by the formula

$$k = d^4G / 8D^3N,$$

where d was the wire diameter (in.), G was the shear modulus (psi), D was the mean coil diameter (in.), and N was the number of coils. The spring constant was multiplied by the spring's displacement to arrive at the spring force F (lbf). When holding the part this force had to correspond to a gripping force between two and three pounds.

Also, this force produced a shearing stress τ (psi) in the coils defined by the equation

$$\tau = 8KFD / \pi d^3,$$

where

$$K = (4C + 2) / (4C - 3)$$

and

$$C = D / d.$$

The ratio C was constrained to fall between 4 and 16; beyond this range, some of the equations above may break down. Typical C values range from 6 to 12.

The safety factor n against fatigue was determined from the equation

$$\frac{\tau}{S_{se}} + \frac{\tau}{S_{su}} = \frac{2}{n},$$

where S_{se}, the endurance shear strength, equaled 45.0 ksi for all springs (conservatively), the ultimate shear strength (ksi)

$$S_{su} = 0.67A / d^m,$$

and A and m were constants that varied with the spring's material. Music wire, the most frequently used spring material, has constants A = 186 ksi, m = 0.163, and G = 11.5 Msi.

The equations above were used in conjunction with the carrier's dimensions to create a series of spreadsheets, which assisted in outputting properties for many combinations of parameters. An example of one the spreadsheets is shown in Table A1. In these sheets, Fpart and Spart were the spring force and spring stress corresponding to holding the part, and Fopen and Sopen corresponded to the spring force and stress from being completely

Table A1: Sample Linear Spring Calculations

Property	Value	d	D	k	Fpart	Fopen	C	Kb	Sut	Spart	Sopen	n
Inner Diameter (Di):	0.0875	0.009	0.097	0.11	0.01	0.10	10.72	1.125	400.8	7.5	36.6	2.639
Degrees with Part:	16	0.010	0.098	0.16	0.02	0.14	9.75	1.139	394.0	8.2	40.4	2.389
Gripping Force:	2.5	0.011	0.099	0.22	0.03	0.20	8.95	1.152	387.9	9.0	44.0	2.186
Degrees when Open:	86	0.012	0.100	0.31	0.04	0.28	8.29	1.166	382.5	9.7	47.6	2.017
Endurance Strength:	45	0.013	0.101	0.41	0.06	0.37	7.73	1.179	377.5	10.4	51.1	1.874
Elastic Modulus:	3.00E+07	0.014	0.102	0.54	0.08	0.49	7.25	1.192	373.0	11.1	54.6	1.752
Extension Length:	0	0.016	0.104	0.86	0.12	0.78	6.47	1.219	365.0	12.5	61.3	1.555
A (Ultimate Strength):	186	0.018	0.106	1.31	0.18	1.18	5.86	1.245	358.0	13.8	67.8	1.402
m (Ultimate Strength):	0.163	0.020	0.108	1.88	0.26	1.70	5.38	1.270	351.9	15.1	74.0	1.280
Number of Coils:	100	0.022	0.110	2.61	0.36	2.36	4.98	1.296	346.5	16.3	80.1	1.180
Center/Center Dist.:	0.875	0.024	0.112	3.50	0.49	3.17	4.65	1.321	341.6	17.5	85.9	1.098
Poisson's Ratio:	0.282	0.026	0.114	4.57	0.64	4.13	4.37	1.346	337.2	18.7	91.5	1.028
Spring Distance:	0.663	0.029	0.117	6.54	0.91	5.92	4.02	1.383	331.2	20.3	99.5	0.943
		0.031	0.119	8.12	1.14	7.34	3.82	1.407	327.7	21.3	104.6	0.895
Music Wire		0.033	0.121	9.91	1.39	8.96	3.65	1.431	324.3	22.3	109.5	0.853
		0.035	0.123	11.94	1.67	10.80	3.50	1.455	321.2	23.3	114.3	0.817
		0.037	0.125	14.20	1.99	12.85	3.36	1.478	318.3	24.2	118.8	0.784
		0.039	0.127	16.71	2.34	15.12	3.24	1.501	315.6	25.1	123.2	0.755
		0.041	0.129	19.48	2.72	17.61	3.13	1.524	313.1	26.0	127.5	0.729
		0.043	0.131	22.50	3.15	20.35	3.03	1.547	310.6	26.8	131.6	0.705
		0.045	0.133	25.78	3.61	23.32	2.94	1.570	308.3	27.7	135.5	0.684
		0.047	0.135	29.33	4.10	26.53	2.86	1.592	306.2	28.4	139.3	0.664
		0.049	0.137	33.15	4.64	29.98	2.79	1.614	304.1	29.2	143.0	0.646
		0.051	0.139	37.24	5.21	33.68	2.72	1.636	302.1	29.9	146.5	0.630
		0.055	0.143	46.25	6.47	41.83	2.59	1.679	298.4	31.3	153.2	0.601
		0.059	0.147	56.36	7.88	50.97	2.48	1.721	295.0	32.5	159.4	0.576

open. The parameters of most interest are Fpart, C, and n. Again, Fpart had to range from two to three, C had to fall between four and sixteen, and n had to be large (at least greater than one). As shown from the sample spreadsheets (Tables A1 and A2), as d decreased, n approached one, but by the time n exceeded one, Fpart had dropped below two pounds. Changing the outside diameter (D) and the number of spring coils (N) did not help. Table A2 demonstrates that the same conditions with a different D and N did not affect significantly these results.

If a spring is found that does match these conditions, it also has to fall within the geomtric constraint that its solid length L_S (the spring's length when fully compressed) had to be smaller than the distance between spring posts. This length equaled the product of the number of coils (N) and the wire diameter (d), plus the spring diameter (D), which represented the space required by the hooks on each end.

In conclusion, many variable combinations were tried in an attempt to discover a linear spring that satisfied the conditions set by the carrier's geometry, the part's gripping force, and the spring's strength. Unfortunately, none were found. If additional combinations can be achieved by modifying the constraints, it is believed that an appropriate linear spring will emerge from the calculations.

Torsion coil. The torsion coil spring is most likely the best candidate for replacing the elastic band. Not only does its rotary nature accommodate a rotating carrier well, but it also can fit around the carrier shaft (either between the carrier halves or under the

Table A2: Sample Linear Spring Calculations: Different D, N

Property	Value	d	D	k	Fpart	Fopen	C	Kb	Sut	Spart	Sopen	n
Inner Diameter (Di):	0.125	0.009	0.134	0.08	0.01	0.07	14.89	1.088	400.8	7.5	36.7	2.630
Degrees with Part:	16	0.010	0.135	0.12	0.02	0.11	13.50	1.098	394.0	8.3	40.6	2.376
Gripping Force:	2.5	0.011	0.136	0.17	0.02	0.15	12.36	1.108	387.9	9.1	44.4	2.168
Degrees when Open:	86	0.012	0.137	0.24	0.03	0.21	11.42	1.117	382.5	9.8	48.1	1.995
Endurance Strength:	45	0.013	0.138	0.32	0.04	0.29	10.62	1.127	377.5	10.6	51.8	1.849
Elastic Modulus:	3.00E+07	0.014	0.139	0.42	0.06	0.38	9.93	1.136	373.0	11.3	55.5	1.724
Extension Length:	0	0.016	0.141	0.68	0.10	0.62	8.81	1.155	365.0	12.8	62.6	1.522
A (Ultimate Strength):	186	0.018	0.143	1.05	0.15	0.95	7.94	1.174	358.0	14.2	69.6	1.365
m (Ultimate Strength):	0.163	0.020	0.145	1.54	0.21	1.39	7.25	1.192	351.9	15.6	76.4	1.240
Number of Coils:	50	0.022	0.147	2.16	0.30	1.95	6.68	1.211	346.5	16.9	83.0	1.138
Center/Center Dist.:	0.875	0.024	0.149	2.93	0.41	2.65	6.21	1.229	341.6	18.3	89.5	1.054
Poisson's Ratio:	0.282	0.026	0.151	3.88	0.54	3.51	5.81	1.247	337.2	19.5	95.8	0.982
Spring Distance:	0.663	0.029	0.154	5.66	0.79	5.12	5.31	1.274	331.2	21.4	104.9	0.894
		0.031	0.156	7.12	0.99	6.43	5.03	1.292	327.7	22.6	110.9	0.845
Music Wire		0.033	0.158	8.79	1.23	7.95	4.79	1.310	324.3	23.8	116.6	0.801
		0.035	0.160	10.72	1.50	9.69	4.57	1.327	321.2	24.9	122.2	0.763
		0.037	0.162	12.89	1.80	11.66	4.38	1.345	318.3	26.1	127.7	0.730
		0.039	0.164	15.34	2.15	13.87	4.21	1.362	315.6	27.1	133.0	0.699
		0.041	0.166	18.07	2.53	16.34	4.05	1.379	313.1	28.2	138.2	0.672
		0.043	0.168	21.09	2.95	19.07	3.91	1.396	310.6	29.2	143.3	0.647
		0.045	0.170	24.41	3.41	22.08	3.78	1.413	308.3	30.2	148.2	0.625
		0.047	0.172	28.05	3.92	25.37	3.66	1.430	306.2	31.2	153.0	0.605
		0.049	0.174	32.01	4.48	28.95	3.55	1.446	304.1	32.2	157.7	0.586
		0.051	0.176	36.30	5.08	32.83	3.45	1.463	302.1	33.1	162.2	0.569
		0.055	0.180	45.90	6.42	41.51	3.27	1.495	298.4	34.9	171.0	0.538
		0.059	0.184	56.90	7.96	51.45	3.12	1.528	295.0	36.6	179.3	0.512

entire carrier), minimizing complications that currently arise with clearance.

The torsion coil spring used nearly the same constraints as the linear coil spring: it had to fit within the carrier's geomtric constraints, apply two to three pounds of gripping force and resist yield and fatigue when fully opened and closed. It also had roughly the same equations. The new equations are listed below.

$$k = d^4E \;/\; 10.8DN$$

$$S_u = A \;/\; d^m$$

$$\sigma = 16K_iFD \;/\; \pi d^3$$

$$K_i = (4C^2 - C - 1) \;/\; [4C(C - 1)]$$

$$\frac{\sigma}{S_e} + \frac{\sigma}{S_u} = \frac{2}{n}$$

Above, k is the spring constant (lbf/turn), E is the elastic modulus (psi), σ is the spring's bending stress (psi), S_e is the spring's endurance strength (psi), and S_u is the spring's ultimate strength (psi). S_e is typically 78.0 ksi for most springs. The remaining variables maintain the same definitions given for linear springs.

The carrier shaft diameter constrains the spring's diameter (D) to fall within 0.5 and 0.75 inches, and C must still remain between 4 and 16. Besides this, only Fpart and n constrained the spring. Tables A3 and A4 show some spreadsheet results.

Once again, no spring was found that fit all the constraints. The tables show that as d decreased, the safety factor went up but the gripping force dropped. Any spring combination with safety factors greater than one could not grip a part with two to three pounds of force.

Table A3: Sample Torsion Spring Calculations

Property	Value	d	D	k	Fpart	Fopen	C	Ki	Sut	Spart	Sopen	n
Inner Diameter (Di):	0.75	0.095	0.845	9.04	2.88	32.10	8.89	1.091	273.0	18.1	175.9	0.690
Degrees with Part:	16	0.090	0.840	7.32	2.34	26.17	9.33	1.087	275.4	17.0	166.9	0.728
Gripping Force:	2.5	0.085	0.835	5.86	1.87	21.07	9.82	1.082	278.0	16.0	157.9	0.772
Degrees when Open:	86	0.080	0.830	4.63	1.48	16.73	10.38	1.077	280.7	15.0	148.8	0.820
Safety Factor (n):	1.4	0.075	0.825	3.60	1.15	13.08	11.00	1.073	283.7	14.0	139.8	0.875
Endurance Strength:	78	0.071	0.821	2.90	0.93	10.61	11.56	1.069	286.3	13.2	132.5	0.925
Elastic Modulus:	3.00E+07	0.067	0.817	2.31	0.74	8.50	12.19	1.065	289.0	12.4	125.2	0.981
Extension Length:	0	0.063	0.813	1.82	0.58	6.71	12.90	1.061	291.9	11.6	117.9	1.044
A (Ultimate Strength):	186	0.059	0.809	1.40	0.45	5.21	13.71	1.058	295.0	10.9	110.5	1.116
m (Ultimate Strength):	0.163	0.055	0.805	1.07	0.34	3.97	14.64	1.054	298.4	10.1	103.2	1.198
Number of Coils:	5	0.051	0.801	0.79	0.25	2.97	15.71	1.050	302.1	9.3	95.8	1.294
Center/Center Dist.:	0.875	0.049	0.799	0.68	0.22	2.54	16.31	1.048	304.1	8.9	92.1	1.348
		0.047	0.797	0.57	0.18	2.16	16.96	1.046	306.2	8.6	88.4	1.406
Music Wire		0.045	0.795	0.48	0.15	1.83	17.67	1.044	308.3	8.2	84.7	1.470
		0.043	0.793	0.40	0.13	1.53	18.44	1.042	310.6	7.8	81.0	1.539
		0.041	0.791	0.33	0.11	1.27	19.29	1.040	313.1	7.4	77.3	1.616

Table A4: Sample Torsion Spring Calculations: Different D, N

Property	Value	d	D	k	Fpart	Fopen	C	Ki	Sut	Spart	Sopen	n
Inner Diameter (Di):	1	0.095	1.095	9.96	3.18	27.31	11.53	1.069	273.0	25.3	189.9	0.639
Degrees with Part:	16	0.090	1.090	8.06	2.57	22.20	12.11	1.066	275.4	23.9	180.2	0.675
Gripping Force:	2.5	0.085	1.085	6.44	2.06	17.83	12.76	1.062	278.0	22.5	170.4	0.715
Degrees when Open:	86	0.080	1.080	5.08	1.62	14.12	13.50	1.059	280.7	21.1	160.6	0.760
Safety Factor (n):	1.4	0.075	1.075	3.94	1.26	11.01	14.33	1.055	283.7	19.7	150.7	0.812
Endurance Strength:	78	0.071	1.071	3.18	1.01	8.91	15.08	1.052	286.3	18.6	142.8	0.858
Elastic Modulus:	3.00E+07	0.067	1.067	2.53	0.81	7.12	15.93	1.049	289.0	17.5	134.9	0.911
Extension Length:	0	0.063	1.063	1.98	0.63	5.60	16.87	1.046	291.9	16.4	127.0	0.970
A (Ultimate Strength):	186	0.059	1.059	1.53	0.49	4.34	17.95	1.043	295.0	15.3	119.0	1.037
m (Ultimate Strength):	0.163	0.055	1.055	1.16	0.37	3.31	19.18	1.041	298.4	14.2	111.1	1.113
Number of Coils:	3.5	0.051	1.051	0.86	0.28	2.46	20.61	1.038	302.1	13.2	103.1	1.203
Center/Center Dist.:	0.875	0.049	1.049	0.74	0.23	2.11	21.41	1.036	304.1	12.6	99.1	1.253
		0.047	1.047	0.62	0.20	1.79	22.28	1.035	306.2	12.1	95.1	1.307
Music Wire		0.045	1.045	0.53	0.17	1.51	23.22	1.033	308.3	11.6	91.1	1.367
		0.043	1.043	0.44	0.14	1.26	24.26	1.032	310.6	11.0	87.1	1.432
		0.041	1.041	0.36	0.12	1.05	25.39	1.030	313.1	10.5	83.1	1.503

Leaf plate. The leaf spring (part (d) of Figure 40) was the most complex spring to design and put into practice. This spring required a detailed and tedious analysis involving curved beam deflection and stress theories. The equations listed below serve only to outline a basis upon which to start calculations; these can be expanded to give a complete analysis.

The spring is assumed to be bent in its center with a radius R (in.) and have two legs of length L (in.) extending into slots cut into the carrier (Figure A1). Its thickness, h (in.), assists in determining the spring's stiffness.

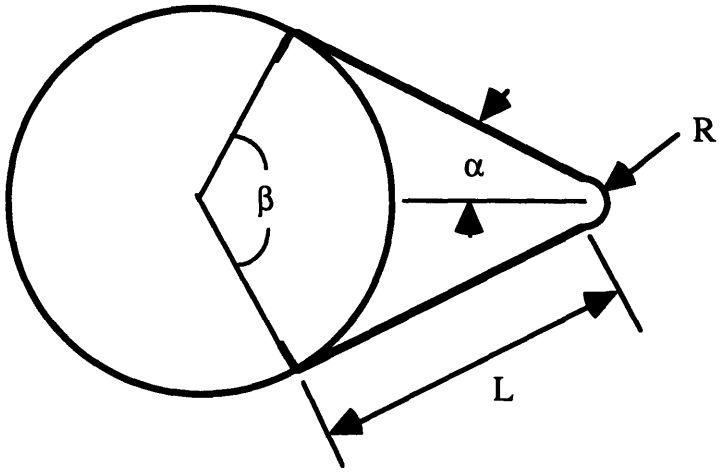

Figure A1: Definitions of leaf spring's variables.

Due to the spring's complex shape, the spring constant must be determined using Castigliano's theorem [19]. The deflection of the spring can be related to the force by taking the derivative (with respect to F) of each of the terms in the equation

$$U = \int \left(\frac{M^2}{2AeE} + \frac{(F\sin\theta)^2 R}{2AE} - \frac{MF\sin\theta}{AE} + \frac{CR(F\cos\theta)^2}{2AG}\right) d\theta,$$

and intergrating. Above, M is the bending moment (lbf-in.), equal to

$$M = FR\sin\theta + FL,$$

A is the cross-sectional area (in.^{2}), e, the eccentricity of the curved portion (in.), equals

$$e = R - r_n,$$

where

$$r_n = \frac{h}{\ln\frac{2R+h}{2R-h}},$$

E is the elastic modulus (psi), F is the force applied (lbf), G is the shear modulus (psi), C is a correction factor (for rectangular cross sections, it equals 1.50), and θ is a dummy variable (ranging from zero to (π - 2α)), about which the equation is integrated. The sizable analytical result would produce an accurate relation between force and deflection.

Determining the spring's stress is more straightforward. The force acting on the spring as a function and α, β, and F_o (the applied force) equals

$$F = F_o\cos(0.5\beta + \alpha),$$

which results in differing stresses on the inside and outside surfaces, σ_i and σ_o:

$$\sigma_i = \frac{F(R+L)(r_n - R + \frac{h}{2})}{bhe(R - \frac{h}{2})}$$

$$\sigma_o = \frac{F(R+L)(R + \frac{h}{2} - r_n)}{bhe(R + \frac{h}{2})}.$$

In the equations above, b is the rectangular spring's width (in.). α and β are related by the equation

$$L\sin\alpha + R\cos\alpha - \sin(\beta/2) = 0.$$

The resulting stresses can be plugged into the equation

$$n = \frac{2S_e S_{ut}}{\sigma(S_{ut} + S_e)}$$

to obtain the safety factors. S_e, the spring's endurance strength, equals

$$S_e = 945 S_{ut}^{0.282}(bh)^{-0.0567}$$

for steels, and S_{ut}, the ultimate tensile strength, varies with type and heat treatment of the steel. Typical heat treatments used on steels for springs results in a bluish tint to the steel; this steel is commonly referred to as spring steel, and has an ultimate strength ranging from 55 to 135 ksi, depending on the carbon content and other alloying components.

Unfortunately, the parameters α, β, L, F, and R, and therefore the other parameters affected by these values, change as the spring opens and closes. The resulting problem may be simplified best by analytically determining the relationships between each variable as the spring opens (and closes), and using time averages of each of the variables. A conservative spring design would use the values of each variable that would maximize (or minimize) each of the spring's properties. Another simplifying assumption would keep the straight portions straight and the curved portions curved while the spring opens, or

$$\alpha R = (\text{constant})$$

over all of α. As a rule of thumb, the minimum attainable radius of hardened low-carbon steels is approximately four times its thickness.

In summary, designing and applying a leaf plate spring is difficult at best. The calculations typically result in accumulated

errors (through time averaging) or excessively conservative results--an effective design can be realized, however, by employing more sophisticated analytical techniques. It was decided that for this thesis, however, the calculations and effort involved in selecting a spring that was not best suited to the carrier would not yield sufficient reward.

APPENDIX B:
Sprocket Tooth Layout

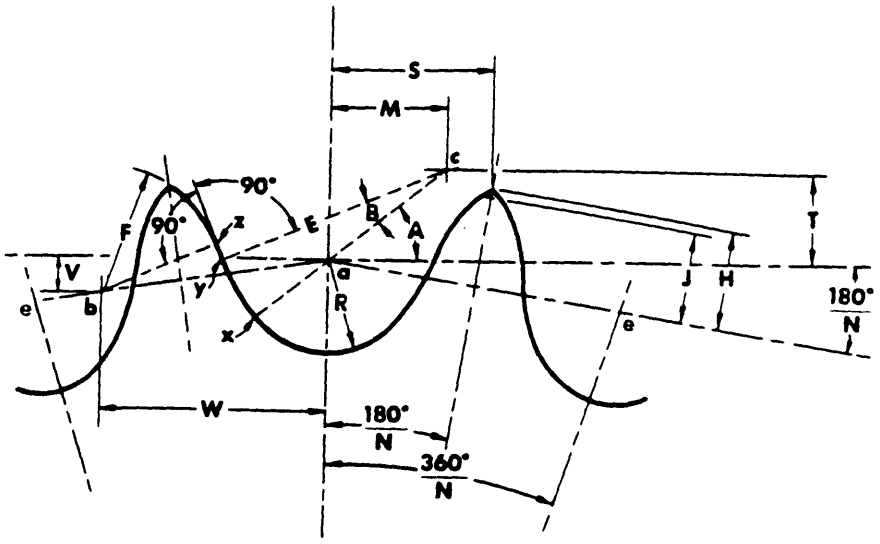

P = CHAIN PITCH (in)

N = NUMBER OF TEETH

D_r = ROLLER DIAMETER

D_s (SEATING CURVE DIAMETER) = 1.005 D_r + 0.003

$R = \frac{D_s}{2} = 0.5025\ D_r + 0.0015$

$A = 35° + \frac{60°}{N}$

$B = 18° - \frac{56°}{N}$

$ac = 0.8\ D_r$

$M = 0.8 D_r \cos\left(35° + \frac{60°}{N}\right)$

$T = 0.8\ D_r \sin\left(35° + \frac{60°}{N}\right)$

$E = 1.3025\ D_r + 0.0015$

CHORDAL LENGTH OF ARC $xy = (2.605\ D_r + 0.003) \sin\left(9° - \frac{28°}{N}\right)$

$yz = D_r\left[1.4 \sin\left(17° - \frac{64°}{N}\right) - 0.8 \sin\left(18° - \frac{56°}{N}\right)\right]$

$ab = 1.4\ D_r$

$W = 1.4\ D_r \cos\frac{180°}{N}$

$V = 1.4\ D_r \sin\frac{180°}{N}$

$F = D_r\left[0.8 \cos\left(18° - \frac{56°}{N}\right) + 1.4 \cos\left(17° - \frac{64°}{N}\right) - 1.3025\right] - .0015$

$H = \sqrt{F^2 - \left(1.4\ D_r - \frac{P}{2}\right)^2}$

$S = \frac{P}{2} \cos\frac{180°}{N} + H \sin\frac{180°}{N}$

APPROXIMATE OUTSIDE DIAMETER OF SPROCKET WHEN J IS 0.3P

$= P\left(0.6 + \cot\frac{180°}{N}\right)$

OUTSIDE DIAMETER OF SPROCKET WHEN TOOTH IS POINTED

$= P \cot\frac{180°}{N} + \cos\frac{180°}{N}(D_s - D_r) + 2H$

THE PRESSURE ANGLE FOR A NEW CHAIN IS $xab = 35° - \frac{120°}{N}$

THE MINIMUM PRESSURE ANGLE IS $xab - B = 17° - \frac{64°}{N}$

THE AVERAGE PRESSURE ANGLE = $26° - \frac{92°}{N}$

APPENDIX C:
Engineering Drawings, Prototype

Drawings included:
- Carrier 1
- Carrier 2
- Carrier Shaft
- Carrier Shaft 2 (dummy shaft)
- Cap
- Sprocket
- Sprocket Spacer
- Driving Main Shaft
- Driven Main Shaft
- Top Flange
- Driving Bottom Flange
- Driven Bottom Flange
- Driven Mount Block
- Mount Plate
- Shim Block
- Mount Shim

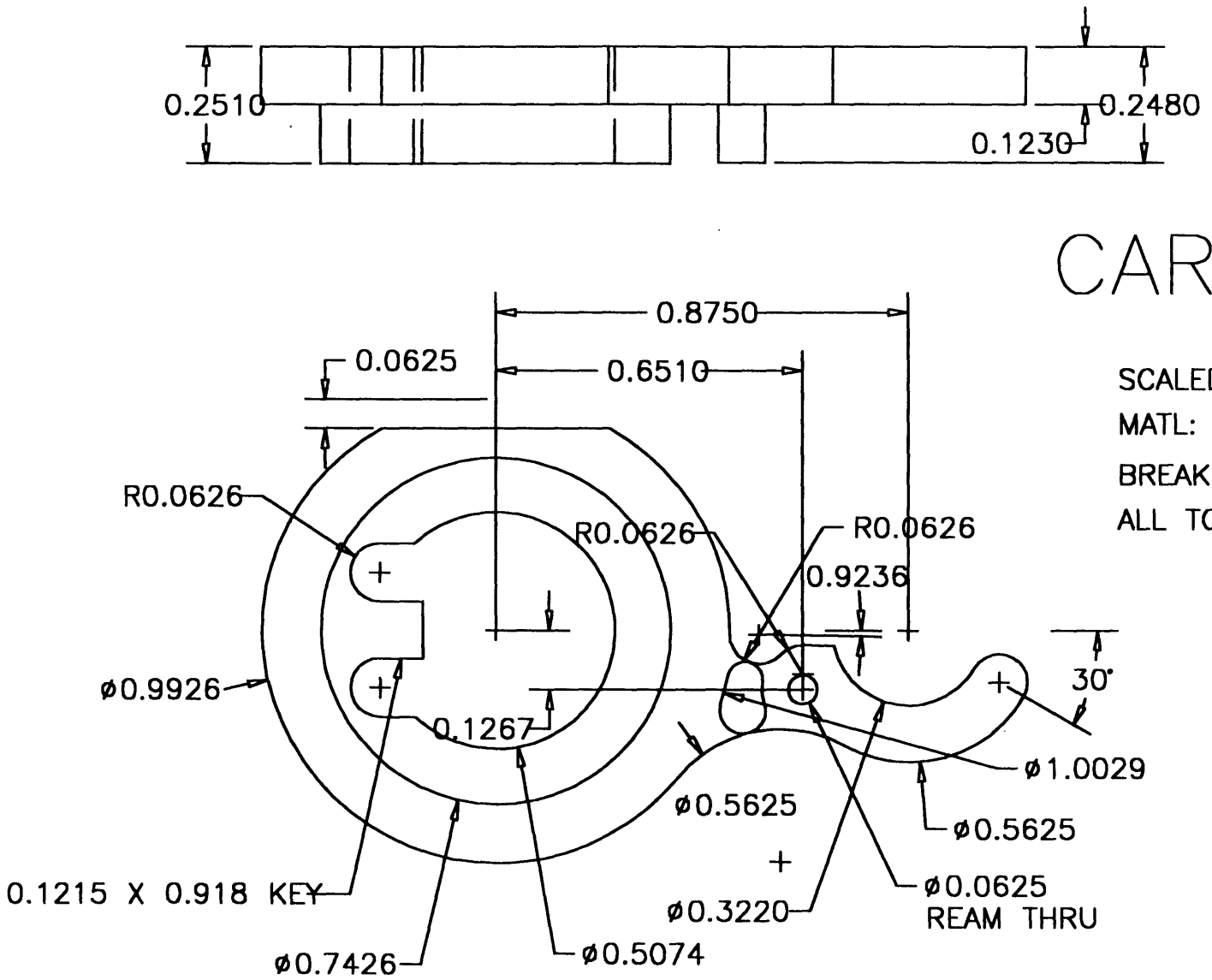
0.2510
0.2480
0.1230
CARRIER 1
0.8750
0.0625
0.6510
SCALED TO FIT QTY: 5(
MATL: 6061-T6 AL
BREAK FIRST THREAD
ALL TOLERANCES 0.0005"
R0.0626
R0.0626
R0.0626
0.9236
30°
ø0.9926
0.1267
ø1.0029
ø0.5625
ø0.5625
0.1215 X 0.918 KEY
ø0.0625
REAM THRU
ø0.3220
ø0.7426
ø0.5074

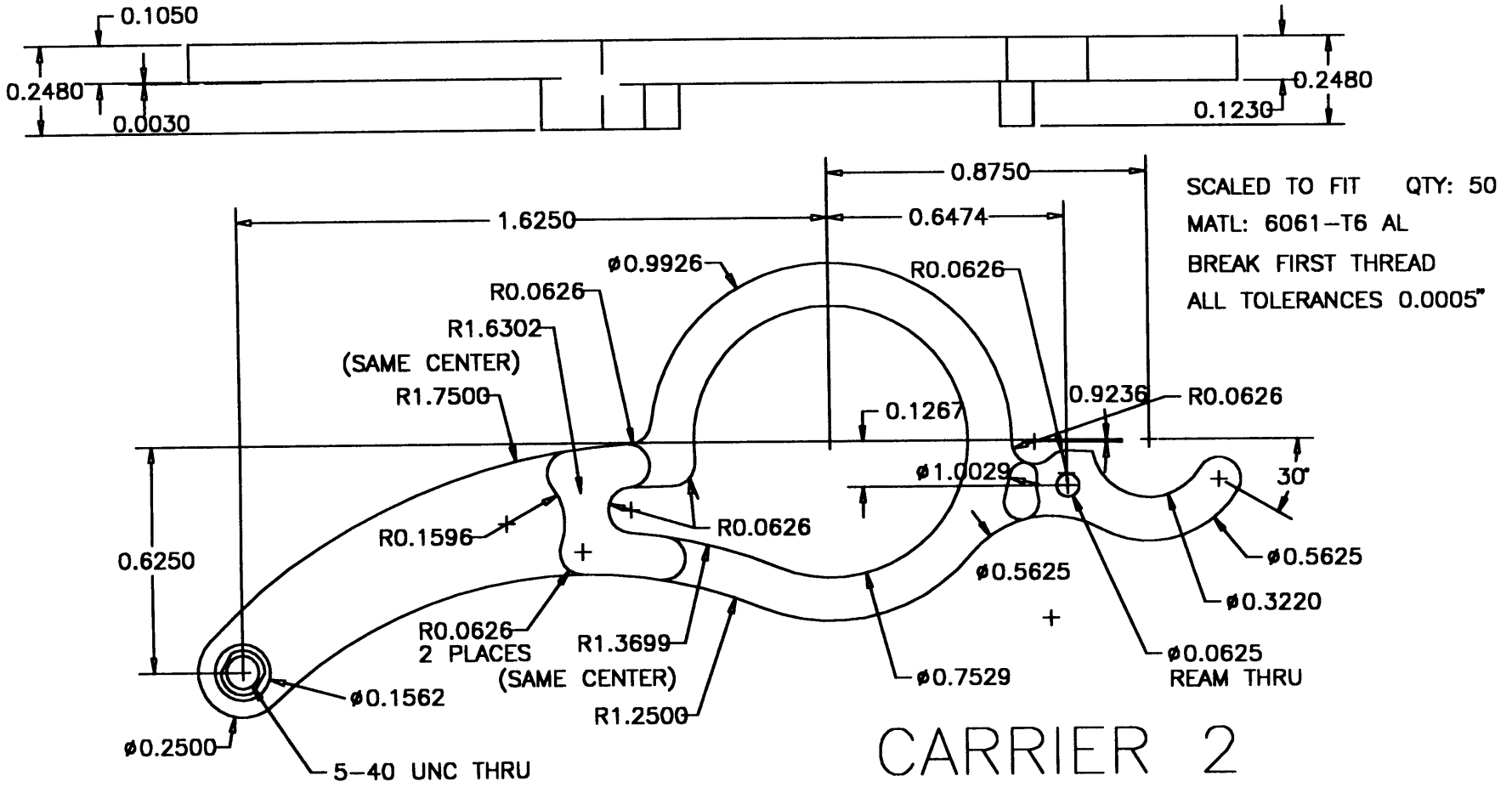
0.1050
0.2480
0.0030
0.2480
0.1230
0.8750
1.6250
0.6474
SCALED TO FIT QTY: 50
MATL: 6061-T6 AL
BREAK FIRST THREAD
ALL TOLERANCES 0.0005"
ø0.9926
R0.0626
R0.0626
R1.6302
(SAME CENTER)
R1.7500
0.1267
0.9236
R0.0626
ø1.0029
30°
R0.1596
R0.0626
0.6250
ø0.5625
ø0.3220
ø0.5625
R0.0626
2 PLACES
R1.3699
(SAME CENTER)
ø0.7529
ø0.0625
REAM THRU
ø0.1562
R1.2500
ø0.2500
5-40 UNC THRU
CARRIER 2

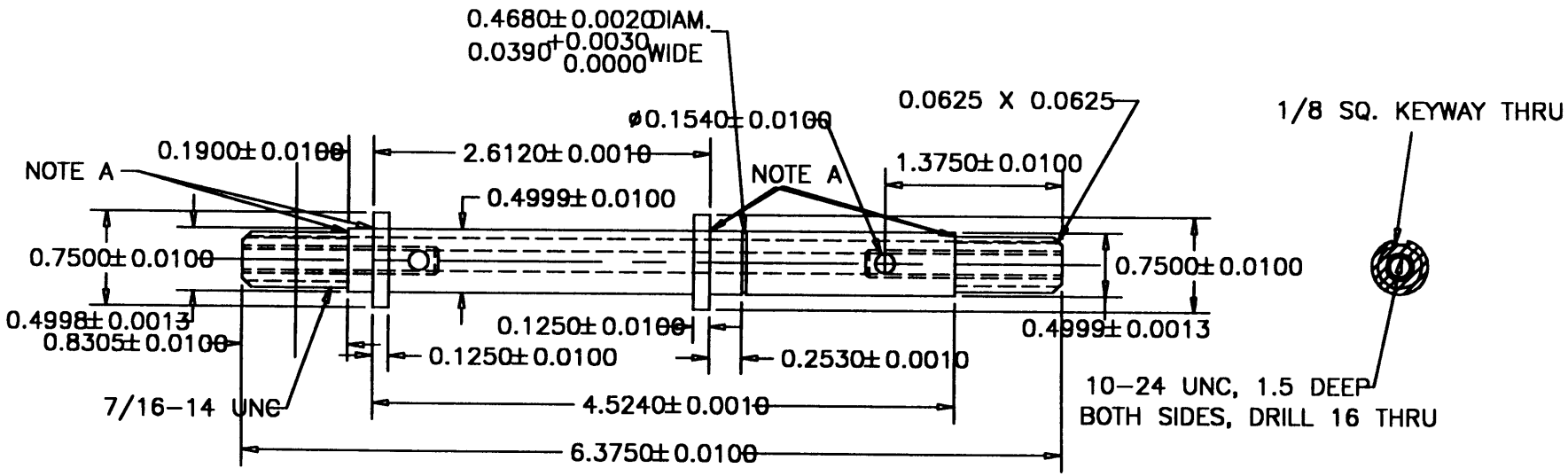

CARRIER SHAFT

SCALED TO FIT QTY: 50
MATL: 6061-T6 AL
BREAK FIRST THREAD

NOTE A: MAX 0.014R FILLET
ALL FILLETS 0.0625R UNLESS NOTED

CARRIER SHAFT 2

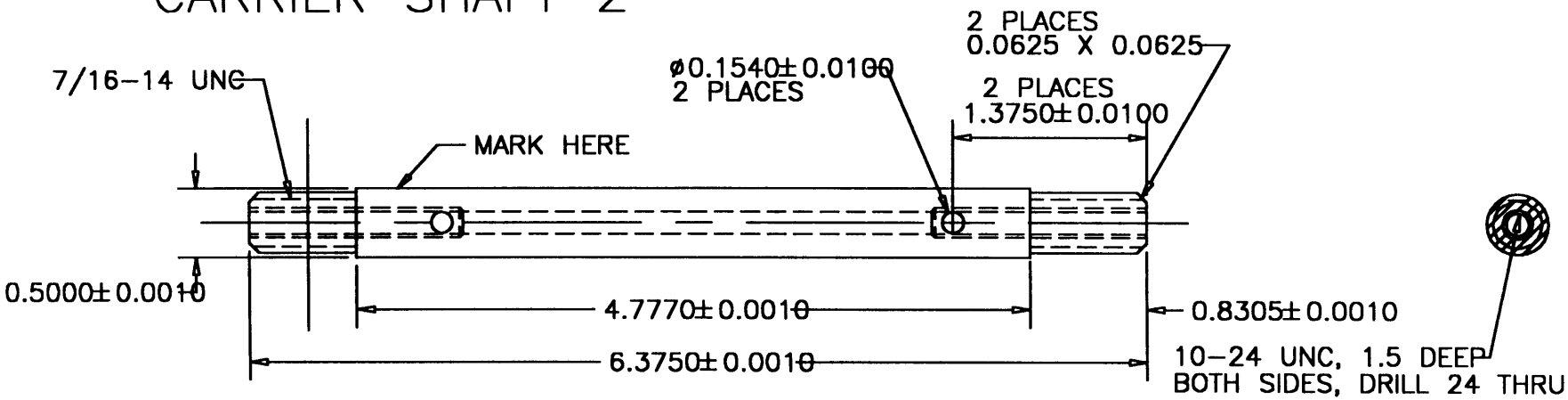

SCALED TO FIT QTY:95 MAT'L: 6061-T6 AL ALL FILLETS MAX 0.014R

CAP 2

SCALED TO FIT QTY: 275
MAT'L: 6061-T6 AL

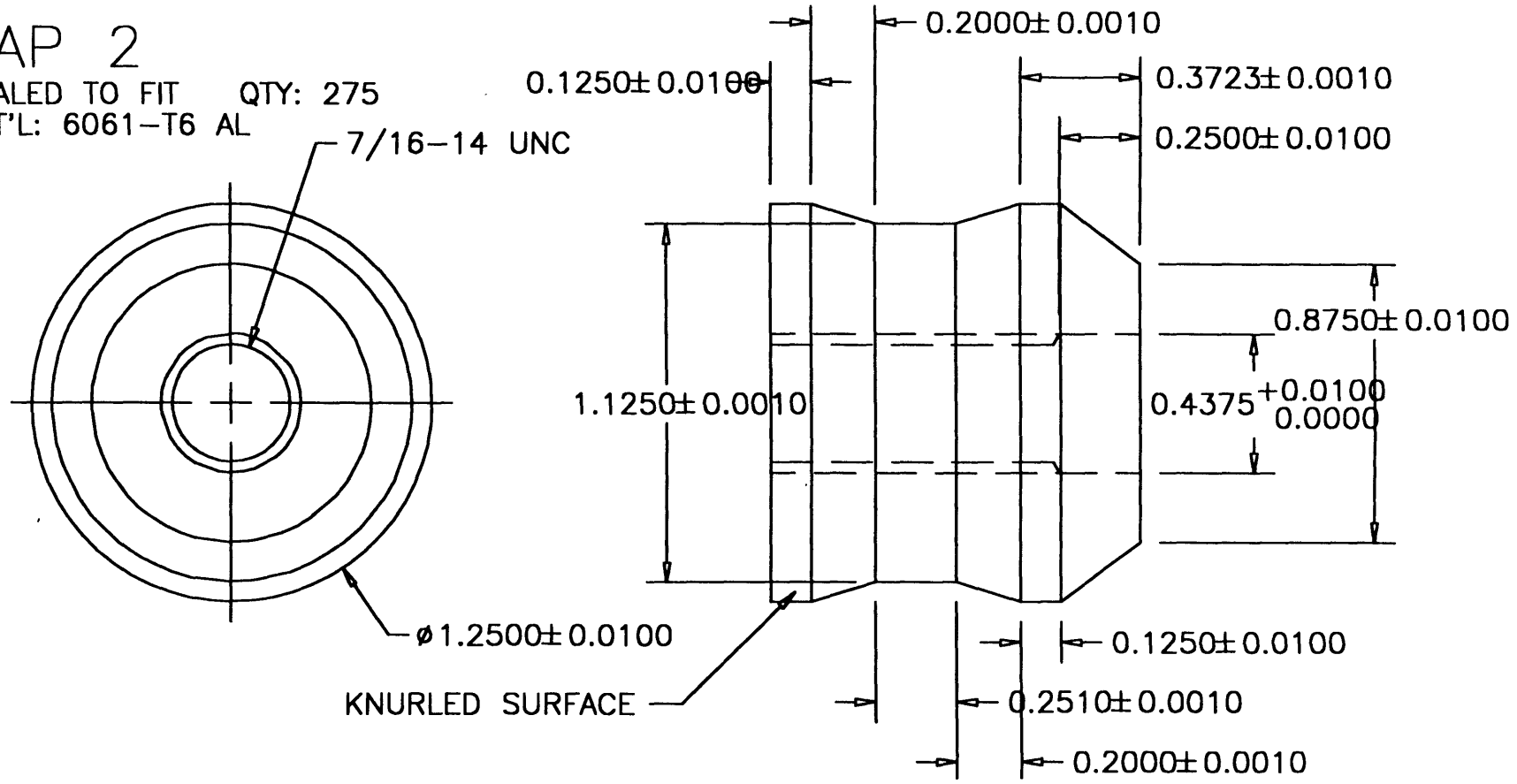

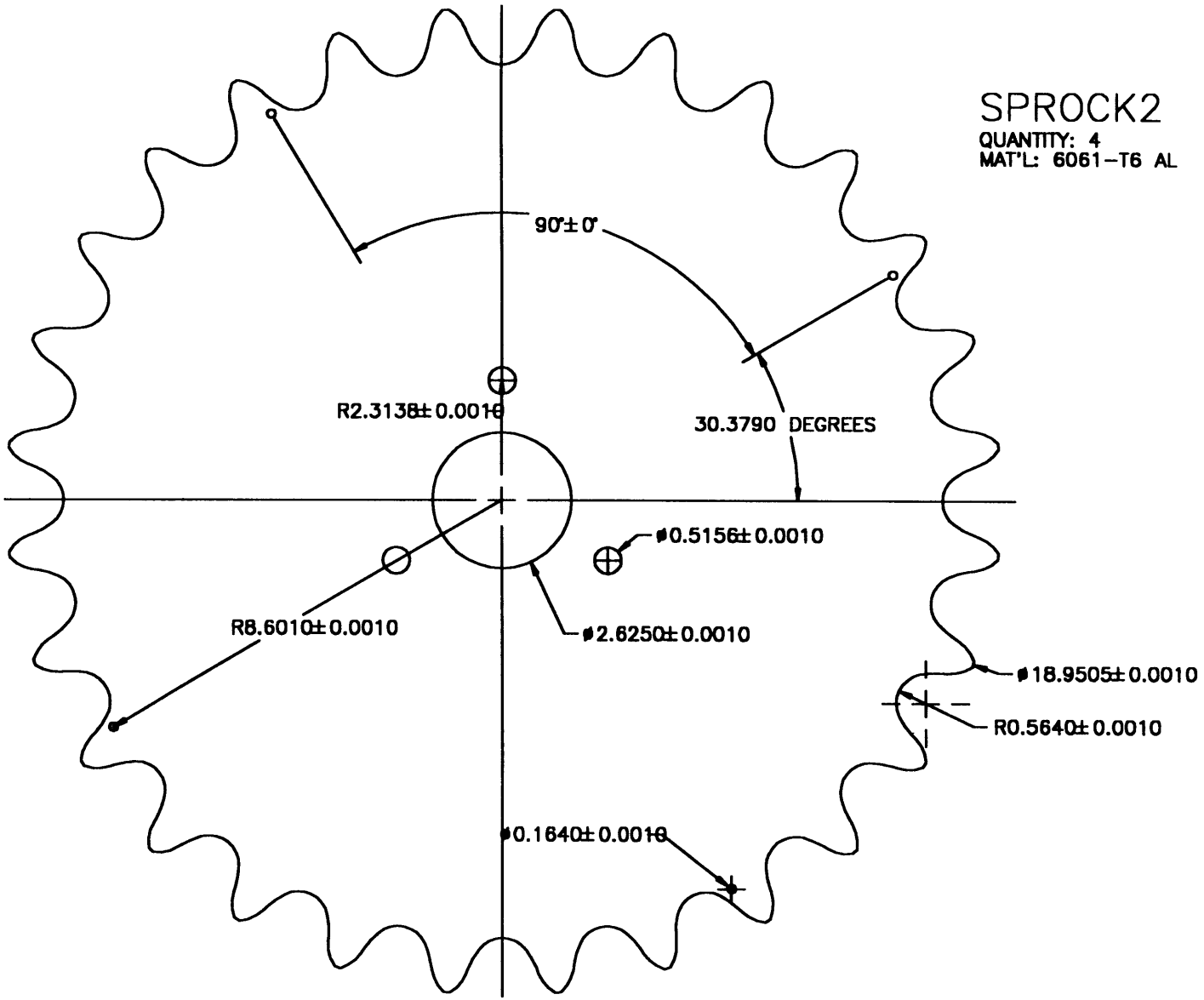
SPROCK2
QUANTITY: 4
MAT'L: 6061-T6 AL
90°±0°
R2.3138±0.0010
30.3790 DEGREES
ø0.5156±0.0010
R8.6010±0.0010
ø2.6250±0.0010
ø18.9505±0.0010
R0.5640±0.0010
ø0.1640±0.0010

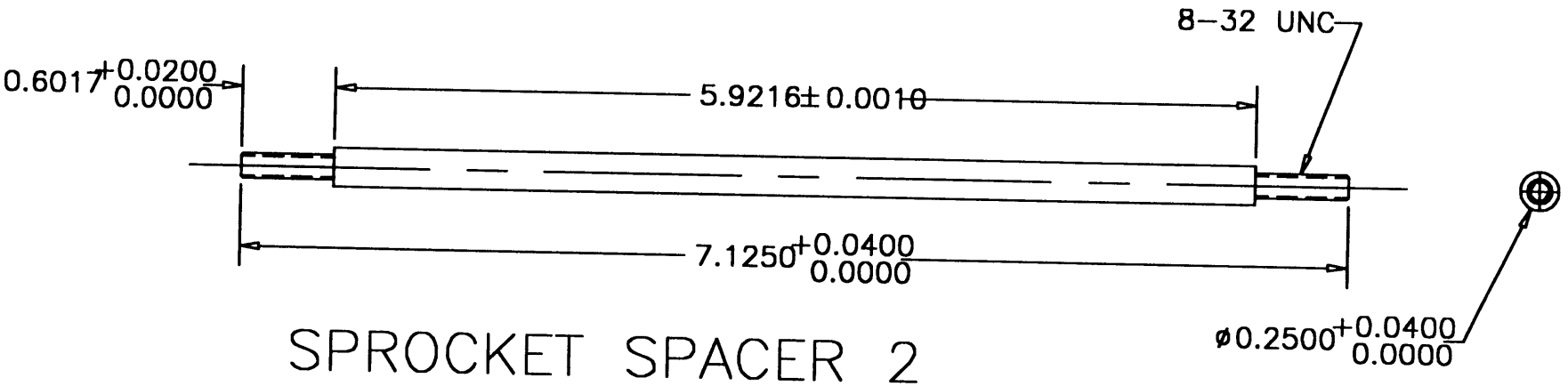

SPROCKET SPACER 2

SCALED TO FIT QTY: 8
MAT'L: LOW CARBON STEEL

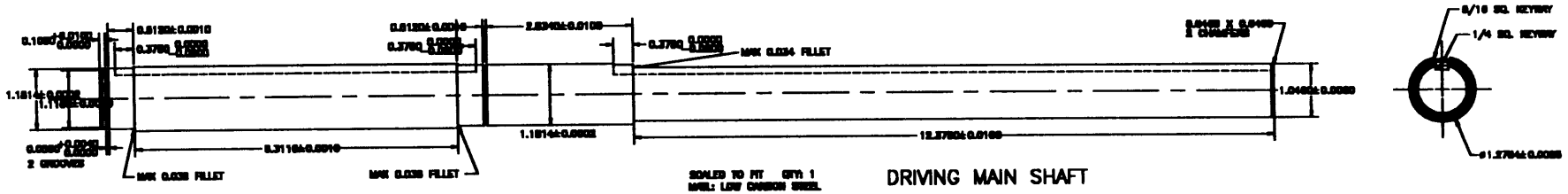

SCALED TO FIT QTY: 1
MATL: LOW CARBON STEEL

DRIVING MAIN SHAFT

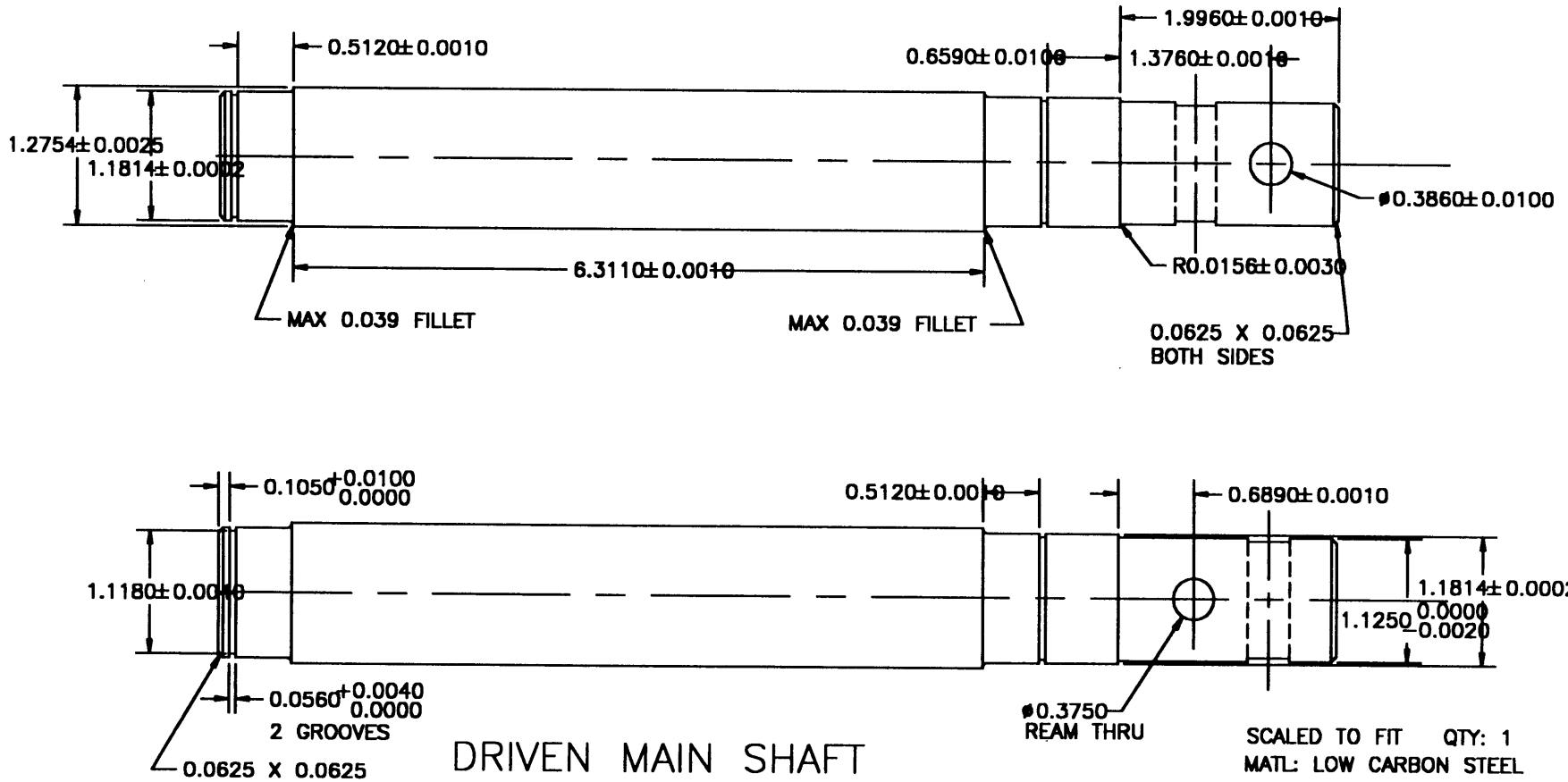

DRIVEN MAIN SHAFT

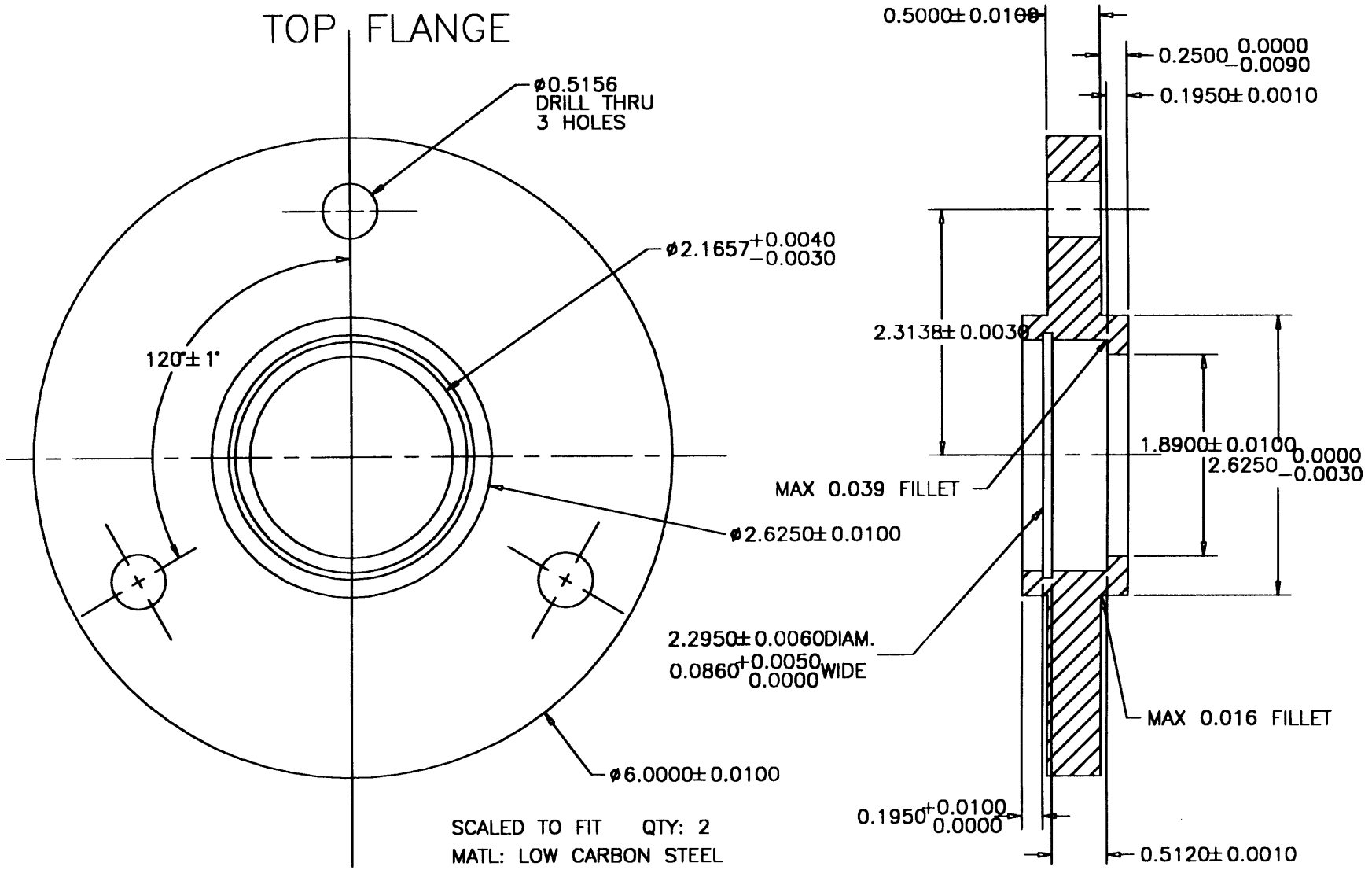
TOP FLANGE
ø0.5156
DRILL THRU
3 HOLES
ø2.1657 +0.0040 −0.0030
120° ± 1°
ø2.6250 ± 0.0100
ø6.0000 ± 0.0100
SCALED TO FIT QTY: 2
MATL: LOW CARBON STEEL
0.5000 ± 0.0100
0.2500 0.0000 −0.0090
0.1950 ± 0.0010
2.3138 ± 0.0030
1.8900 ± 0.0100
2.6250 0.0000 −0.0030
MAX 0.039 FILLET
2.2950 ± 0.0060 DIAM.
0.0860 +0.0050 0.0000 WIDE
MAX 0.016 FILLET
0.1950 +0.0100 0.0000
0.5120 ± 0.0010

DRIVING BOTTOM FLANGE

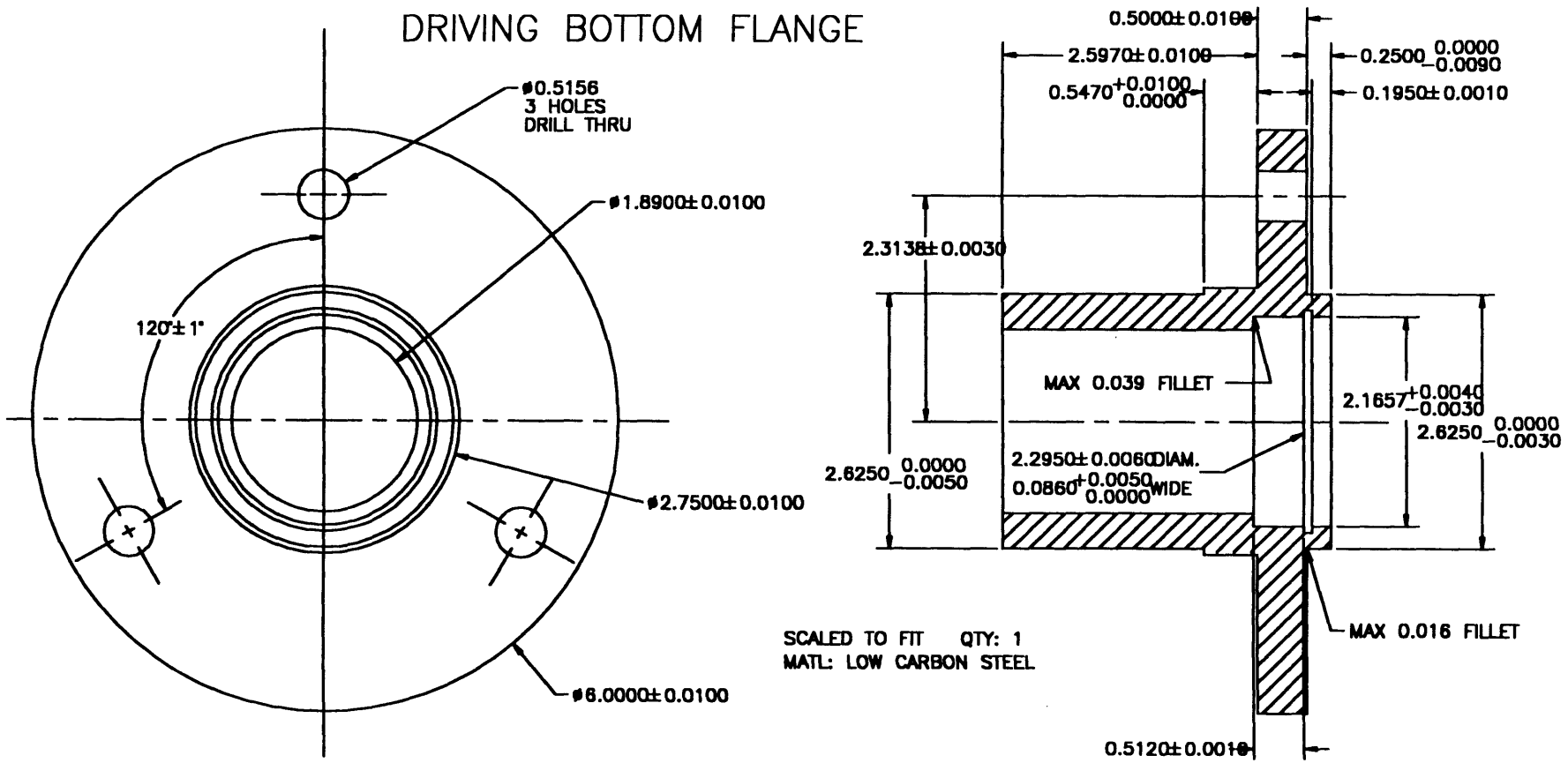

SCALED TO FIT QTY: 1
MATL: LOW CARBON STEEL

DRIVEN BOTTOM FLANGE

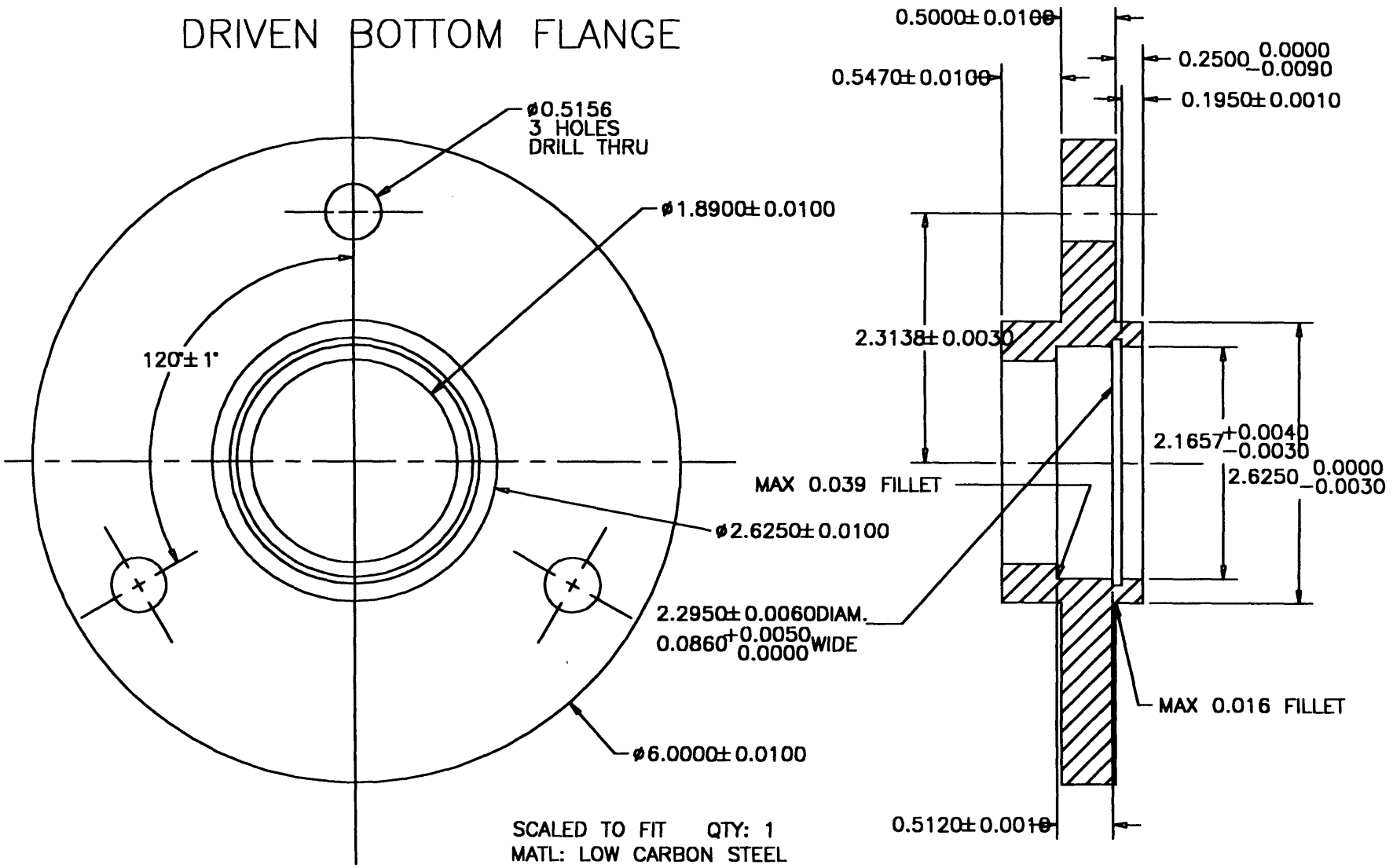

SCALED TO FIT QTY: 1
MATL: LOW CARBON STEEL

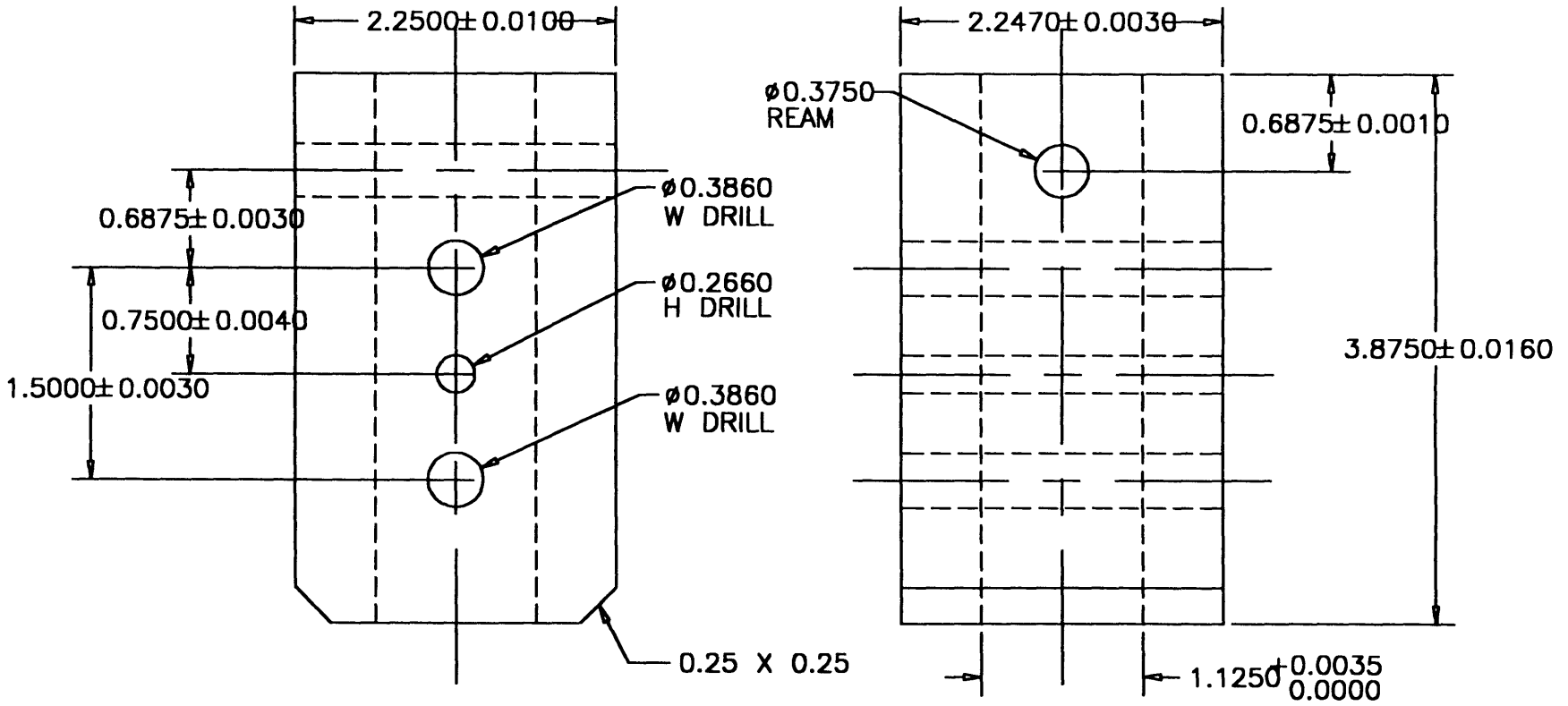

DRIVEN MOUNT BLOCK

SCALED TO FIT QTY: 1
MATL: LOW CARBON STEEL

MOUNT PLATE

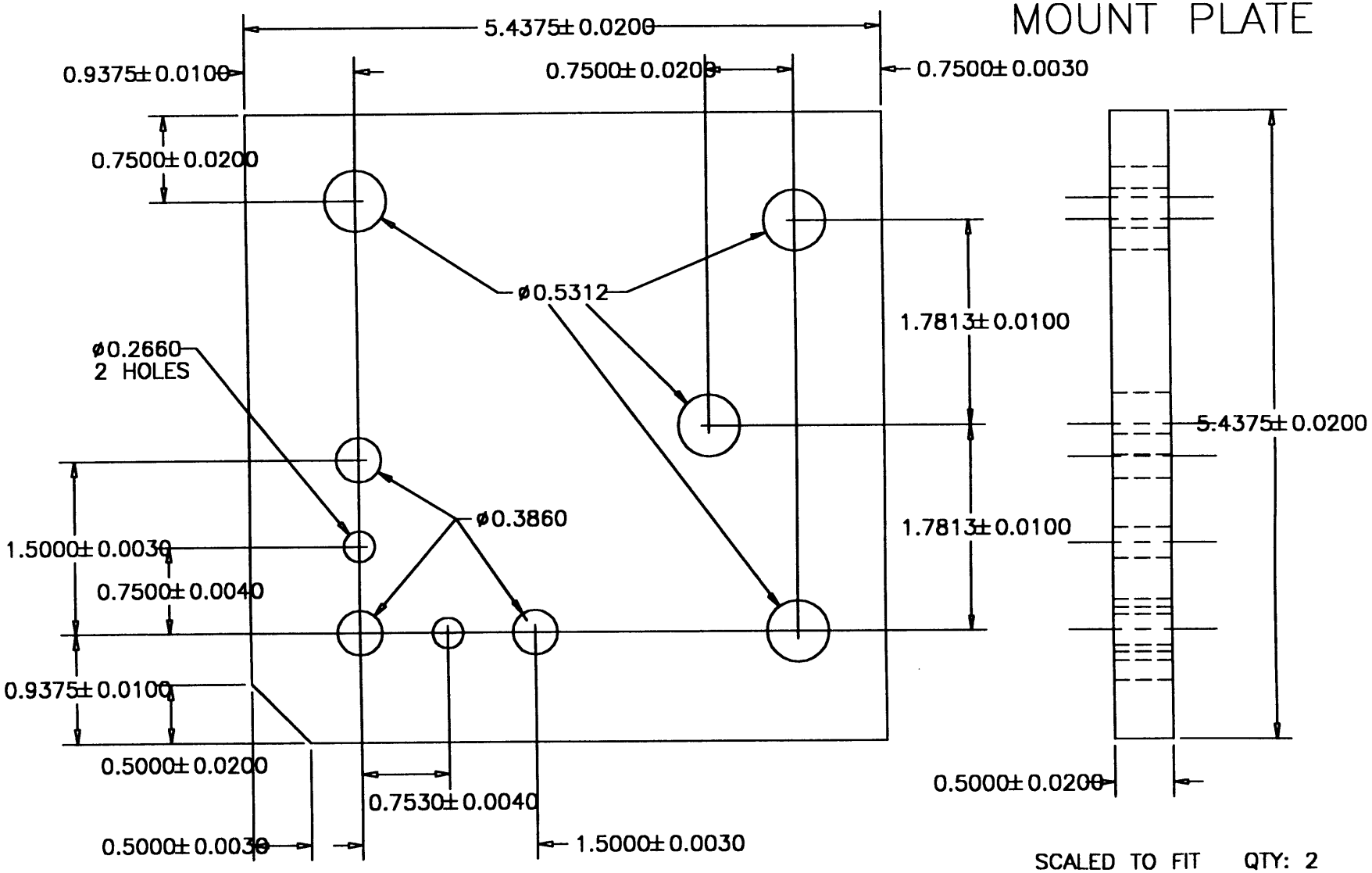

SCALED TO FIT QTY: 2
MATL: LOW CARBON STEEL

SHIM BLOCK

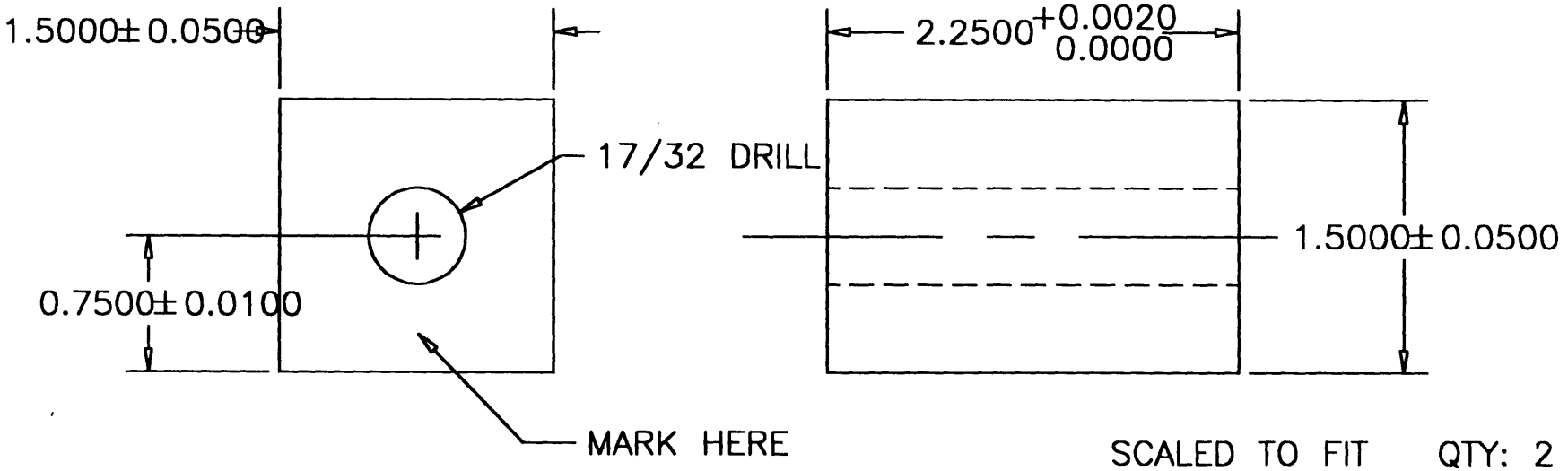

SCALED TO FIT QTY: 2

MATL: LOW CARBON STEEL

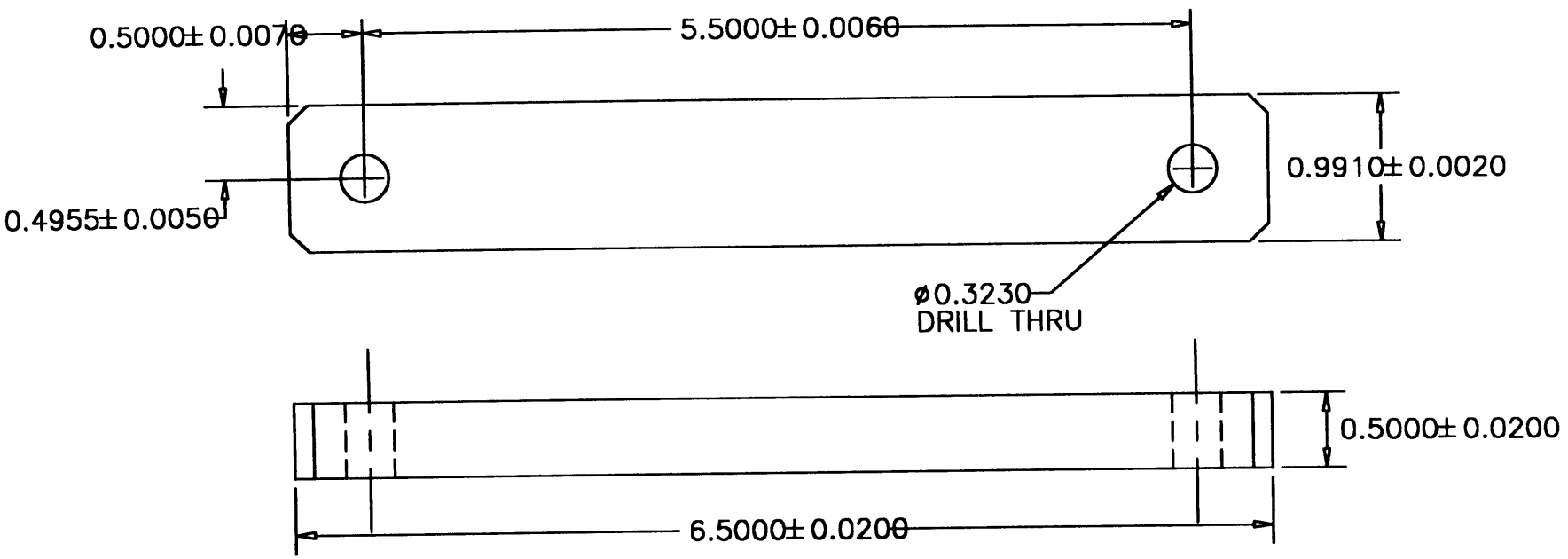

MOUNT SHIM

SCALED TO FIT QTY: 2
MAT'L: LOW CARBON STEEL